THE JOURNAL
OF
CHEMICAL PHYSICS

VOLUME 7 NOVEMBER, 1939 NUMBER 11

Rotatory Dispersion and Absorption Spectra of Carboxylic Acids and Hydrocarbons Containing a Phenyl or Cyclohexyl Group

ALEXANDRE ROTHEN AND P. A. LEVENE
Rockefeller Institute for Medical Research, New York, New York

(Received July 5, 1939)

The configurational relationships of aliphatic and aromatic disubstituted carboxylic acids having been established, it was possible to study the vicinal effect of the phenyl group on the carboxyl group. It was found that the effect of the phenyl group is not different from that of a normal hexyl or a cyclohexyl group. This phenomenon is due, perhaps, to the fact that the absorption bands of the phenyl group nearest to the visible region are not optically active.

THE knowledge of the configurational relationship of optically active aliphatic acids and of those containing a phenyl group seemed to offer an opportunity for the study of the mutual effect on optical rotation of two chromophoric groups with absorption bands in the near ultraviolet region. The task seemed accessible to solution through the comparison of the rotatory dispersion curves of the corresponding acids of the two types. Inasmuch as, according to Kuhn, the weaker absorption bands located in the longer wave-length region furnish the strongest partial rotation, the phenyl group was expected to furnish the first partial rotatory contribution of the acids containing a phenyl group. However, it was found that the region λ2700 to λ2500 (the characteristic absorption region of the phenyl group) is not anisotropic either in the phenylated acids or in the phenylated hydrocarbons. It was possible to measure the rotation beyond the short wave-length side of this region ($\lambda < 2500$) without noticing the familiar anomaly of a dispersion curve within an active absorption band. In other words, this region which contributes very little to the ordinary refraction[1] does not furnish a detectable rotatory contribution. A similar condition was observed in the phenylated carbinols and corresponding halides.[2] On the other hand, the second absorption region of the phenyl group and the first absorption band of the carboxyl group are located so close to each other that the dispersion curve does not permit a decision as to the origin of the first rotatory contribution of these acids.

With a sufficient degree of probability, however, the choice can be made on the basis of a comparison of the dispersion of the consecutive members of the following general type, homologous with respect to n_2, in the aliphatic and phenylated series.

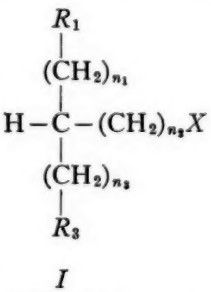

($R_1 = CH_3$; $R_3 = C_6H_5$, C_6H_{11} or C_6H_{13}; $X = COOH$ or CH_3)

I

[1] T. M. Lowry and C. B. Allsopp, Proc. Roy. Soc. **A133**, 26 (1931).

[2] P. A. Levene and A. Rothen, J. Biol. Chem. **127**, 237 (1939).

TABLE I. *Maximum rotations of configurationally related phenyl, cyclohexyl and aliphatic acids and of configurationally related phenylhydrocarbons* $[M]_D^{25}$, $R = C_6H_5 = A$; $R = C_6H_{11} = B$; $R = C_6H_{13} = C$.

$CH_3-CH-R-COOH$† $A+112$, $B+25$, $C+26$	$CH_3-CH-R-CH_2COOH$ $A-81$, $B+8.5$* $C-8$			
$C_2H_5-CH-R-COOH$ $A+140$, $B-1.3$* $C+23$	$C_3H_7-CH-R-CH_2COOH$ $A-\infty 85$	$C_2H_5-CH-C_6H_5-C_4H_9$ -10*		
$CH_3-CH-CH_2R-COOH$ $A+31$, $B+28$ $C+27$	$CH_3-CH-CH_2R-CH_2COOH$ $A-3.4$ (homog.) $+4.9$* (heptane) $B-13$, $C-\infty 8$	$CH_3-CH-CH_2C_6H_5-C_2H_5$ -9.5		
$CH_3-CH-(CH_2)_2R-COOH$ $A+50$, $B+30$ $C+27$	$CH_3-CH-(CH_2)_2R-CH_2COOH$ $A-52$, $B-19$, $C-\ldots$	$CH_3-CH-(CH_2)_2R-(CH_2)_3COOH$ $A-6.5$, $B-5$ (homog.) -7 (heptane)	$CH_3-CH-(CH_2)_2R-(CH_2)_3COOH$ $A-14.3$, $B-6.0$, $C-\ldots$	$CH_3-CH-(CH_2)_2C_6H_5-C_2H_5$ -35

* Anomalous dispersion.
† The sequence of the groups in the formulas of this table corresponds to their relative spatial distribution.

On the Direction of the Corresponding Partial Rotations of Members of Homologous Series

Before proceeding with the analysis of the dispersion of the compounds given in Table I, it should be recalled[3] that it was previously shown that in homologous series with respect to n_1 or n_3, the sign of the partial rotation of X remains the same in all members even when the total rotations are of opposite sign. The same regularity has now been observed in the series of acids containing a cyclohexyl group.

In this connection, the case of *ethylcyclohexylacetic acid* is especially interesting since the dispersion could be measured over a wide wavelength range from λ6300 to λ2465. (See Table VI and Fig. 4.) The molecular rotation varies from $-1.29°$ to $+260°$ and it can be seen that the agreement reached between the values found and those calculated from a two-term Drude formula is excellent, especially if one considers the great change in the magnitude of the rotation. It should be noted that the lower homolog with respect to n_1 (methylcyclohexylacetic acid) has a normal dispersion and hence it is self-explanatory why these two homologs are of opposite sign when configurationally related. The constant of dispersion of the first Drude term is appreciably higher in ethylcyclohexylacetic than in methyl-

TABLE II. *Rotatory dispersion in heptane of dextro 2-phenylbutyric acid-1 (ethylphenylacetic acid), constant of sample:* $n_D^{25} = 1.5140$ *conc. 0.1840M, l = 40 cm, 10 cm for λ3980 to λ2800, 1 cm for λ2780 and λ2750, 0.5 cm for λ2410.*

$$[M]^{25}_{max} = \frac{59.933}{\lambda^2 - 0.047} - \frac{18.851}{\lambda^2 - 0.030}$$ *

λ	α^{25}	λ	α^{25}
5875.6	9.164 (+.001)	3215	12.85 (−.25)
5780.1	9.527 (.000)	3160	13.82 (−.18)
5460.7	10.925 (.000)	3110	14.85 (−.15)
4358.3	19.565 (.000)	3025	16.82 (−.48)
4046.6	24.15 (−.02)	2985	17.82 (−.08)
3980	6.35 (.00)	2951	18.82 (−.08)
3965	6.39 (−.03)	2895	20.76 (+.06)
3880	6.85 (.00)	2840	22.82 (−.08)
3710	7.85 (−.02)	2800	24.72 (+.1)
3459	9.86 (−.11)	2780	2.55 (−.02)
3360	10.85 (−.25)	2750	2.75 (.00)
		2410	0.95 (+.2)

* The figures in parentheses represent the absolute difference from the calculated values.

[3] P. A. Levene and A. Rothen, Chapter on Rotatory Dispersion in H. Gilman, *Organic Chemistry* (John Wiley & Son, 1938). First edition. New York, 1779.

cyclohexylacetic acid. It might very well be that this first term is the sum of two terms whose relative importance is different in the two homologues. Definite conclusions cannot be drawn since the dispersion data could not be obtained close enough to the active absorption region.

The behavior of methylbenzylpropionic acid is another illustration. This acid is levorotatory in homogeneous state whereas it rotates to the right in a solution of heptane. The data in Table III show that the dispersion is anomalous in heptane solution and normal in homogeneous state. The first rotatory contribution remains negative in either solvent. It should be emphasized again that no case is known where a substance exhibiting opposite signs of rotation in two different mediums would have the same type of dispersion in both. The medium affects the relative magnitude of the different partial rotations but not their sign.

Allocation of the First Active Absorption Region of the Phenylated Carboxylic Acids

It can be seen from Table I that a sufficient number of members homologous with respect to n_2 were available only for the phenethyl series.

Two phenomena stand out in their optical behavior. First, there is observed a change in the direction of rotation when the value of n_2 changes from 0 to 1, this change being also observed in the phenyl and benzyl series. Second, with further increase in the values of n_2 there is observed a periodic change in the direction of the shift of rotation of the consecutive members. A similar behavior is observed in the corresponding carboxylic acids containing a cyclohexyl group, as well as in

Table III. *Rotatory dispersion in heptane of configurationally related*

A. Levo 3-phenylbutyric acid-1 (methylphenylpropionic acid) conc. 0.3164M l=40 cm $[M]^{25}_{max} = -\frac{23.86}{\lambda^2-0.0526}$;

B. Levo 3-phenylcaproic acid-1 (propylphenylpropionic acid) conc. 0.4617M l=20 cm $\alpha^{25} = -\frac{0.5577}{\lambda^2-0.0548}$;

C. Dextro 3-phenyl-2-methylpropionic acid-1 (methylbenzylacetic acid) $n_D^{25}=1.5128$, $d_4^{25}=1.044$, *conc.* $=0.4959M$, *l=40 cm.* $[M]^{25}_{max} = +\frac{9.049}{\lambda^2-0.05566}$;

D. 4-phenyl-3-methylbutyric acid-1 (methylbenzylpropionic acid) $n_D^{25}=1.5097$ *conc.* $=1.111M$, *l=20 cm dextro* $[M]^{25}_{D_{max}} = +4.8$;

E. 4-phenyl-3-methylbutyric acid-1 (methylbenzylpropionic acid (Homogeneous state) l=5 cm levo $[M]^{25}_{D_{max}} = -3.4$.

λ	A	α^{25}	B	α^{25}	C	α^{25}	D	α^{25}	E	α^{25}
6678.1	−1.758	(−.003)	−1.405	(−.015)	—		—		—	
5875.6	−2.359	(−.010)	−1.919	(+.001)	5.748	(+.012)	—		—	
5780.1	—		−1.996	(.000)	5.966	(.000)	+0.355		−0.296	
5460.1	−2.824	(.000)	−2.292	(+.001)	6.866	(+.017)	+0.396		−0.365	
4358.3	−5.05	(.00)	−4.127	(.000)	12.37	(.00)	+0.53		−0.89	
4046.6	—		—		15 40	(+.03)	+0.59		—	

Table IV. *Rotatory dispersion in heptane of configurationally related.*

A. Dextro 4-phenylbutyric acid-1 (methylphenethylacetic acid) $n_D^{25}=1.5096$, *conc. 0.2813M, l=40 cm, 10 cm from λ3840 to λ2820,* $[M]^{25}_{max} = \frac{17.065}{\lambda^2-0.042} - \frac{1.893}{\lambda^2-0.030}$;

B. Levo 5-phenyl-3-methylvaleric acid-1 (methylphenethylpropionic acid) $n_D^{25}=1.5077$ *conc. 0.522M, l=40 cm, 10 cm from λ3440 to λ3000, 5 cm from λ2925 to λ2885,* $[M]_D^{25} = -\frac{35.052}{\lambda^2-0.042} + \frac{19.764}{\lambda^2-0.030}$.

λ	$A\alpha^{25}$		$B\alpha^{25}$	
5875.6	7.016	(−.012)	−3.239	(+.005)
5780.1	7.297	(.000)	−3.363	(.000)
5460.7	8.320	(−.005)	−3.867	(.008)
4358.3	14.47	(.00)	−6.93	(.00)
4046.6	17.55$_5$	(−.055)	−8.55	(−.02)
3840	5.15	(+.08)	—	
3590	6.17	(−.03)	—	
3440	—		−3.60	(.00)
3425	7.18	(+.01)	—	
3300	—		−4.10	(−.07)
3285	8.20	(.00)	—	
3210	—		−4.60	(−.05)
3168	9.21	(−.07)	—	
3130			−5.10	(−.02)
3085	10.23	(+.03)	—	
3000	11.25	(−.05)	−6.10	(−.02)
2935	12.26	(−.06)	—	
2925	—		−3.40	
2885	—		−3.65	
2878	13.28	(−.05)	—	
2820	14.29	(−.26)	—	
2740			0.48	(0.5 cm)
2340			0.30	(0.05 cm)

Table V. *Rotatory dispersion in heptane of configurationally related.*

A. Levo 6-phenyl-4-methylcaproic acid-1 (methylphenethylbutyric acid) $n_D^{25}=1.5062$, *conc. 0.6351M, l=40 cm* $[M]^{25}_{max} = -\frac{14.376}{\lambda^2-0.042} + \frac{12.876}{\lambda^2-0.030}$;

B. Levo 7-phenyl-5-methylheptylic acid-1 (methylphenethylvaleric acid) $n_D^{25}=1.5030$, *conc. 0.3650M, l=100 cm* $d_4^{25}=1.0020$ $[M]^{25}_{max} = -\frac{20.770}{\lambda^2-0.042} + \frac{17.050}{\lambda^2-0.030}$.

λ	A	α^{25}	B	α^{25}
5875.6	−0.316	(−.001)	−1.726	(−.005)
5780.1	−0.332	(.000)	−1.807	(.000)
5460.7	−0.398	(+.007)	−2.099	(−.003)
4358.3	−0.805	(.000)	−4.06	(.000)
4046.6	−1.03	(−.02)	−5.21	(+.03)

TABLE VI. *Rotatory dispersion in heptane of levo 2-cyclohexylbutyric acid (ethylcyclohexylacetic acid) conc. 1.140 M, l=40 cm, 10 cm from λ3700 to λ2580*

$$[M]^{25}_{max} = -\frac{7.7605}{\lambda^2-0.04393} + \frac{8.8257}{\lambda^2-0.01903}.$$

λ	$[M]^{25}$ OBSERVED	
5875.6	−1.286	(−.014)
5780.1	−1.267	(.000)
5460.7	−1.103	(+.010)
4358.3	+1.509	(.000)
4046.6	+3.95	(+.17)
3700	+7.89	(−.70)
3520	+12.5	(−.3)
3415	+17.2	(+1.0)
3285	+21.8	(−.2)
3220	+26.5	(+1.0)
3010	+45.0	(+2.1)
2935	+54.3	(+2.1)
2877	+63.6	(+2.3)
2824	+72.9	(+1.6)
2785	+82.2	(+4.4)
2744	+91.5	(+1.0)
2710	+100.7	(.0)
2684	+110.0	(.0)
2660	+119.3	(+0.7)
2617	+137.9	(+0.5)
2598	+147.2	(.0)
2580	+156.5	(−0.7)
2465	+260	(1 cm) (+5)

the members of aliphatic carboxylic acids homologous with respect to n_2 discussed previously.[4] For these acids it was shown that the periodic change in the total rotation could be attributed to changes in the partial rotation of the carboxyl group. This similarity in behavior of aliphatic and phenylated acids points to a variation in the partial rotation of the carboxyl group as the cause of the observed periodicity in both series. Hence the first partial rotation of the members of the series of phenylated acids may be assigned to the carboxyl group.

It may be emphasized, in this place, that the reality of the periodic change in the shift of rotation with the change in the value of n_2 is evidenced also by the observations on the changes in the values of the dispersion constants of the individual members. For if it is true that the periodic change is brought about in the main by variations in one partial rotation, then the homologs with a high rotation should have a low dispersion and vice versa (admitting that the first two partial rotations are of opposite sign and that all dispersions are normal). It can be observed that this is true in the phenethyl series of acids.

[4] P. A. Levene and A. Rothen, J. Org. Chem. **1**, 76 (1936).

(See Tables IV and V.) Methylphenethylacetic and methylphenethylpropionic acids are of opposite sign but their maximum rotations are of the same order of magnitude and their dispersion curves are not much different. On the contrary, methylphenethylbutyric acid with a low rotation is highly dispersive. Finally, the magnitude of the rotation of methylphenethylvaleric acid is intermediate between that found for methylphenethylpropionic and methylphenethylbutyric acid and the dispersion is also intermediate between the dispersions of those two latter acids. This parallelism between maximum rotations and dispersions gives additional confidence to the belief that the given values for the maximum rotations are not far from the true values.

A further argument in favor of the assignment of the first rotatory contribution to the carboxyl group may be found in a comparison of the rotations of the consecutive members homologous with respect to n_3 of the series of phenylated hydrocarbons, on one hand, and of those of the phenylated carboxylic acids on the other. (See Tables I and IX.) In the former, where the first rotatory contribution can definitely be attributed to the phenyl group, the change of n_3 from 0 to 1 leads to a change of sign of the first partial rotation (which is evident from the fact that the rotatory dispersion of the first member is anomalous, whereas that of the second member is normal,

TABLE VII. *Rotatory dispersion in heptane of configurationally related*

A. Dextro 2-cyclohexylpropionic acid-1 (methylcyclohexylacetic acid) conc. 0.7228 M, l=40 cm,

$$[M]^{25}_{max} = \frac{14.454}{\lambda^2-0.036} - \frac{7.2314}{\lambda^2-0.020};$$

B. Dextro 3-cyclohexylbutyric acid-1 (methylcyclohexylpropionic acid) $n_D^{25}=1.4678$, conc. 0.746 M, l=40 cm $[M]^{25}_{D_{max}}=7.8$;

C. Dextro 3-cyclohexyl-2-methylpropionic acid-1 (methylhexahydrobenzylacetic acid) $n_D^{25}=1.4612$, conc. 0.575 M, l=40 cm $[M]^{25}_{max} = \frac{8.896}{\lambda^2-0.0342}$;

D. Levo 4-cyclohexyl-3- methylbutyric acid-1 (methylhexahydrobenzylpropionic acid) $n_D^{25}=1.4623$, conc. 0.3569 M, l=10 cm, $[M]^{25}_{max} = -\frac{\sim 4.00}{\lambda^2-0.0449}$.

λ	A	α^{25}	B	α^{25}	C	α^{25}	D	α^{25}
5875.6	2.768	(+.004)	+0.028		2.885	(−.006)	−0.312	(−.004)
5780.1	2.872	(.000)	+0.030		3.002	(−.004)	−0.3285	(.000)
5460.7	3.287	(+.002)	+0.027		3.407	(.000)	−0.372	(−.003)
4358.3	5.79	(.00)	−0.005		5.77	(.00)	−0.655	(.000)
4046.6	7.09	(.02)	−0.05		6.93	(−.01)	−0.78	(−.019)
			−1.60 for λ2750					

TABLE VIII. *Rotatory dispersion of configurationally related*

A. Dextro 4-cyclohexyl-2-methylbutyric acid-1 (methylhexahydrophenethylacetic acid), $n_D^{25}=1.4623$, $d_4^{25}=0.968$. *In heptane: conc. 0.5438 M, l=40 cm* $[M]^{25}_{max}=\frac{10.763}{\lambda^2-0.035}$. *Homogeneous: l=10 cm,* $[M]^{25}_{max}=\frac{9.3188}{\lambda^2-0.038}$.

B. Levo 5-cyclohexyl-3-methylvaleric acid-1 (methylhexahydrophenethylpropionic acid), $n_D^{25}=1.4632$, $d_4^{25}=0.959$. *In heptane: conc. 0.5080 M, l=40 cm* $[M]^{25}_{max}=-\frac{6.639}{\lambda^2-0.0337}$. *Homogeneous: l=20 cm,* $[M]^{25}_{max}=-\frac{5.822}{\lambda^2-0.039}$.

C. Levo 6-cyclohexyl-4-methylcaproic acid-1 (methylhexahydrophenethylbutyric acid), $n_D^{25}=1.4650$, $d_4^{25}=0.953$. *In heptane: conc. 0.412 M, l=40 cm,* $[M]^{25}_{max}=-\frac{2.52}{\lambda^2+0.002}$. *Homogeneous: l=10 cm,* $[M]^{25}_{max}=-\frac{1.740}{\lambda^2}$.

D. Levo 7-cyclohexyl-5-methylheptylic acid-1 (methylhexahydrophenethylvaleric acid), $n_D^{25}=1.4653$, $[M]^{25}_{max}=-\frac{2.049}{\lambda^2-0.022}$ *(homogeneous).*

λ	*A* (HEPTANE)	*A* (HOMOG.)	*B* (HEPTANE)	*B* (HOMOG.)	*C* (HEPTANE)	*C* (HOMOG.)	*D*
	α^{35}	α^{35}	α^{25}	α^{25}	α^{25}	α^{25}	α^{25}
5875.6	5.739	—	−1.169	− 4.737	—	—	−2.751
5780.1	5.948	12.482	−1.219	− 4.939	−0.320	−0.582	−2.846
5460.7	6.770	14.222	−1.394	− 5.618	−0.359	−0.648	−3.210
4358.3	11.50	24.34	−2.36	− 9.65	−0.56	−1.02	−5.285
4046.6	13.82	—	−2.83	−11.67	—	−1.15	−6.25

both hydrocarbons rotating in the same direction in the visible region). In the latter series, the change from $n_3=0$ to $n_3=1$ does not result in a change of sign.

Still additional grounds for the allocation of the first rotatory contribution to the carboxyl group may be found in the changes in rotation of the members homologous to n_2 in series of acids containing a cyclohexyl group. It is logical to expect a different vicinal effect from the cyclohexyl than from the phenyl group and yet consecutive changes in the value of n_2 in cyclohexyl series bring about changes in rotation similar to those observed in the phenylated and in the aliphatic acids. These changes are particularly striking in the series of hexahydrophenethyl acids.

The first two members, homologous with respect to n_2, exhibit the same dispersion but are of opposite sign. (See Table VIII.) In other words, the first contribution changes its sign with the increase of n_2 from 0 to 1. This is in accord with the events observed in all other series as mentioned above. The third member, methylhexahydrophenethylbutyric acid, has the same sign as the second member but exhibits an anomalous dispersion. (The dispersion constant has a zero value from measurements in the visible spectrum.) It follows then that the first contribution has again changed its sign. The last member, methylhexahydrophenethylvaleric acid, exhibits a normal dispersion. In this series, then, the direction of the first partial rotation of the successive members homologous with respect to n_2 is +, −, +, −. This is the first example, to our knowledge, where a change of sign of the partial rotation of a chromophoric group occurs with a change of n_2 from 1 to 2.

TABLE IX. *Rotatory dispersion of configurationally related*

A. Levo ethylbutylphenylmethane (3-phenylheptane), constants of sample: $n_D^{25}=1.4848$, $d_4^{25}=0.8558$, *l=20 cm from λ5875.6 to λ4046.6, 5 cm from λ3580 to λ2120* $[M]^{25}_{max}=-\frac{\sim 3.34}{\lambda^2-0.0054}$ *(homogeneous).*

B. Levo methylethylbenzylmethane (1-phenyl-2-methylbutane) constants of sample: $n_D^{25}=1.4870$, $d_4^{25}=0.8571$ *l=20 cm from λ5875.6 to λ4046.6, 5 cm from λ3850 to λ3090,* $[M]^{25}_{max}=-\frac{7.8247}{\lambda^2-0.038}+\frac{5.2173}{\lambda^2-0.018}$ *(homogeneous).*

C. Levo methylethylphenethylmethane (1-phenyl-3-methylpentane) constants of sample: $n_D^{25}=1.4859$, $d_4^{25}=0.8585$, *l=10 cm from λ5875.6 to λ4046.6, 1 cm from λ3645 to λ2865.* $[M]^{25}_{max}=-\frac{10.43}{\lambda^2-0.0462}$ *(homogeneous).*

A		*B*		*C*	
λ	α^{25}	λ	α^{25}	λ	α^{35}
5875.6	−1.336 (.000)	5875.6	−3.027 (−.008)	5875.6	−3.474 (+.016)
5780.1	−1.374 (−.007)	5780.1	−3.161 (.000)	5780.1	−3.593 (+.001)
5460.7	−1.552 (+.001)	5460.7	−3.649 (.000)	5460.7	−4.112 (+.009)
4358.3	−2.46 (.00)	4358.3	−6.74 (.00)	4358.3	−7.215 (+.025)
4046.6	−2.88 (+.01)	4046.6	−8.43 (+.01)	4046.6	−8.80 (.00)
3580	−0.90 (+.02)	3850	−2.45 (−.01)	3645	−1.22 (.03)
3230	−1.15 (.00)	3750	−2.70 (+.01)	3140	−2.00 (+.03)
3120	−1.30 (.00)	3630	−2.90 (−.09)	3000	−2.42 (+.06)
		3560	−3.10 (−.10)	2930	−2.50 (+.05)
		3467	−3.45 (−.06)	2865	−2.70 (+.02)
		3360	−3.95 (−.02)		
		3235	−4.45 (−.10)		
		3170	−4.95 (+.02)		
		3090	−5.45 (−.03)		

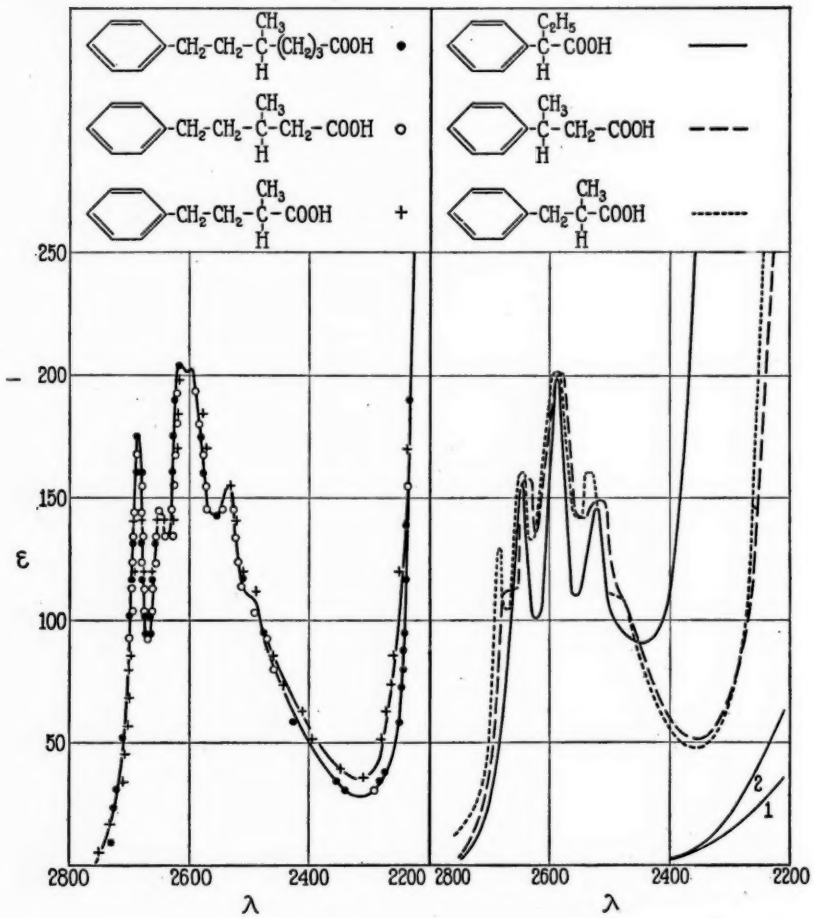

FIG. 1. Absorption spectra. Molecular extinction coefficients are plotted against wave-length expressed in A. Solvent = normal heptane. Curve 1 corresponds to methylhexahydrophenethylbutyric and methylhexahydrophenethylvaleric acids. Curve 2 corresponds to methylcyclohexylacetic acid.

THE VICINAL EFFECT OF THE PHENYL GROUP ON THE PARTIAL ROTATION OF THE CARBOXYL GROUP

Having assigned the first partial rotation to the carboxyl group in the phenylated acids, it is possible to compare its direction in the phenylated acids with that in aliphatic acids.

Acid with $n_2=0$, $n_3=0$

From previous work,[4] it is known that in the visible region of the spectrum configurationally related methylphenylacetic acid (or ethylphenylacetic acid) and methylhexylacetic acid rotate in the same direction. From dispersion measurements on aliphatic acids, it had been concluded that the direction of rotation of these acids was determined by the direction of the partial rotation of the carboxyl group. From Table II it now may be seen that *the substitution of a phenyl group for a hexyl group does not alter the direction of rotation of the carboxyl group.* The dispersion curve can be expressed by a two term Drude formula, the first term determining the direction of the total rotation.

Acids with $n_2=0$ and $n_3>0$

Methylbenzylacetic acid is correlated to the methylheptylacetic acid of the same sign of rotation in the visible region and methylphenethylacetic acid is correlated similarly to methyloctylacetic acid. In the aliphatic acids the direction of rotation in the visible is determined by the partial

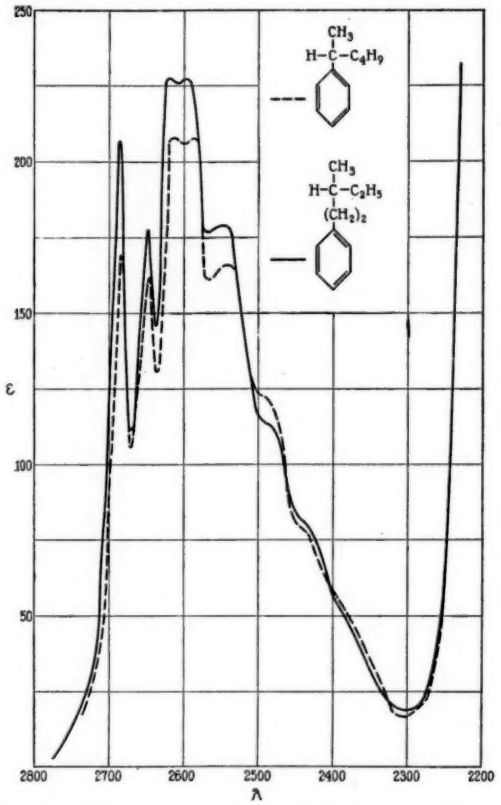

FIG. 2. Absorption spectra. Molecular extinction coefficients are plotted against wave-length expressed in A. Solvent = normal heptane.

rotation of the carboxyl group. In methylbenzylacetic acid likewise the partial rotation of the carboxyl group determined the direction of rotation in the visible. This conclusion follows from the normal course of the rotatory dispersion curve.

In methylphenethylacetic acid the partial rotation of the carboxyl group is also responsible for the direction of rotation in the visible since its dispersion curve may be expressed by two Drude terms, the first determining the direction of rotation in the visible.

Thus, in these two aliphatic acids and in the two phenylated acids correlated to them, the partial rotation of the carboxyl group has the same sign. It follows that in all phenylated acetic acids, irrespective of the value of n_3, the vicinal effect of the phenyl group is the same.

It is apparent from Table III that a one term formula is sufficient to represent the dispersion of a number of phenyl acids in the visible region. The constant of dispersion of this term is high ($\lambda_0^2 \leq 0.054$) and does not correspond to an active band. This high value results from the fact that the two main contributions are of opposite sign but their magnitudes are sufficiently different to permit the use of one term without appreciable error for a considerable wave-length interval. However, it is apparent from Fig. 2 that the dispersion in the ultraviolet deviates from the course required by a simple term. The low relative precision in the experimental determination did not warrant the calculation of a two-term formula.

THE EFFECT OF SUBSTITUTION OF A CYCLOHEXYL- FOR A HEXYL-GROUP IN THE SERIES OF DISTRIBUTED CARBOXYLIC ACIDS WITH n_1 AND $n_2 = 0$ AND HOMOLOGOUS WITH RESPECT TO n_3

From Table I it may be seen that the three acids of this series rotate in the same direction. (The opposite sign observed for ethylcyclohexylacetic acid is easily explained since the rotatory dispersion of this compound is anomalous, as mentioned above).

From the data given in Table VII and VIII, it may be seen that the dispersion of the three acids follows a normal course, thus indicating that the first partial rotatory contribution, which in this case in unquestionably that of the carboxyl group, determines the direction of the total rotation. Hence, here also the change in the distance of the cyclohexyl group from the asymmetric carbon atom remains without effect on the direction of rotation of the carboxyl group.

Rotatory dispersion of the phenylated hydrocarbons may be seen in Table IX. The order of magnitude of the observed angles did not warrant the calculation of a two-term formula, but it may be seen from the value of the dispersion constant obtained for a one-term formula from measurements in the visible region that the dispersion of ethylbutylphenylmethane is unquestionably anomalous.

The dispersion of methylethylbenzylmethane has been analyzed and has been expressed by a two-term formula. The constant of the first term corresponds to the second absorption region of the phenyl group (about λ1950). The low magnitude of the maximum molecular rotation is in

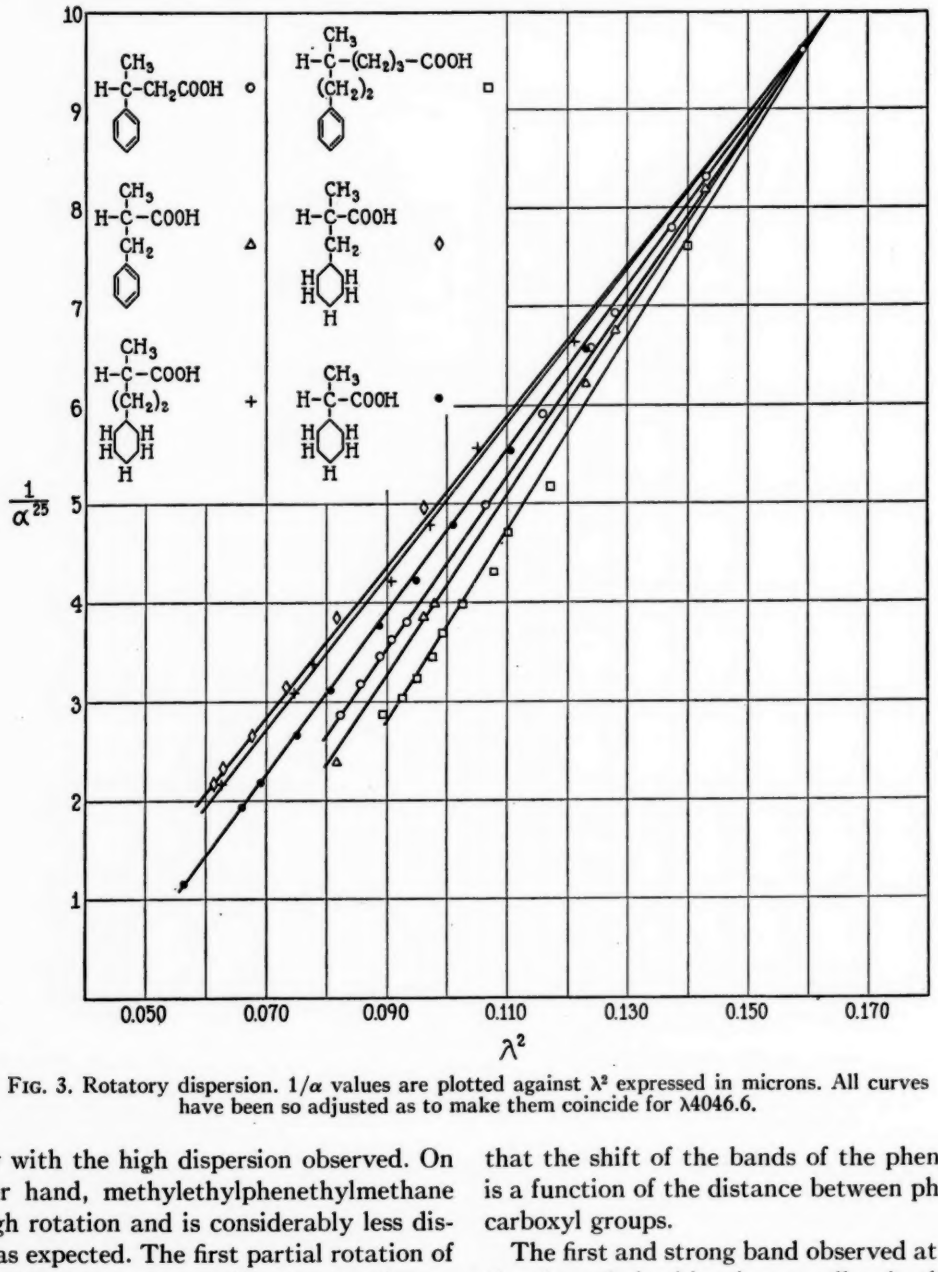

FIG. 3. Rotatory dispersion. $1/\alpha$ values are plotted against λ^2 expressed in microns. All curves have been so adjusted as to make them coincide for λ4046.6.

harmony with the high dispersion observed. On the other hand, methylethylphenethylmethane has a high rotation and is considerably less dispersive, as expected. The first partial rotation of the phenyl group, corresponding to the absorption region λ1950, is greater when the phenyl group is two carbon atoms removed from the asymmetric carbon than when it is either directly attached to, or one carbon atom removed from the asymmetric carbon atom.

ABSORPTION SPECTRA

Absorption spectra of most of the compounds may be seen in Fig. 1 and Fig. 2. It is apparent that the shift of the bands of the phenyl group is a function of the distance between phenyl and carboxyl groups.

The first and strong band observed at λ2688 in the phenethyl acid series as well as in the hydrocarbons has practically disappeared when there is only one intermediate carbon atom between carboxyl and phenyl groups. It is, however, apparent but weaker and slightly displaced (λ2684) when there are two intermediate carbon atoms between the chromophoric groups. On the other hand, the weaker band at λ2652 in the phenethyl series is stronger in the phenyl series and is located at λ2648. Two close bands are distinguish-

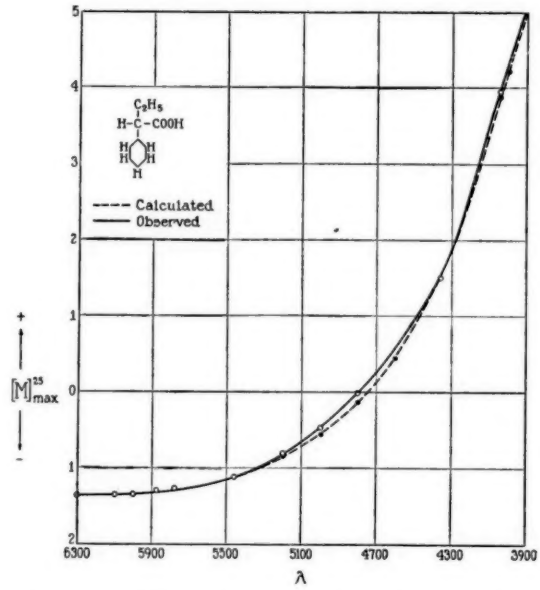

FIG. 4. Rotatory dispersion of ethylcyclohexylacetic acid. Maximum molecular rotations are plotted against wave-length expressed in A.

able in the phenethyl series at λ2620 and λ2596. There is only one band in the phenyl series at λ2588.

It should be noted that these effects are similar to those observed in the case of other phenyl derivatives. Absorption spectra obtained by reflexion in the solid state of a series of phenyl acid amides have been recently published.[5] The shifts of the bands and their changes in intensity run parallel with our determinations on analogous free acids in heptane solution. For convenience of comparison, data have been arranged in Table X.

TABLE X. *Absorption bands of phenylated acids and their amides.*

	I	II	III	IV	V	VI	VII
Phenylacetamide	2690 weak	2655 strong	—	2592	—	2520	2490
Phenylheptyl amide	2695 strong	2662 weak	2629	2610	2563	2550	2495
Methylphenylacetic acid	2684 weak	2648 strong	—	2588	—	2528	2492
Methylphenethylacetic, propionic, etc. acids	2688 strong	2652 weak	2620	2596	—	2552	2496

[5] T. Guilmart, Bull. Soc. Chim. France **5**, 1209 (1938).

SUMMARY

1. Shifts in the absorption bands in disubstituted carboxylic acids containing a phenyl group as a function of the distance of the two chromophoric groups (phenyl and carboxyl) were observed.

2. The first absorption region of the phenyl group furnishes no detectable rotatory contribution in acids of the above type.

3. Grounds are advanced for allocating the first rotatory contribution to the carboxyl group of these acids.

4. The phenyl as well as the cyclohexyl group in the acids of this group have a similar vicinal effect as a hexyl group with respect to sign of rotation.

EXPERIMENTAL

All acids were carefully fractionated and titrated. The rotatory measurements were carried out as previously described[6] and the same precision is claimed. For many compounds the precision attained in the ultraviolet region, on account of the small rotations observed, did not warrant the publication of individual measurements. Dispersion curves are given in Fig. 3 for those compounds where the inaccuracy of reading the values from the graph are of the same order of magnitude as the experimental errors. Individual measurements are given in tables, as in the past, for compounds for which the precision of the rotatory measurements was such that a graphical representation would have been of insufficient accuracy.

Absorption spectra were determined with a Hilger sector photometer.

[6] P. A. Levene, A. Rothen and R. E. Marker, J. Chem. Phys. **1**, 662 (1933).

The Near Ultraviolet Absorption of Substituted Benzenes*

A. L. SKLAR
The Catholic University of America, Washington, D.C.
(Received July 21, 1939)

The intensification of ultraviolet absorption in substituted over unsubstituted benzene is here attributed to the destruction of the sixfold symmetry of the benzene by the partial migration of an electron to the ring or out of it. Toluene, aniline, phenol, and fluorobenzene are treated. The electric moment produced by a migration of an electron from the radical into the benzene ring is calculated by the method of antisymmetric molecular orbitals and the extent of migration by a minimum condition. The results are in agreement with empirical data. It is concluded that a radical will produce a large intensification of the absorption if it has a low ionization potential, a pair of nonbonding P electrons, and a not too large ring-radical distance. On this basis the SH group is predicted to be very effective.

INTRODUCTION

IT is known empirically that the absorption of an organic compound is determined by two factors: first by its skeleton of unsaturated bonds, and second by the groups or radicals attached to the skeleton. The former has been treated, for certain cases, in a previous paper.[1] In order to consider the effect of the latter, we will compare the long wave-length electronic absorption of the compounds shown in Fig. 1.

It will be noticed that in these compounds the atoms attached to the ring are consecutive in the periodic table, yet the intensity of absorption of the longest wave-length electronic band does not vary monotonously. Toluene and fluorobenzene absorb weakly, only twice as much as unsubstituted benzene, while aniline and phenol absorb about twenty times as strongly as benzene.

The long wave-length electronic band of these compounds occurs at about 2700A. This band has been shown to be due in benzene to an $A_{1g} \rightarrow B_{2u}$ transition, forbidden[1, 2] by the sixfold symmetry of the ring. It appears in benzene only very weakly through the interaction with vibrations of a suitably low degree of symmetry (E_{1g}). The sixfold symmetry can also be disturbed by a substitution. A monosubstitution reduces the symmetry sufficiently to make the transition allowed to an extent which depends upon the interaction of ring and radical. In order to obtain an experimental measure of the effect of the substitution on the absorption one must, accordingly, compare the enhancement in the different substituted benzenes over benzene itself.

It is found empirically that a large intensification usually goes hand in hand with a large directing power.[3] The NH_2 and OH groups exert both effects outstandingly, whereas the action of CH_3 or of a halogen is feeble. That a connection exists between these two phenomena is to be expected, since the directing power has been shown[4] to be due to the effect of the substitution upon the symmetrical charge distribution of benzene. The difference between the two phenomena is principally that the directing effects depend upon the perturbation of the ground state (and also upon the group being attached) whereas the intensification depends upon the perturbation of both the ground and the excited state. The same fundamental mechanism, however, underlies both

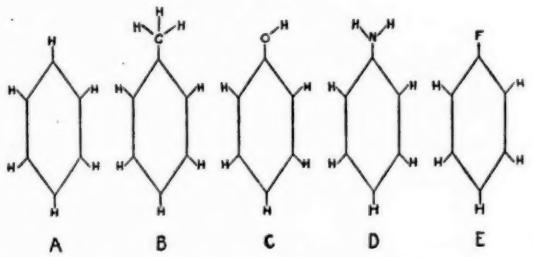

FIG. 1. A, benzene; B, toluene; C, phenol; D, aniline; E, fluorobenzene.

* This research was supported by a grant from the Penrose Fund of the American Philosophical Society.

[1] A. L. Sklar, J. Chem. Phys. **5**, 669 (1937).

[2] H. Sponer, G. Nordheim, A. L. Sklar and E. Teller, J. Chem. Phys. **7**, 207 (1939).

[3] Watson, *Modern Theories of Organic Chemistry* (Oxford, 1937).

[4] C. K. Ingold, Chem. Rev. **15**, 225 (1934). (Includes references to literature.)

phenomena, namely, a distortion of the sixfold symmetry of benzene.

In developing a theory of directing power it has been found necessary to consider at least two effects of the substitution: a distortion of charge distribution by induction and a migration of charge between ring and substituent.[5] The latter effect turned out to be the larger one.[6] These same two effects will influence the intensity of absorption.

The induction, caused by the polarity of the ring-radical bond, may be treated as a perturbation which will mix the energy levels. Two levels, only one of which is forbidden in combination with the ground state, may be mixed and make the forbidden transition partially allowed. It is, however, empirically clear that the inductive effect does not produce large intensifications.[7] This may be seen from the absorption of the anilinium ion, 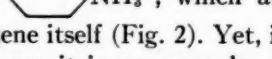 , which absorbs as weakly as benzene itself (Fig. 2). Yet, in view of its integral charge, it is an example, par excellence, of a large induction effect. On the other hand, aniline and phenol are considerably less polar than the anilinium ion and absorb twenty times as strongly. The first-mentioned molecules

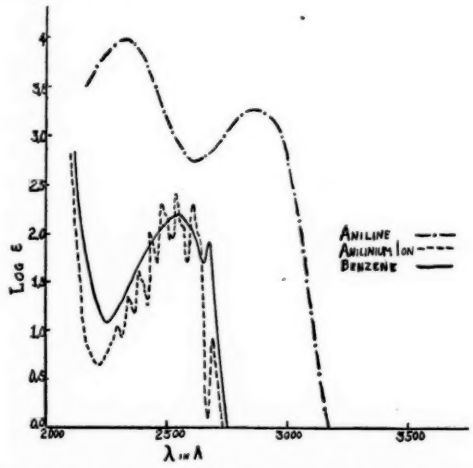

FIG. 2. Data from Landolt-Börnstein, Phys. Chem. Tab. Egb. I, 443, Egb. II, 665, Egb. III, 1377.

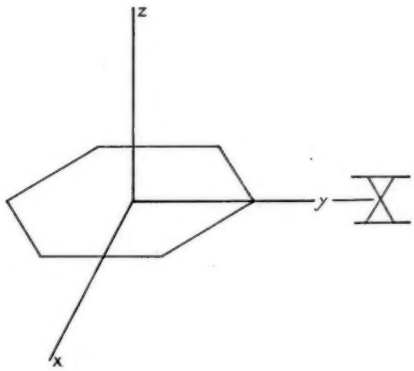

FIG. 3.

permit an electron to migrate into the ring, since the N and O atoms have pairs of electrons which do not form chemical bonds. The anilinium ion, on the other hand, does not allow migration into the ring since the ionization potential of the $C_6H_5NH_3^+$ ion is extremely large, due firstly to the positive charge and secondly to the fact that all the electrons (except the deeply bound $1S$) in the nitrogen are now bonding electrons. Furthermore, the Pauli principle forbids an electron to enter the NH_3^+ group. We must, accordingly, look to the migration effect for large intensifications in absorption. It will be shown in the following that this effect does give a satisfactory account of the absorption of the compounds in Fig. 1.

THE MIGRATING ELECTRONS

Since the only electrons in the substituent to interact with the absorbing ring electrons are those whose orbitals have a node in the benzene plane (P orbitals), we must first consider the state of the radical electrons. If the atom attached to the ring has nonbonding electrons, it is clear that these will migrate so much more easily than the bonding electrons, whose ionization potential is higher, that the migration of the latter can in this case be neglected.

The fluorine atom is in a

$$[(1S)^2(2S)^2(2P_x)^2(2P_z)^2(2P_y)]$$

state, where the direction of the axes may, without any loss in generality, be taken as in Fig. 3. That is, for fluorobenzene we may treat the migration of a pair of P_z electrons, since S, P_x, and P_y

[5] E. Hückel, Zeits. f. Physik **72**, 310 (1931); Sutton, Proc. Roy. Soc. **A133**, 668 (1931); C. K. Ingold, reference 4; G. W. Wheland and L. Pauling, J. Am. Chem. Soc. **57**, 2086 (1935).

[6] G. W. Wheland and L. Pauling, reference 5.

[7] This cannot yet be understood theoretically since a preliminary estimate for this effect does not turn out to be particularly small.

electrons do not interact with the P_z ring electrons. Oxygen, in its ground state, has only one pair of nonbonding P electrons. Only when the OH bond is coplanar with the ring does this pair become a P_z pair capable of migration into the ring, which will stabilize this orientation of the OH bond.[8] Accordingly for phenol as for fluorobenzene, we consider the migration of a pair of nonbonding P_z electrons.

The nitrogen atom also has a pair of nonbonding electrons. However, in the ground state of nitrogen this pair is in the $2s$ state and will not interact with the ring. In ammonia-like compounds, on the other hand, the nitrogen atom is not in its ground state[9] and the nonbonding pair may be taken to be in the state ζ_N where

$$\zeta_N=(0.35)^{\frac{1}{2}}\psi_{2S}+(0.65)^{\frac{1}{2}}\psi_{2P}, \qquad (1)$$

where the axis of the P function is the threefold axis of ammonia. This may be seen from the circumstance that if the pair were in the ψ_{2S} state, ammonia would form a right-angled tetrahedron. On the other hand, if the pair were in the ψ_{2P} state ammonia would be plane. The flattened pyramidal structure can only be obtained by a linear combination, the above coefficients having been adjusted to give the experimental angles. This probably overestimates the contribution of ψ_{2P} since the repulsion of the hydrogens could spread the tetrahedron without hybridizing the states. A more accurate estimate might well yield a somewhat lower value for the 0.65 in Eq. (1). The equilibrium position for the pyramidal axis is taken to be in a plane normal to the benzene plane, since the unbound pair migrates most easily in this configuration and hence effects the greatest decrease in energy. We may resolve the ψ_{2P} function of Eq. (1), which is referred to the pyramidal axis, along the axes shown in Fig. 3, since a P function transforms like a vector under a rotation. For aniline we accordingly treat the migration of a pair of electrons in a state ζ_N, where

$$\zeta_N=(0.35)^{\frac{1}{2}}\psi_{2S}+(0.65)^{\frac{1}{2}}[(0.15)^{\frac{1}{2}}\psi_{P_y}+(0.85)^{\frac{1}{2}}\psi_{P_z}]. \qquad (1')$$

[8] L. Pauling, J. Am. Chem. Soc. **58**, 94 (1936); O. R. Wulf and U. Liddel, J. Am. Chem. Soc. **57**, 1464 (1935).
[9] J. H. Van Vleck and A. Sherman, Rev. Mod. Phys. **7**, 199 (1935).

In toluene we have no unbound pair and accordingly the entire migration is due to the bound electrons, in agreement with the weakness of the effect in toluene. In the preceding cases the migration of bound electrons was neglected in comparison to that of the unbound. We must now investigate the orbitals for the C−C and the three C−H bonds. It is clear that the C−C orbital has no P_z component since the C−C bond is in the plane of the ring, and accordingly, the electrons forming this bond will not migrate into the P_z ring orbitals. The functions for the three CH bonds may be written

$$\zeta_j(\mathrm{CH})=\eta(\psi_{\mathrm{C}j}+\psi_{\mathrm{H}}),$$

where the normalization factor

$$\eta^2=2(1+\int\psi_{\mathrm{C}}\psi_{\mathrm{H}}d\tau),$$

ψ_{H} is the atomic orbital of the attached hydrogen atom and the $\psi_{\mathrm{C}j}$ are the sp^3 hybridized (tetrahedral) carbon functions:

$$\begin{aligned}
\psi_{\mathrm{C}_1}&=\tfrac{1}{2}\psi_{2S}+\tfrac{1}{2}\sqrt{3}(-\tfrac{1}{3}\psi_{P_y}+\tfrac{2}{3}\sqrt{2}\psi_{P_z}),\\
\psi_{\mathrm{C}_2}&=\tfrac{1}{2}\psi_{2S}+\tfrac{1}{2}\sqrt{3}(-\tfrac{1}{3}\psi_{P_y}+\sqrt{\tfrac{2}{3}}\psi_{P_x}-\tfrac{1}{3}\sqrt{2}\psi_{P_z}), \qquad (2)\\
\psi_{\mathrm{C}_3}&=\tfrac{1}{2}\psi_{2S}+\tfrac{1}{2}\sqrt{3}(-\tfrac{1}{3}\psi_{P_y}-\sqrt{\tfrac{2}{3}}\psi_{P_x}-\tfrac{1}{3}\sqrt{2}\psi_{P_z}).
\end{aligned}$$

All three pairs of electrons forming the CH bonds will migrate into the ring. However, each migrating pair will, in the first order, contribute independently to the electric moment. Now we will see later* that the contribution to the electric moment is proportional to the square of the coefficient of ψ_{P_z} in ζ. We may accordingly calculate the electric moment due to the migration of one pair of electrons from state ψ_{C_1} and then include a factor $1+(\frac{1}{2})^2+(\frac{1}{2})^2=1.5$ which takes care of the effect of the pairs of electrons in orbitals ψ_{C_2} and ψ_{C_3}. This factor, 1.5, makes the coefficient of ψ_{P_z} in ψ_{C_1} equal to unity, as it evidently must.

Effect of Migration on Intensity

The monosubstituted benzene is now treated like a diatomic molecule by the method of antisymmetric molecular orbitals. The single-electron orbitals are

$$\psi(\nu)=a\Phi(\nu)+b\zeta(\nu), \qquad (3)$$

* See reference 16.

where $\zeta(\nu)$ is the orbital of the radical attached to the ring which has been described above and $\Phi(\nu)$ is a ring function. Since the Pauli principle forbids the ring electrons to enter the radical we may set the b (Eq. (3)) equal to zero for the first six electrons and write their one electron orbitals: $\psi_m(\nu)=\varphi_m(\nu)$ where φ_m is an occupied orbital of the benzene ring. In the orbital for the pair of migrating electrons of the radical b is large compared to a. Since the pair can migrate into the various unoccupied benzene orbitals we must write the orbitals for the migrating electrons:

$$\psi(\nu)=\sum_j a_j\varphi_j(\nu)+b\zeta(\nu), \tag{4}$$

j runs over all unoccupied states. The extent of migration into φ_k is determined by $a_k/b=\lambda_k$.

Since the substituted benzene has a twofold axis of symmetry, the calculation is simplified if one uses as φ the real one electron functions $\varphi_{\pm k}$ where:

$$\left.\begin{aligned}\varphi_0&=\phi_0\\ \varphi_l&=(\phi_l+\phi_{-l})2^{-\frac{1}{2}}\\ \varphi_{-l}&=i(\phi_l-\phi_{-l})2^{-\frac{1}{2}}\\ \varphi_3&=\phi_3\end{aligned}\right\} l=1,\ 2. \tag{5}$$

The $\phi_{\pm l}$ are the usual complex functions[10]

$$\phi_{\pm l}(\nu)=(6\sigma_l)^{-\frac{1}{2}}\sum_{k=1}^{6}\exp\left[\frac{2\pi i}{6}(\pm l)K\right]K(\nu). \tag{6}$$

The simplification is due to the fact that φ_{-l} and φ_{+l} are respectively even and odd to a rotation by π about the twofold axis since this rotation changes l to $-l$ in the complex ϕ_l and also changes the sign of the P_z functions, $K(\nu)$. Accordingly electrons on the radical cannot enter φ_{-l} states since both ζ and the perturbing potential are even with respect to the rotation about the twofold axis.

The $\varphi_{\pm l}$ orbitals are:

$$\begin{aligned}\varphi_0&=(\ 6\sigma_0)^{-\frac{1}{2}}[\ \mathrm{I}+\mathrm{II}+\mathrm{III}+\ \mathrm{IV}+\mathrm{V}+\mathrm{VI}]\\ \varphi_1&=(12\sigma_1)^{-\frac{1}{2}}[2\mathrm{I}+\mathrm{II}-\mathrm{III}-2\mathrm{IV}-\mathrm{V}+\mathrm{VI}]\\ \varphi_{-1}&=(\ 4\sigma_1)^{-\frac{1}{2}}[\quad \mathrm{II}+\mathrm{III}\quad\ -\mathrm{V}-\mathrm{VI}]\\ \varphi_2&=(12\sigma_2)^{-\frac{1}{2}}[2\mathrm{I}-\mathrm{II}-\mathrm{III}+2\mathrm{IV}-\mathrm{V}-\mathrm{VI}]\\ \varphi_{-2}&=(\ 4\sigma_2)^{-\frac{1}{2}}[\quad \mathrm{II}-\mathrm{III}\quad\ +\mathrm{V}-\mathrm{VI}]\\ \varphi_3&=(\ 6\sigma_3)^{-\frac{1}{2}}[\ \mathrm{I}-\mathrm{II}+\mathrm{III}-\ \mathrm{IV}+\mathrm{V}-\mathrm{VI}],\end{aligned} \tag{7}$$

where I, II, $\cdots$ are the functions of the first, second $\cdots$ nucleus, here taken to be P_z hydrogen like functions, and[10]

$$\sigma_l=1+2s_1\cos\frac{2\pi}{6}l+2s_2\cos\frac{4\pi}{6}l+(-1)^l s_3,$$
$$s_k=\int I(\nu)\cdot\{I+K\}(\nu)d\tau. \tag{8}$$

The molecular orbitals for both the ground and excited state may now be written as products of eight single-electron orbitals. The product is expanded up to first powers in $\lambda_k=a_k/b$ and then antisymmetrized. The particular products of single-electron functions for the two levels[11] responsible for the 2700A bond has been previously discussed.[10] In the ground state, ψ^0, the six electrons fill the three lowest orbitals; namely, φ_0 and the doubly degenerate φ_1, φ_{-1}. The excited state, Ψ', is the lowest of the four states formed by exciting an electron from the doubly degenerate orbital φ_{+1}, φ_{-1} to the similarly degenerate φ_{+2}, φ_{-2}. The antisymmetrized molecular orbitals of the 8-electron system for the ground ($t=0$) and lower excited state ($t=1$) are

$$\Psi_t=(8!)^{-\frac{1}{2}}\sum_P(-1)^P P\Psi^t\chi^t, \tag{9}$$

where[12, 13]

[10] M. Goeppert-Mayer and A. L. Sklar, J. Chem. Phys. **6**, 645 (1938).

[11] It is easily checked that for the ground and excited state the proper products of real functions, φ_l, are the same as for the complex functions ϕ_l.

[12] In Eq. (9′) the first term in Ψ^0,

$$\{\varphi_0(1)\varphi_0(2)\varphi_1(3)\varphi_1(4)\varphi_{-1}(5)\varphi_{-1}(6)\}\zeta(7)\zeta(8),$$

corresponds to a state in which 6 electrons are in the ring and two on the substituent. The next terms

$$\{\varphi_0(1)\varphi_0(2)\varphi_1(3)\varphi_1(4)\varphi_{-1}(5)\varphi_{-1}(6)\}\varphi_j(7)\zeta(8)$$

correspond to states with seven electrons in the ring and one on the substituent. For these latter states it is not strictly correct to use for the φ_j the one electron orbitals made up of hydrogen like atomic functions for the neutral carbon atom calculated in Eq. (7), because the effective charge is different. However, the difference between the effective charges of a neutral benzene and of a negative benzene ion can be estimated by the rules of Zener and Slater, reference 13, to be only $1/6\times0.35$. Since this difference represents only 2 percent of the effective charge, we have simplified the calculation by neglecting this difference and writing, in Eq. (9′), all φ_k's with the same effective charge.

[13] C. Zener, Phys. Rev. **36**, 51 (1930); J. C. Slater, *ibid.* **36**, 57 (1930).

$$\Psi^0=\mu_0^{-\frac{1}{2}}\{\varphi_0(1)\varphi_0(2)\varphi_1(3)\varphi_1(4)\varphi_{-1}(5)\varphi_{-1}(6)\}$$
$$\times\{\zeta(7)\zeta(8)+\sum_j\lambda_j[\varphi_j(7)\zeta(8)+\zeta(7)\varphi_j(8)]\},\ j=2,3$$

$$\Psi'=\mu_1^{-\frac{1}{2}}\left\{\frac{1}{\sqrt{2}}\varphi_0(1)\varphi_0(2)[\varphi_1(3)\varphi_1(4)\varphi_{-1}(5)\varphi_2(6)-\varphi_{-1}(3)\varphi_{-1}(4)\varphi_1(5)\varphi_{-2}(6)]\right\}$$
$$\times\{\zeta(7)\zeta(8)+\sum_j\lambda_j[\varphi_j(7)\zeta(8)+\zeta(7)\varphi_j(8)]\},\ j=1,2,3 \quad (9')$$

$$\chi^0=\alpha_1\beta_2\alpha_3\beta_4\alpha_5\beta_6\alpha_7\beta_8,$$
$$\chi'=\alpha_1\beta_2\alpha_3\beta_4\frac{1}{\sqrt{2}}(\alpha_5\beta_6-\beta_5\alpha_6)\alpha_7\beta_8.$$

P is the permutation operator whose function is to antisymmetrize the complete molecular orbital and α, β are the two spin functions. μ_t is the normalization factor for Ψ^t.

Since φ_l is antisymmetrical and φ_{-l} symmetrical with respect to a rotation by π about the twofold axis of symmetry, it will be noticed that Ψ_0 and Ψ_1 are, respectively, symmetric and antisymmetric to this operation and, accordingly, the product $\Psi_0\Psi_1$ is antisymmetrical. It is then clear that the y component (cf. Fig. 3) of the electric moment vanishes, since the y coordinate is symmetrical to the rotation by π about the twofold axis. Furthermore, both Ψ_0 and Ψ_1 are symmetrical to a reflection in the plane of the ring and since the z coordinate is antisymmetrical to this operator, the z component of the electric moment also vanishes. Accordingly, the only contribution to the intensity is the moment:

$$\mathbf{x}=\int\Psi_0 x\Psi_1 d\tau. \quad (10)$$

We will now consider each of the twelve terms in the expanded form for the x component of the electric moment; of these one term does not contain λ_k, five are linear and six quadratic in λ_k. The term independent of λ_k evidently vanishes since it represents no interaction between ring and substitution; the transition accordingly remains forbidden. The terms linear in λ contain, as a factor, the overlap integral between ring and radical, $\int\varphi_k(\nu)\zeta(\nu)d\tau_\nu$. This reduces their magnitude to that of the quadratic terms, since λ_k, as will be seen later, is of the order of magnitude of the overlap integral. Accordingly, all nonvanishing terms in the electric moment are of the same order.

To simplify the evaluation of the integrals we break the 8! interchanges in Ψ_t into 8×7 groups of 6! each and write, for example:

$$\Psi_0=\mu_0^{-\frac{1}{2}}(8\cdot7)^{-\frac{1}{2}}\sum_{P'=1}^{56}(-1)^{P'}P'\{(6!)^{-\frac{1}{2}}\sum_{P''=1}^{6!}(-1)^{P''}P''$$
$$\times\varphi_0(1)\varphi_0(2)\varphi_1(3)\varphi_1(4)\varphi_{-1}(5)\varphi_{-1}(6)\chi'\}$$
$$\times\{\zeta(7)\zeta(8)+\sum_{j=2}^{3}\lambda_j[\varphi_j(7)\zeta(8)+\zeta(7)\varphi_j(8)]\}\chi'', \quad (11)$$

where

$$\chi'=\alpha_1\beta_2\alpha_3\beta_4\alpha_5\beta_6 \quad \text{and} \quad \chi''=\alpha_7\beta_8.$$

In the above expressions each set of 6! permutations involves interchanges of the six electrons in the benzene ring among themselves. The 56 groups of 6! terms involve an additional interchange of a radical electron either with a ring electron or with a second radical electron. Accordingly, the first bracket contains an antisymmetric molecular orbital of unsubstituted benzene of sixfold symmetry. If we further group the expression for the coordinate x into two parts:

$$x=\sum_{j=1}^{6}x(j)+\sum_{k=7}^{8}x(k), \quad (12)$$

the evaluations are further simplified since the first sum also has sixfold symmetry.

The individual products in the electric moment $\mathbf{x}$ (Eq. (10)) may now be calculated straightforwardly. The result is

$$\mathbf{x}=\frac{r}{2}\sigma_2^{-\frac{1}{2}}\left\{\frac{T}{\sqrt{3}}[(\sigma_1^{-\frac{1}{2}}\lambda_1+\sigma_2^{-\frac{1}{2}}\lambda_2)\sigma_1^{-\frac{1}{2}}(1-s_2)+\sqrt{2}(\sigma_1\sigma_3)^{-\frac{1}{2}}\lambda_3(1-\tfrac{3}{2}s_1+\tfrac{1}{2}s_2)]+\sigma_1^{-\frac{1}{2}}\lambda_2^2(1-s_2)+\sqrt{2}\sigma_3^{-\frac{1}{2}}\lambda_1\lambda_3\times(1-\tfrac{3}{2}s_1+\tfrac{1}{2}s_2)\right\}(\mu_0\mu_1)^{-\frac{1}{2}}, \quad (13)$$

where

$$T=\int I(\nu)\zeta(\nu)d\tau$$

in which $I(\nu)$ is the atomic orbital of the ring atom at the position of substitution and r is the carbon-carbon distance in benzene; for σ_k and s_k see Eq. (8). If one neglects the overlap integrals s_k, as is frequently but not necessarily done, the above expression is simplified to:

$$\mathbf{x} \backsimeq \frac{r}{2}\left\{\frac{T}{\sqrt{3}}(\lambda_1+\lambda_2+\sqrt{2}\lambda_3)+\lambda_2{}^2+\sqrt{2}\lambda_1\lambda_3\right\}(\mu_0\mu_1)^{-\frac{1}{2}}. \quad (13)$$

The oscillator strength, f, is given in terms of $\mathbf{x}$ by the expression:[14]

$$f=\left(\frac{8\pi^2mc}{3h}\right)\nu G\mathbf{x}^2, \quad (14)$$

where ν is the frequency in cm^{-1} and G is "the number of orbitals, belonging to the final level, with which any one orbital of the initial level can combine."

We have, then, evaluated the dependence of the intensity on the extent of migration, λ, and now proceed to consider the latter.

Extent of migration

The wave function for the migrating electron has been given in Eq. (4) as:

$$\psi(\nu)=\sum a_j\varphi_j(\nu)+b\zeta(\nu). \quad (4)$$

The magnitude of the migration from the radical orbitals $\zeta(\nu)$ into the ring orbital $\varphi_j(\nu)$ is determined by $\lambda_j=a_j/b$ which may be determined by minimizing the energy, U.

$$U=\int\psi(\nu)H_\nu\psi(\nu)d\tau, \quad (15)$$

where

$$H_\nu=\nabla_\nu+H_\varphi(\nu)+H_\zeta(\nu).$$

H_φ is the potential of the ring and H_ζ that of the radical. This is to be minimized under the constraint that $\int\psi^2d\tau=1$, which may be expanded by Eq. (4) into the condition that

$$\sum_j a_j{}^2+2b\sum_j a_jT_j+b^2=1, \quad (16)$$

where

$$T_j=\int\varphi_j(\nu)\zeta(\nu)d\tau.$$

From Eqs. (4) and (15) we obtain:

$$U=\sum_j a_j{}^2\left(\omega_j+2\sum_{k>j}\frac{a_k}{a_j}\int\varphi_kH_\zeta\varphi_jd\tau\right)+2b\sum a_j\rho_j+b^2\omega, \quad (17)$$

where

$$\rho_j=\tfrac{1}{2}\left\{\int\varphi_jH_\varphi\zeta d\tau+\int\zeta H_\zeta\varphi_jd\tau+T_j(W_j+W)\right\},$$

$$W_j=\int\varphi_j(\nabla+H_\varphi)\varphi_jd\tau\,;\quad W=\int\zeta(\nabla+H_\zeta)\zeta d\tau\,;$$

$$\omega_j=W_j+\int\varphi_jH_\zeta\varphi_jd\tau\,;\quad \omega=W+\int\zeta H_\varphi\zeta d\tau.$$

ω is the negative of the lowest ionization potention of the radical in the compound while ω_k is effectively the electron affinity of the benzene ring in the compound.

Equations (16) and (17) yield as minimal condition:

$$\sum_j\left[\left(a_j\omega_j+b\rho_j+\sum_{k>j}a_k\int\varphi_kH_\zeta\varphi_jd\tau\right)-\mu(a_j+bT_j)\right]\delta a_j+\left[(b\omega+\sum_j a_j\rho_j)-\mu(b+\sum a_jT_j)\right]\delta b=0, \quad (18)$$

where μ is an undetermined multiplier of La Grange.

Since the magnitude of the migration, λ_k, is not very large, we may take the a_k's to be small whereas b is approximately unity. The overlap integral, T_k, is also a small quantity. Furthermore, $\int\varphi_kH_\zeta\varphi_jd\tau$ is very small for $k\neq j$ since φ_k is strictly orthogonal to φ_j. We now neglect in Eq. (18) all terms which are second order and keep only those terms which are zero and first order in small quantities. Eq. (18) then simplifies to

$$\sum_j[(a_j\omega_j+b\rho_j)-\mu(a_j+bT_j)]\delta a_j+[b\omega-\mu b]\delta b=0, \quad (18')$$

which yields the extent of migration λ_j to be:

$$\lambda_j=\frac{\rho_j-T_j\omega}{\omega-\omega_j}. \quad (19)$$

[14] R. S. Mulliken, J. Chem. Phys. **7**, 15 (1939).

It is clear, as was to be expected, that λ_j is determined by $(\rho_j-\tau_j\omega)$, the interaction energy of the ring and radical, and by $(\omega-\omega_j)$, the difference between the ionization potential of the radical and the electron affinity of the ring.

Since Eq. (19) yields the extent of migration and Eqs. (13) and (14) give the effect on the oscillator strength, we may now proceed to a numerical evaluation of the latter.

Numerical Calculations

As can be seen from Eq. (19), in order to determine λ_k, and accordingly the intensity, we must evaluate ρ_k, τ_k, ω_k and ω. In order to calculate ρ_k we must first evaluate the interaction integrals $\int\varphi_k H_\varphi\zeta d\tau$ and $\int\zeta H_\zeta\varphi_k d\tau$. A direct integration would be extremely tedious even with hydrogen-like wave functions, since the effective charge of the ring atoms is different from that of the radical atoms. However, an interaction integral involving two different effective charges may be rather well approximated as follows:

$$\int\varphi_k(z_1)H\zeta(z_2)d\tau \backsimeq \tfrac{1}{2}T_k(z_1z_2) \times\left[\frac{\int\varphi_k(z_1)H\zeta(z_1)d\tau}{T_k(z_1z_1)}+\frac{\int\varphi_k(z_2)H\zeta(z_2)d\tau}{T_k(z_2z_2)}\right], \quad (20)$$

where the parameters z_1 and z_2 are the effective charges of the hydrogen-like functions φ_k and ζ, and

$$T_k(z_mz_n)=\int\varphi_k(z_m)\zeta(z_n)d\tau. \quad (21)$$

The justification for the above approximation is that at large distances an integral involving wave functions of two different nuclei, $\int\psi_a H_a\psi_b d\tau$, is quite well approximated by the product of the overlap integral, $\int\psi_a\psi_b d\tau$ times the integral $\int\psi_c H_a\psi_c d\tau$ where ψ_c is a function of a hypothetical nucleus located at the place where the functions ψ_a and ψ_b overlap most. The latter integral, which is a Coulomb integral, is relatively insensitive to the form of the wave function. In other words, the two nuclei integrals should for a fixed internuclear distance be proportional to the overlap integral T_k; as the screening constant is varied this is indeed found to be the case in the range of values which enter these calculations. Therefore we may write

$$\int\varphi_k(z_1)H_\varphi\zeta(z_2)d\tau=T_k(z_1z_2)\int\psi_c H_\varphi\psi_c d\tau, \quad (20')$$

and furthermore,

$$\int\varphi_k(z_1)H_\varphi\zeta(z_1)d\tau=T_k(z_1z_1)\int\psi_c' H_\varphi\psi_c' d\tau,$$

$$\int\varphi_k(z_2)H_\varphi\zeta(z_2)d\tau=T_k(z_2z_2)\int\psi_c'' H_\varphi\psi_c'' d\tau.$$

Since the Coulomb integral $\int\psi_c H_\varphi\psi_c d\tau$ does not depend critically upon the form of the wave function, we may write

$$\int\psi_c H_\varphi\psi_c d\tau = \tfrac{1}{2}\left\{\int\psi_c' H_\varphi\psi_c' d\tau+\int\psi_c'' H_\varphi\psi_c'' d\tau\right\}. \quad (20'')$$

Eqs. (20'), (20'') and (20''') yield Eq. (20).

The overlap integral $T_k(Z_1Z_2)$ may be expanded by means of Eq. (7). Since the overlap decreases exponentially, only the overlap of wave functions on neighboring nuclei will be treated in the numerical evaluations, although the preceding equations have included all overlaps. The $T_k(z_1, z_2)$ then take the form

$$\begin{aligned} T_1&=(3\sigma_1)^{-\frac{1}{2}}T(z_1z_2),\\ T_2&=(3\sigma_2)^{-\frac{1}{2}}T(z_1z_2),\\ T_3&=(6\sigma_3)^{-\frac{1}{2}}T(z_1z_2), \end{aligned} \quad (22)$$

where $T(z_1, z_2)=\int I(\nu)\zeta(\nu)d\tau$; $I(\nu)$ being the function of the ring atom at the position of substitution.

The integral $T(z_1, z_2)$ had been evaluated for the special case when $z_1=z_2$.[15]

$$\epsilon^{-1}T(z_1z_1)=\frac{1}{120}e^{-\rho/2}\{\rho^3+12\rho^2+60\rho+120\}$$

where $\rho=zr$. The more general case, $z_1\neq z_2$, can be evaluated fairly simply by integration in

[15] *Handbuch der Physik* (Springer, 1933), Vol. XXIV$_1$, p. 643.

elliptic coordinates, yielding

$$\epsilon^{-1}T(z_1z_2)=\frac{(z_1z_2)^{5/2}}{32\pi}\int r_1\sin\theta_1\cos\varphi_1 \times e^{-z_1r_1/2}r_2\sin\theta_2\cos\varphi_2 e^{-z_2r_2/2}d\tau$$
$$=\frac{e^{-P}}{4m^5}\left[\frac{2(\sigma_1\sigma_2)}{\sigma_1+\sigma_2}\right]^5\{(P^3+5P^2+12P+12)m^2 \times[m\cosh m-\sinh m] -P^2(P+1)[m(m^2+12)\cosh m -(5m^2+12)\sinh m]\}, \quad (23)$$

where $m=\frac{1}{2}(\sigma_1-\sigma_2)$, $P=\frac{1}{2}(\sigma_1+\sigma_2)$, $\sigma_k=\frac{1}{2}z_kR$, R=interatomic distance in atomic units, and ϵ=the coefficient of P_z in $\zeta(\nu)$.[16]

In the evaluation one may take the sum of atomic radii as the internuclear distances.[17] The effective charges of atoms, z_k, has been obtained by Zener[18] in two ways. First, they have been computed for the ground state and secondly estimated from the ionization potential. Since these two methods yield values within five percent of one another, we have used the mean of the two results. In calculating the extent of migration the above values for z are to be diminished by 0.06, as discussed in reference 12. The values for z thus obtained are $z_C=3.2$; $z_N=3.9$; $z_O=4.5$; $z_F=5.2$.

Equation (23), with these z's, then yields values for $\epsilon^{-1}T(z_1z_2)$.

In order to evaluate the integrals occurring in ρ_k one must now write down the potentials H_φ and H_ζ for the radical electron. The H_φ is taken to be the potential of a neutral benzene ring while H_ζ is that of the singly positively charged substituent. That is, we consider the radical as being brought up to its equilibrium position under the restriction that no migrations occur and then picture an electron as taken out from the radical. This electron is then permitted to distribute itself in the molecular field which consists of the neutral benzene ring and the ionic substituent.

With Eq. (20) and the above described H_φ and H_ζ the integrals $\int\zeta H_\varphi\zeta d\tau$; $\int\varphi_kH_\zeta\varphi_kd\tau$; $\int\zeta H_\zeta\varphi_kd\tau$; and $\int\varphi_kH_\varphi\zeta d\tau$ may be evaluated from previously tabulated integrals,[19] the first two being in terms of the Coulomb and Coulomb penetration integrals, the latter two being given by the hybrid Coulomb-exchange and its corresponding penetration integral. The only quantities now missing for the determination of λ_k are the augmented ionization potentials ω_k and ω.

The ω is the ionization potential of the radical in the compound and may, with sufficient accuracy, be taken to be the ionization potential of RX, where R is an alkyl group and X is, respectively, CH_3, NH_2, OH or F. The ionization potentials of amines, alcohols and even ethane have, unfortunately, not yet been reported. Accordingly, we have tentatively approximated the ω by the ionization potential of CH_4, NH_3, H_2O and CH_3F. The ionization energies of the first three compounds have been measured[20] to be 14.5, 11.1, and 12.5 volts, respectively. That of CH_3F, however, had to be obtained from the measured values for the other methyl halides. This was done by roughly extrapolating the relatively small difference between the ionization energy of CH_3X and of X atoms. Fifteen volts was tentatively estimated for the ionization energy of methyl fluoride. This is sufficiently accurate for our purposes, since in the fluoride case the ionization energy does not enter critically into the intensity as it does in the case of phenol and aniline. A higher value for the ionization energy of CH_3F would not affect the calculation but a value much below 15 volts (say 12 volts) would seriously change matters. This latter is, however, highly improbable.

$$W_k=\int\varphi_k(\nabla+H_\varphi)\varphi_kd\tau$$

as well as W can easily be expanded in terms of previously calculated integrals.[19] It need only be recalled that H_φ is the potential of a neutral ring. The W_k, hence, contain an electron affinity term and the penetration integrals Q_{kk} and $Q_{k,\,k+1}$ of reference 19 (there Eq. (17)). Since Q represents

[16] Since T_k and each term in ρ_k is proportional to ϵ (the ratios in the bracket of Eq. (20) are independent of ϵ) the λ_j's are proportional to ϵ. It is hence clear that the electric moment is homogeneous of the second degree in ϵ.

[17] L. Pauling and M. L. Huggins, Zeits. f. Kryst. **87**, 205 (1934).

[18] C. Zener, Phys. Rev. **36**, 51 (1930).

[19] A. L. Sklar and R. H. Lyddane, J. Chem. Phys. **7**, 374 (1939).

[20] H. Sponer, *Molekülspectren* (Springer, 1935), Table 24.

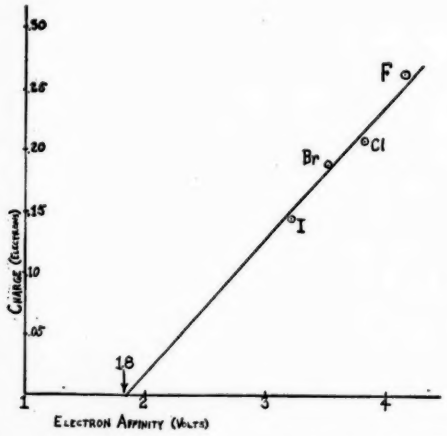

FIG. 4. Electron affinities are taken from J. E. Mayer and L. Helmholtz, Zeits. f. Physik **75**, 19 (1932); interatomic distances from Landolt-Börnstein, Phys. Chem. Tab. Egb. III, 113.

the energy of penetration within a neutral carbon atom, it is certainly very small for large distances. In fact all Q_{ik} except Q_{11} and Q_{12} turn out to be negligible, the W_k reducing to

$$W_k=\left\{E+2\left(1+2s_1\cos\frac{2\pi}{6}k\right)^{-1}\times\left(Q_{22}+Q_{12}\cos\frac{2\pi}{6}k\right)\right\}, \quad (24)$$

where

$$E=\int I(\nu)(\nabla+H_I)I(\nu)d\tau,$$

in which

$$H_\varphi=\sum_{k=1}^{6}H_k.$$

E may be taken to be the electron affinity of the methyl radical (or more correctly, that of the secondary propyl radical). The electron affinity of the methyl radical has not been measured. It can, however, be estimated by the following extrapolation method.[21] In the series of compounds CH_3X, the greater the electron affinity of the X atom, the larger will be the dipole moment of the C−X bond. In fact, no moment should result if the electron affinity of CH_3 and X were the same. One can, accordingly, estimate the electron affinity of the CH_3 radical by plotting the charge on the X atom against the electron affinity of X and then extrapolate to zero charge. The plot, shown in Fig. 4, yields 1.8 volts for the electron affinity of the CH_3 radical.

The calculation may be somewhat refined by including in H_φ and H_I the electrostatic energy of the dipole associated with the benzene radical bond. This correction has been applied in the numerical computations, but was found to be quite small.

The above data and Eq. (20) yield λ_k and accordingly, from Eq. (13), the electric moment of the transition. The latter and Eq. (14) give values for the oscillator strength, f. The results are tabulated in Table I.

COMPARISON WITH EXPERIMENT

A comparison of the theoretical results with experiment may be obtained from measurements of the extinction, ϵ, in solution.[22] The area under the extinction curves yields $\int\epsilon d\nu$; $\nu=1/\lambda$. This immediately gives values for the oscillator strength in the condensed phase $\bar{f}$:[23]

$$\bar{f}=\frac{n}{N}\frac{c^2m}{\pi e^2}10^3\int\epsilon d\nu, \quad (25)$$

where n is the index of refraction of the solution, N is Avogadro's number.

Since we have treated the molecules as independent, a comparison of the calculated values should be made with the f values in the vapor.

The correction[21] for the Lorentz-Lorenz force has been applied to arrive at the f values in the vapor.

$$f=\left(\frac{3}{n_0^2+2}\right)^2\bar{f}. \quad (26)$$

TABLE I. *Since experimental values for* C_6H_5F *are not available, the experimental data in the table are the values for the next halogenated benzene,* C_6H_5Cl.

COMPOUND	THEOR. f	EXPT. $\bar{f}$ Measured in solution	EXPT. f Corrected to vapor
$C_6H_5CH_3$	5	8	5
$C_6H_5NH_2$	140	150	88
C_6H_5OH	60	120	75
C_6H_5F	3	(6)*	(4)*

[21] The author is indebted to Professor J. E. Mayer for discussions on this matter.

[22] K. L. Wolf and Herold, Zeits. f. physik. Chemie **B13**, 201 (1931).

[23] N. Chako, J. Phys. Chem. **2**, 644 (1934).

The experimental values tabulated in Table I have been obtained from the measurements of Wolf and Herold.[22] Both $\bar{f}$, the value in solution, and f, the corresponding value in vapor, are given in the table.

Conclusions

A very precise numerical comparison between calculated intensities and experimental ones cannot, at present, be made. This is due, among other things, to the fact that the experimental values were obtained in solution and that the correctness of the Lorentz-Lorenz correction has not been tested experimentally.[24] Furthermore, several experimental data used in the theoretical calculation have only been estimated or measured roughly. However, the values are probably not far off.

One can say from Table I that the migration effect does give a satisfactory account of the intensification of substituted benzenes both in magnitude and in the variation from one group to another. The calculation does show that aniline and phenol are very strongly and that toluene and fluorobenzene are weakly absorbing.

The physical mechanism behind the above order may briefly be summarized. The weakness of the fluorobenzene is to be attributed to the electro-negativity of the fluorine atom which causes the ionization potential ω to be large. That toluene also absorbs weakly may be traced to the circumstance that in CH_4 there are no nonbonding electrons (except the tightly bound $1S$) and accordingly the ionization energy of the carbon atom is augmented by the binding energy of the CH bond. Furthermore, the P_z electrons are shared by the C and H atoms and hence are further from the ring.

The NH_2 and OH groups each have a pair of unbound electrons. Now since NH_3 has a considerably lower ionization potential than H_2O one would expect $C_6H_5NH_2$ to be much more strongly absorbing than C_6H_5OH. That aniline absorbs only very little more than phenol may, at least in part, be attributed to the character of the pair of nonbonding electrons. In the OH radical the pair, as previously discussed, is in a P_z state whereas in the NH_2 radical the pair is partially in an S and partially in a P_z state. Since an S electron on the radical will not interact with the P_z ring electrons, the above effect tends to diminish the effectiveness of the NH_2 group.

A large intensification should be expected for those substituted benzenes in which the radical has a small ionization potential, a pair of unbound P_z electrons, and small a ring-radical distance. One of the most favorable cases should be the mercaptan group S−H since the sulfur atom has the same electron configuration (except that its outer shell is an M shell) as oxygen and since the ionization energy of H_2S is considerably below that of H_2O. The effect of the slightly larger atomic radius of sulfur is compensated by the larger extension of the charge distribution of its P_z state. The absorption of the thio-phenols has not been measured, but it is now under investigation.

In conclusion I would like to express my thanks to Professor K. F. Herzfeld for stimulating and directing this research and to Dr. R. H. Lyddane for checking the calculations.

[24] Results of Victor Henri and Lucy W. Pickett (J. Chem. Phys. **7**, 439 (1939)) seem to indicate that the change from liquid to vapor is much less than that given by Eq. (26).

The Infra-Red Absorption by Hydrogen Selenide, Deuterium Selenide and Deutero-Hydrogen Selenide

DONALD M. CAMERON, WILLIAM C. SEARS AND HARALD H. NIELSEN
Mendenhall Laboratory of Physics, Ohio State University, Columbus, Ohio

(Received August 3, 1939)

The infra-red spectra of H_2Se, D_2Se and HDSe have been measured and the positions of the three fundamental frequencies for each molecule have been determined. These are; for H_2Se $\nu_1=2260$ cm^{-1}, $\nu_2=1074$ cm^{-1}, $\nu_3=2350$ cm^{-1}; for D_2Se, $\nu_1=1630$ cm^{-1}, $\nu_2=745$ cm^{-1}, $\nu_3=1696$ cm^{-1}; for HDSe, $\nu_1=1691$ cm^{-1}, $\nu_2=905$ cm^{-1} and $\nu_3=2352$ cm^{-1}. Interpretation of the observed data has led to the adoption of an obtuse model where the H—Se—H bond angle is slightly in excess of 90°. The H—Se distances are evaluated to be 1.6A and the H—H distance is equal to 2.3A. The product relations of Redlich are made use of as a verification of a correct assignment of frequencies and for a correct determination of the band centers.

I. INTRODUCTION

THE absorption spectra of the hydrides and deuterides of oxygen and sulphur have been studied quite extensively in the infra-red[1] so that the fundamental vibration frequencies of these molecules is known with considerable certainty. Considerable progress has, moreover, been made recently toward a rotational analysis of these spectra; particularly is this true for the bands in the spectrum of water vapor.[2] Concerning the infra-red spectra of the selenium hydrides very little has hitherto been known. An exploratory prism curve of the spectrum of H_2Se was carried out by Mischke[3] and more recently Raman lines due to H_2Se, D_2Se and HDSe have been reported by Dadieu and Engler.[4] We have considered these preliminary results of sufficient interest to warrant a further investigation of these spectra. Our measurements have been carried out under high dispersion in order that the character of each band might be determined.

II. EXPERIMENTAL

A. Preparation of the H_2Se, D_2Se and HDSe

The gas, hydrogen-selenide, is readily prepared by allowing distilled water to react with aluminum selenide, the reaction taking place as follows: $Al_2Se_3+6H_2O\rightarrow 3H_2Se+2Al(OH)_3$. The aluminum selenide alloy may be prepared by carefully heating together approximately combining weights of finely ground selenium and aluminum in a sealed Pyrex tube over a Bunsen flame. Prior to the sealing of the tube, the air had been removed by evacuation. The combination between the metals takes place as indicated by the equation $2Al+3Se\rightarrow Al_2Se_3$. Four different samples of gas were prepared, one using ordinary distilled water, a second using 99.8 percent D_2O, a third using 20 percent heavy water and a fourth from 80 percent heavy water. The first two samples were nearly pure gases while the third and fourth contained approximately 50 percent H_2Se, 40 percent HDSe and 10 percent D_2Se and 10 percent H_2Se, 40 percent HDSe and 50 percent D_2Se, respectively. The purpose of the samples three and four was to make available mixtures of gases rich in HDSe, but containing little D_2Se and H_2Se, respectively, so that the absorption bands due to the hybrid molecule which lay in regions where also H_2Se and D_2Se had absorption bands might be investigated with little falsification due to the presence of these. In all cases before samples of gas were generated the alloy was dried carefully to drive off all occluded water vapor. This precaution is extremely important when preparing pure D_2Se.

B. The spectrometer and the absorption cells

The spectrometer used to make these measurements is the same used by other workers in this

[1] E. K. Plyler and W. W. Sleator, Phys. Rev. **37**, 1493–1507 (1931); E. K. Plyler, Phys. Rev. **39**, 77 (1932); A. D. Sprague and H. H. Nielsen, J. Chem. Phys. **5**, 85 (1937); A. H. Nielsen and H. H. Nielsen, J. Chem. Phys. **5**, 277 (1937).

[2] P. Cross, Phys. Rev. **47**, 7 (1935); R. Mecke, Zeits. f. Physik **81**, 313, 445, 465 (1933); H. M. Randall, D. M. Dennison, Nathan Ginsburg and L. R. Weber, Phys. Rev. **52**, 160 (1937).

[3] Walter Mischke, Zeits. f. Physik **106**, 67 (1931).

[4] Armi Dadieu and Wolf Engler, Wiener Anzeiger **128**, 13 (1935).

laboratory. Many of the absorption bands in the spectra of these gases lie in regions which have hitherto been almost inaccessible for measurements, namely in the region of the intense CO_2 fundamental band near 4.3μ and in the region of the very intense water vapor fundamental absorption band near 6.2μ. It was consequently found necessary to surround the optical parts of the spectrometer by a box which was made as nearly air tight as possible. When measurements were to be made near 4.3μ, trays containing Ascarite were placed inside to remove as much of the atmospheric carbon dioxide as possible and when measurements near 6.0μ were to be made the trays were filled with phosphoric anhydride to remove as completely as possible all of the atmospheric water vapor. To hasten the removal of the atmospheric gases from the enclosed air the diffusion was enhanced by operating a fan placed inside the box. In all cases it has been found that enough of the CO_2 or water vapor can be removed so that no falsification of the absorption patterns under investigation was detectable.[5]

[5] The falsification of absorption patterns of bands overlapping badly with atmospheric bands has been especially annoying in the past. The intensity of many of the water vapor lines has necessitated the use of widened spectrometer slits so that enough radiant energy might pass through to give measureable galvanometer deflections. This has made resolution of many such bands practically impossible so that mere envelopes have had to suffice. Almost universally such bands have been found to have an apparent rotational structure which shows itself to be a mirror image of the water vapor absorption pattern, i.e., where ever a strong water vapor line occurs there will manifest itself an apparent deep transmission window in the absorption band of the molecule under investigation. Several explanations have been given for this, but the real reason we believe to be the following one. When the spectrometer is correctly adjusted for measurements in a certain spectral region all higher order radiations should have been eliminated either by a filter or by a monochromator device. It is, however, seldom feasible to remove this higher order radiation completely so that in general about 5 percent of the total galvanometer deflection will be due to higher order. If now a cell containing gas which absorbs in the region for which the spectrometer is set, is placed in the light beam there will be only very slight falsification by these 5 percent if at this setting there is no atmospheric line. Where there occurs a strong atmospheric line, however, all of the first-order radiation may be absorbed by the atmosphere so that the total galvanometer deflection will be due to the 5 percent of higher radiation. This radiation will in general not be absorbed by the molecule being investigated so that at such a point there may very well occur an apparent transmission of nearly 100 percent. It has been possible to remove enough of the atmospheric gases in the above manner so that the second-order radiation represents a rather negligible amount of the total galvanometer deflection even where the atmospheric absorption is most intense.

For the measurements three echelette gratings were made use of, one ruled with 3600 lines per inch for the region near 4.3μ, a second ruled with 2000 lines per inch for the region near 6.5μ and a third with 900 lines ruled to the inch for the region 8.0μ to 14.0μ.

Two lengths of absorption cells were required, one 10 cm long filled to atmospheric pressure and used for the measurements made on the pure gases, and a second 27 cm long filled to atmospheric pressure and used when measurements on the HDSe bands were made. In all cases it was found possible to operate with slit widths equivalent to about 0.5 cm^{-1}. Deflections were recorded with the absorption cell in the light path and with the cell out of the light path at intervals on the circle of the spectrometer equivalent to the above slit widths so that the data could be recorded in terms of percent absorbed.

C. Absorption bands due to H_2Se and D_2Se

Two regions of intense absorption were located when the spectrum of H_2Se was measured with a prism spectrometer of the Wadsworth type. These fall near 4.3μ and 9.0μ. A third peak of less intensity was found near 2.8μ and a much less intense band was detected at 2.1μ. Two regions of intense absorption were likewise found in the prism spectrum of deuterium selenide, these falling near 6.0μ and 13.0μ. Only the regions of most intense absorption by these molecules have been studied under high dispersion; i.e., for H_2Se the regions near 4.2μ and 9.0μ and for D_2Se the bands near 6.0μ and at 13.0μ.

The 4.2μ region in H_2Se *and the 6.0μ region in* D_2Se.—The 4.3μ absorption region in H_2Se is resolvable into a group of sharp lines on the high frequency side of a strong central line and into a set of double lines on the low frequency side. This region is believed to consist of two overlapping bands. The one of these which has the broad gathered Q branch is interpreted to be the fundamental band ν_3, using the notation of Dennison.[6] Its center is taken to be 2350 cm^{-1}. The other of these bands does apparently not have any strong central group of lines and it is believed to be the other fundamental ν_1, the center of which appears to be at 2260 cm^{-1}. The separations between principal absorption peaks

[6] D. M. Dennison, Rev. Mod. Phys. 3, 280 (1931).

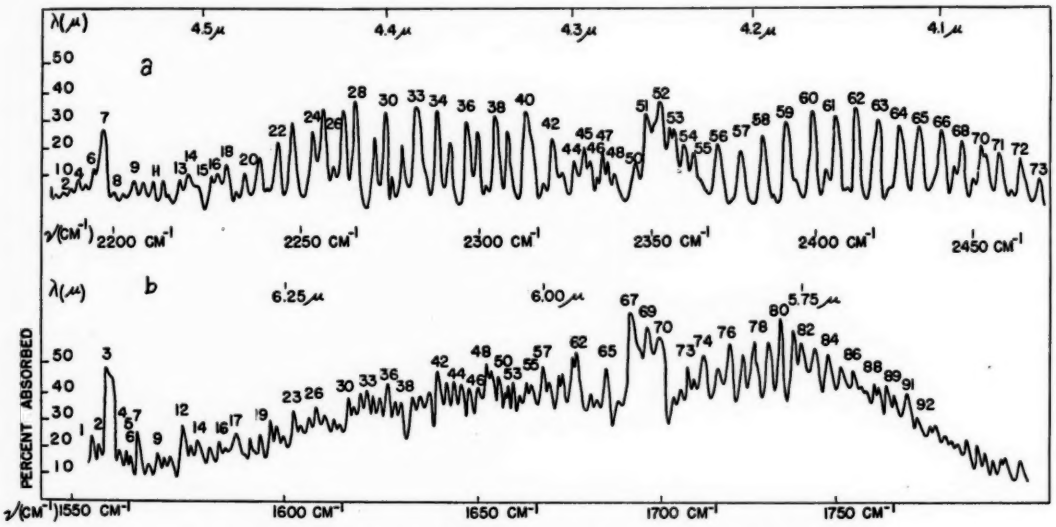

FIG. 1. (a) Absorption by H_2Se at 4.3μ. (b) Absorption by D_2Se at 6.0μ.

is very nearly the same for both bands and is on the average equal to about 7.6 cm^{-1}.

The 6.0μ absorption region in the D_2Se spectrum is undoubtedly the counter part of the 4.3μ bands in the spectrum of H_2Se and to which it bears a striking resemblance. As in the preceding case, resolution shows this region to consist of a set of essentially sharp lines on the high frequency side of a central line and into a set of double lines on the low frequency side. These are again believed to be the fundamental bands ν_3 and ν_1 with centers lying close to 1696 cm^{-1} and 1630 cm^{-1} and on the average the rotational lines in the two bands are separated from each other by an interval of about 3.7 cm^{-1}. The absorption patterns of these regions are shown respectively in Fig. 1, (a) and (b), original circle settings having been replaced by abscissae of wave-lengths and frequencies. In Tables I and II are set down the frequency positions of the principal absorption lines as determined from these measurements.

The 9.0μ region in H_2Se *and the 13.0μ region in* D_2Se.—The region near 9.0μ is the most intense in the spectrum of H_2Se and must almost certainly be attributed to the fundamental deformation frequency ν_2. When examined under high dispersion and resolving power it splits up into a rotational structure which is quite irregular in appearance near the middle of the band, but which at the extremities consists of rather sharp lines separated quite uniformly from each other by a spacing which on the average is close to 7.8 cm^{-1}. This band has no strong central line (as is the case in ν_3 at 2350 cm^{-1}) but there is a noticeable dip in the envelope of the absorption pattern near 1074 cm^{-1} and this point is identified as the center. A more exact determination of the center can hardly be affected before a complete rotational analysis of this region is feasible.

The corresponding region in the spectrum of D_2Se lies near 13.0μ and when it is examined under high dispersion it resembles in general structure and appearance the 9.0μ band in the H_2Se spectrum. As in that spectrum so also here

TABLE I. *Frequency positions of principal* H_2Se *absorption lines.*

Line No.	Frequency Position	Line No.	Frequency Position	Line No.	Frequency Position	Line No.	Frequency Position
1	2184.0 cm^{-1}	19	2232.7 cm^{-1}	37	2299.6 cm^{-1}	55	2362.5 cm^{-1}
2	2186.8	20	2235.0	38	2304.5	56	2369.8
3	2188.3	21	2238.9	39	2308.0	57	2376.8
4	2190.2	22	2244.1	40	2312.8	58	2383.8
5	2192.7	23	2247.3	41	2319.1	59	2391.2
6	2195.2	24	2253.6	42	2320.5	60	2398.3
7	2197.0	25	2256.6	43	2322.5	61	2405.5
8	2200.2	26	2259.6	44	2326.0	62	2412.3
9	2205.2	27	2261.8	45	2329.6	63	2419.1
10	2207.7	28	2265.2	46	2331.7	64	2426.0
11	2210.2	29	2270.5	47	2336.7	65	2432.9
12	2213.1	30	2273.9	48	2338.0	66	2439.9
13	2217.2	31	2275.9	49	2343.1	67	2443.4
14	2219.4	32	2279.0	50	2344.8	68	2446.1
15	2222.6	33	2282.6	51	2348.1	69	2450.0
16	2225.5	34	2287.4	52	2351.7	70	2453.2
17	2227.4	35	2290.8	53	2355.6	71	2459.4
18	2230.0	36	2296.3	54	2359.6	72	2465.4
						73	2471.8

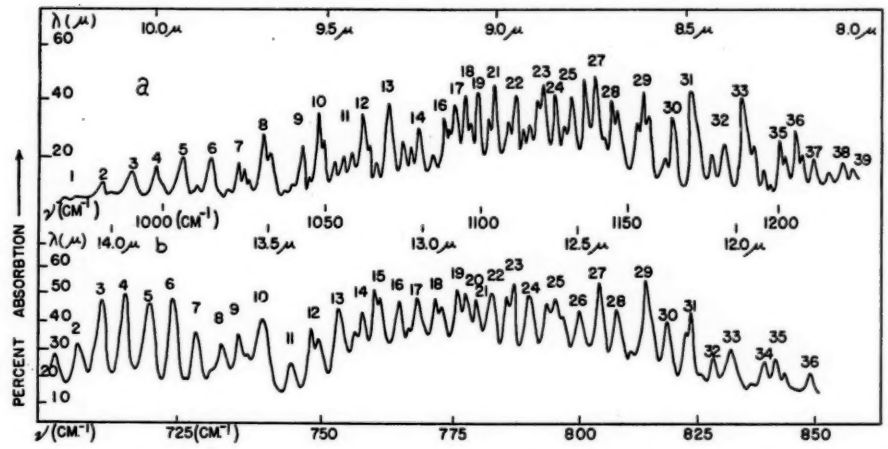

FIG. 2. (a) Absorption by H_2Se at 9.0μ. (b) Absorption by D_2Se at 13.0μ.

is the rotational structure near the center quite complex, but a small distance away from the center a fairly uniform spacing of 3.9 cm^{-1} manifests itself. The center of this band is taken to be at 745 cm^{-1} where again there is a minimum in the envelope of the band; this time much more discernible than in the H_2Se band. A diagram of the absorption bands ν_2 for H_2Se and D_2Se is given in Fig. 2, (a) and (b), respectively, where as before percent absorption has been plotted against a scale of frequencies and wave-lengths. Frequency positions of the principal absorption lines in these two bands are listed in Tables III and IV.

TABLE II. *Frequency positions of principal* D_2Se *absorption lines at 6.2*μ.

Line No.	Frequency Position	Line No.	Frequency Position	Line No.	Frequency Position
1	1554.2	32	1619.3	63	1679.8
2	1555.9	33	1620.6	64	1681.8
3	1558.7	34	1622.0	65	1684.4
4	1560.9	35	1624.2	66	1687.7
5	1562.0	36	1626.0	67	1691.7
6	1563.6	37	1628.5	68	1693.7
7	1564.9	38	1630.3	69	1695.7
8	1567.7	39	1632.8	70	1699.1
9	1569.9	40	1635.3	71	1703.1
10	1571.1	41	1637.1	72	1705.1
11	1572.8	42	1639.6	73	1707.8
12	1575.7	43	1641.5	74	1711.9
13	1577.4	44	1644.0	75	1716.0
14	1579.7	45	1645.9	76	1718.7
15	1582.0	46	1647.8	77	1722.8
16	1584.3	47	1649.6	78	1726.0
17	1588.4	48	1651.5	79	1729.8
18	1591.9	49	1652.8	80	1735.0
19	1594.8	50	1654.7	81	1736.8
20	1596.6	51	1656.0	82	1740.3
21	1598.4	52	1657.3	83	1743.8
22	1600.2	53	1658.8	84	1747.3
23	1602.5	54	1660.4	85	1751.6
24	1604.9	55	1663.0	86	1754.8
25	1607.3	56	1664.3	87	1758.8
26	1608.5	57	1666.9	88	1762.4
27	1610.3	58	1668.8	89	1765.3
28	1612.7	59	1670.7	90	1767.5
29	1614.5	60	1672.0	91	1771.1
30	1615.7	61	1674.6	92	1774.0
31	1617.5	62	1675.9		

D. Absorption bands due to HDSe

In the spectrum of deutero-hydrogen selenide three rather intense absorption regions appear. Their presence is determined in the following manner: first, measurements are made on a mixture of selenide containing 50 percent H_2Se, 40 percent HD_2Se and 10 percent D_2Se and then measurements are made on a mixture of the gases containing 10 percent H_2Se, 40 percent HDSe and 50 percent D_2Se. The first mixture shows intense bands where absorption occurs due to H_2Se and HDSe and very faint absorption where there are bands due to D_2Se; the second sample exhibits strong absorption bands due to HDSe and D_2Se and only weak bands due to H_2Se. The regions of absorption which occur intensely in both cases must be ascribed to HDSe. The three regions already referred to lie near 4.3μ, 6.0μ and 11.0μ.

The 4.3μ *region in* HDSe.—This region when investigated under high dispersion becomes at least partially resolved into rotational structure. In this band a strong minimum of absorption is found at the center and it has been identified as

ν_3 of the HDSe molecule. The center of this band lies at 2352 cm^{-1}, almost exactly coincident with the center of the 4.3μ absorption band in H_2Se. The absorption curve for HDSe in this region has been carefully compared with the curve obtained earlier for H_2Se at these wave-lengths to guard against falsification by the small amount of H_2Se present and absorbing here. No consistent coincidence of absorption lines in the two patterns could be detected and it is believed that the falsification due to the absorption by H_2Se must be negligibly small. At some distance from the center on either side the rotational structure becomes quite uniform and an average spacing of about 5.0 cm^{-1} between adjacent lines seems to prevail. When relative intensities of the absorption are plotted against a scale of frequencies, the curve in Fig. 3(a) is obtained. Frequency positions of the more prominent lines, to which arbitrary numbers have been affixed, are set down in Table V.

The 6.0μ region in HDSe.—The region near 6.0μ has been measured and has also been, at least partially, resolved into rotational structure. In contrast to the band at 4.3μ in this spectrum this one shows a very intense and sharp central line as may be seen by referring to Fig. 3(b). This band has been identified as the fundamental frequency ν_1 of the HDSe. Its central line lies at 1691 cm^{-1}, almost exactly coincident with the center of the 6.0μ band in the spectrum of H_2Se.

TABLE III. *Frequency positions of principal* H_2Se *absorption lines at 9.0μ.*

Line No.	Frequency Positions	Line No.	Frequency Positions
1	974.9 cm^{-1}	21	1104.9
2	982.7	22	1112.8
3	991.5	23	1122.0
4	998.7	24	1126.8
5	1005.6	25	1132.9
6	1013.9	26	1137.9
7	1021.9	27	1140.7
8	1030.2	28	1147.4
9	1041.6	29	1158.9
10	1048.1	30	1170.0
11	1057.7	31	1176.5
12	1063.5	32	1188.6
13	1069.0	33	1195.9
14	1078.7	34	1199.6
15	1083.8	35	1209.6
16	1086.8	36	1214.7
17	1091.4	37	1224.3
18	1094.5	38	1234.7
19	1098.6	39	1238.0
20	1102.8		

Also here a careful comparison has been made with the absorption band in the spectrum of D_2Se in this region to verify that no major falsifications in the absorption pattern have arisen because of the small amount of D_2Se present and absorbing here. No consistent coincidence could be established here either and it is felt that any such falsification is certainly small. In Table VI is given the frequency positions of the principal peaks of this band.

The 11.0μ region in HDSe.—This region has been investigated under high resolving power and at least to some extent it has been split up into rotational structure. The envelope of this band has the same general appearance as the envelope of the one measured near 4.3μ, there being a minimum discernible near 905 cm^{-1}. This point has been chosen as the center of the band which has been identified as the frequency ν_2 of the HDSe molecule. On the high frequency side of the center is found a series of fairly sharp lines separated quite uniformly from each other by an interval of about 5 cm^{-1}. The absorption curve is reproduced in Fig. 3(c) where as in other cases percent absorption has been plotted against a scale of frequencies and wave-lengths. The positions of the principal lines in the bands are set down in Table VII.

TABLE IV. *Frequency positions of principal* D_2Se *absorption lines at 13.0μ.*

Line No.	Frequency Positions	Line No.	Frequency Positions
1	704.6		
2	708.5	19	775.7
3	712.4	20	777.6
4	716.4	21	779.5
5	720.5	22	782.3
6	724.3	23	785.2
7	728.3		786.8
8	732.7	24	790.1
9	736.4	25	793.9
10	739.9		795.7
11	744.9		797.3
12	748.4	26	800.4
	750.4	27	804.1
13	752.4	28	808.0
14	756.3	29	813.9
	757.7	30	818.5
15	760.5	31	822.4
16	764.4		823.7
17	768.3	32	828.2
18	772.2	33	832.0
		34	839.7
		35	842.1
		36	850.5

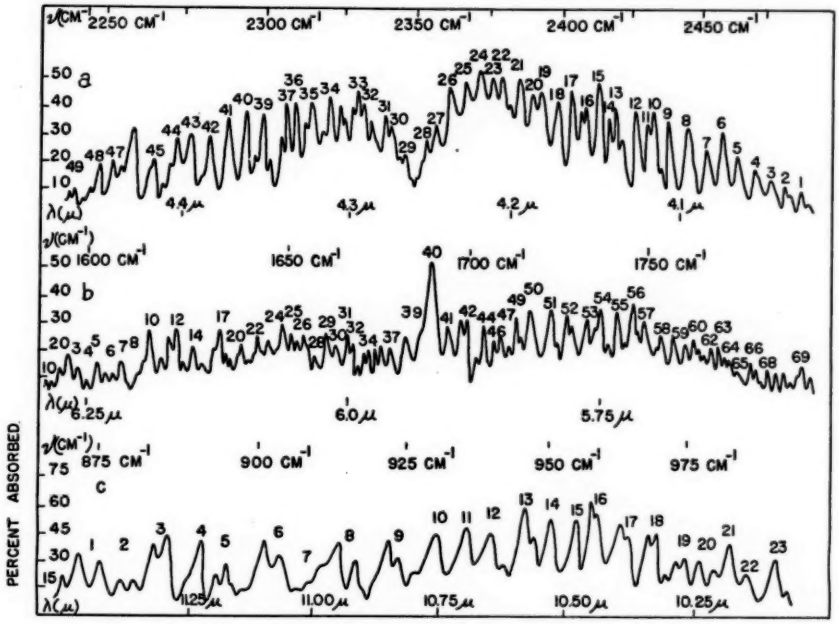

FIG. 3. Absorption bands of HDSe.

III. Discussion of the Results

The absorption bands in asymmetric molecules of this kind are of two types. One type arises when the electric moment alternates along the axis of the smallest moment of inertia and frequently has a gathered Q branch at the center. The other kind originates with alternations of the electric moment parallel to the intermediate moment of inertia and has a Q branch where the components spread out from the center away from each other leaving the middle of the band free from lines. This difference in general character of their rotational characters gives an important clue toward fixing which frequencies are which and, indeed, ultimately determining the shape of the molecular model.

The oscillations of the nonlinear XY_2 type molecule divide themselves into two symmetry classes. The frequencies ν_1 and ν_2 make up the one of these symmetry classes and give rise to alternations of the electric moment parallel to the axis of symmetry while the frequency ν_3 which belongs to the other symmetry class produces a change of electric moment perpendicular to the symmetry axis. ν_1 and ν_3 are oscillations of the molecule where the atoms move essentially along the XY bonds; in the first case they are oscillating in the same phase, in the second case their motions are out of phase. The masses and restoring forces being essentially the same in each case, one may expect the frequencies ν_1 and ν_3 to take very nearly the same values. The frequency ν_2, on the other hand, which originates principally from a deformation of the YXY bond angle only may be expected to take a value appreciably less than ν_1 or ν_3. Since, however, ν_1 and ν_2 both produce an electric moment parallel to the same

TABLE V. *Frequencies of principal* HDSe *absorption lines at 4.3μ.*

Line No.	Frequency Position	Line No.	Frequency Position	Line No.	Frequency Position
1	2488.4	20	2389.1	39	2299.8
2	2482.8	21	2384.6	40	2293.6
3	2477.1	22	2379.1	41	2288.1
4	2471.1	23	2376.5	42	2282.0
5	2465.2	24	2371.0	43	2275.3
6	2458.8	25	2367.0	44	2272.0
7	2452.9	26	2361.9	45	2266.0
8	2446.3	27	2357.5	46	2258.7
9	2440.0	28	2352.5	47	2255.4
10	2433.8	29	2346.0	48	2252.7
11	2431.5	30	2341.0	49	2248.8
12	2426.9	31	2339.6	50	2241.6
13	2420.7	32	2332.5		
14	2417.7	33	2330.4		
15	2413.1	34	2321.9		
16	2407.8	35	2315.3		
17	2403.3	36	2310.8		
18	2398.8	37	2306.6		
19	2384.6	38	2304.6		

TABLE VI. *Frequencies of principal* HDSe *absorption lines at 6.2μ.*

LINE No.	FREQUENCY POSITION	LINE No.	FREQUENCY POSITION	LINE No.	FREQUENCY POSITION
1	1594.0 cm^{-1}	24	1650.0	47	1710.5
2	1596.6	25	1653.4	48	1712.6
3	1599.3	26	1656.0	49	1714.6
4	1600.2	27	1657.9	50	1718.7
5	1603.1	28	1659.8	51	1724.9
6	1606.9	29	1662.4	52	1729.8
7	1609.1	30	1665.2	53	1735.0
8	1612.7	31	1668.1	54	1739.6
9	1614.5	32	1670.1	55	1743.8
10	1616.3	33	1671.4	56	1748.8
11	1619.3	34	1674.0	57	1752.3
12	1622.4	35	1675.3	58	1757.3
13	1624.8	36	1677.9	59	1760.9
14	1627.6	37	1680.1	60	1767.5
15	1630.0	38	1683.8	61	1769.6
16	1632.8	39	1685.8	62	1772.6
17	1633.7	40	1691.1	63	1774.0
18	1635.9	41	1696.4	64	1775.5
19	1637.1	42	1700.4	65	1781.4
20	1639.3	43	1703.1	66	1785.1
21	1642.1	44	1704.8	67	1786.6
22	1644.6	45	1707.1	68	1789.9
23	1647.1	46	1708.5	69	1797.8

TABLE VII. *Frequency positions of principal absorption lines in* HDSe *at 11.0μ.*

LINE No.	FREQUENCY POSITIONS	LINE No.	FREQUENCY POSITIONS
1	874.0	13	945.5
2	879.8	14	950.0
3	885.8	15	954.3
4	892.3	16	958.3
5	898.3	17	963.4
6	903.5	18	968.9
7	910.3	19	974.5
8	915.2	20	979.2
9	922.5	21	983.5
10	930.0	22	988.0
11	935.0	23	992.7
12	939.9		

axis their rotational character should be the same, whereas the rotational characteristics of the band ν_3 might well be quite different. This supplies an important clue toward determining without ambiguity which frequencies are which, and indeed, ultimately toward fixing the shape of the molecular model.

In the case of the spectrum of H_2Se we have attributed the 4.3μ region to two overlapping bands of considerable intensity, one near 2350 cm^{-1} which has a rather prominent gathered Q branch and another at 2260 cm^{-1} which has no gathered Q branch. The band in the H_2Se spectrum at 9.0μ gives, moreover, no evidence of a gathered Q branch and it may therefore be inferred that it is similar in rotational structure to the band at 2260 cm^{-1}. Similarly in the spectrum of D_2Se two bands have been found with no gathered Q branches, one lying at 1630 cm^{-1}, and the other at 745 cm^{-1}, and a third band showing a distinct gathered Q branch has been located at 1696 cm^{-1}. Thus we believe to have observed in the spectra of H_2Se and D_2Se the three fundamental bands and in each case two of these are essentially alike while the third is different. In view of the above argument we feel justified in making the assignments of these as indicated in Section II. These assignments are summarized in Table VIII together with positions of observed Raman lines, these latter being set in parentheses.

On the basis of a molecule oscillating with simple harmonic motion Redlich[7] has shown that the frequencies of two isotopic molecules belonging to the same symmetry classes must obey certain product relations. For the H_2Se and D_2Se molecules these will be:

$$\left(\frac{\nu_1\nu_2}{\nu_1'\nu_2'}\right)^2=\left(\frac{m_D m_{Se}}{m_H{}^2 m_{Se}}\right)\times\left(\frac{M_{H_2Se}}{M_{D_2Se}}\right)$$

and

$$\left(\frac{\nu_3}{\nu_3'}\right)^2=\left(\frac{m_D m_{Se}}{m_H{}^2 m_{Se}}\right)\times\left(\frac{M_{H_2Se}}{M_{D_2Se}}\right)\left(\frac{A}{A'}\right).$$

TABLE VIII. *Assignment of vibrational frequencies in* H_2Se, D_2Se *and* HDSe.

	H_2Se	D_2Se	HDSe
ν_1	2260 cm^{-1}	1630 cm^{-1}	912 cm^{-1}
ν_2	1074 cm^{-1}	745 cm^{-1}	1691 cm^{-1} (1671)
ν_3	2350 cm^{-1} (2312)	1696 cm^{-1} (1665)	2352 cm^{-1} (2313)

The value of such relations is, of course, that they serve as a check on the manner in which the observed vibration bands are identified and indeed also serve as a guide as to where the centers of bands are to be chosen. To be able to apply these to any advantage the moments of inertia of the molecules must be known. The values of these may be estimated from the frequency intervals between rotational lines in the

[7] O. Redlich, Zeits. f. physik. Chemie **B28**, 371 (1935).

bands ν_1 and ν_3 at 4.3μ in the H_2Se spectrum and at 6.0μ in the spectrum of D_2Se. In these bands the frequency intervals between lines is quite uniform from one end to the other save just at the centers. This leads one to conclude that the molecule is very nearly a symmetric molecule where $B \approx C = A/2$. When this approximation is made and one remembers that prominent lines occur in the spectrum when the molecule makes the transitions corresponding to $\Delta J = 0, \Delta K = \pm 1$

TABLE IX. *Values of* $\Pi(\nu_i/\nu_i')^2$.

Computed values	1.98	3.92
Experimental values	1.92	3.95

we obtain for A the value 7.3×10^{-40} g cm^2 and $C = 3.6 \times 10^{-40}$ g cm^2. Applying the same methods to the bands at 6.0μ in the D_2Se spectrum one obtains the value $A' = 14.6 \times 10^{-40}$ g cm^2 and $C' = 7.3 \times 10^{-40}$ g cm^2. With the aid of these and the values assigned to ν_1, ν_2 and ν_3 for the two molecules we may make use of the product relations of Redlich. The calculated values are compared with the values determined from the spectrum in Table VIII and it will be seen that the agreement is well within 10 percent. Better agreement can probably not be expected in as much as the development by Redlich assumes the oscillational motion to be harmonic which of course is true only in first approximation. Having adopted the above assignment of vibrational frequencies it is possible to draw certain conclusions concerning the forces binding the molecule together. In order to do so it is in general necessary to make certain assumptions concerning the nature of these forces. One assumption which has justified itself in a great many instances is the one, that to a satisfactory approximation the interatomic forces may be replaced by the so-called valence forces. This is a very useful approximation since the results obtained are so readily translated into physical and chemical notation. Lechner[8] has treated the problem of the nonlinear $X-Y-X'$ with three different masses (of which the XY_2 type is a special case) oscillating harmonically using a potential energy relation consistent with the valence forces. On this basis he has arrived at certain equations which relate the frequencies to the force constant f associated with the displacements of the particles X, X' and Y relative to each other along the XY and $X'Y$ distances, the force constant d associated with the deformation of the $X-Y-X'$ bond angle and the equilibrium value of the bond angles $(\pi-\alpha)$ itself. These equations are in principle sufficient for each individual molecule to determine the constants f, d and α.

The positions of the fundamental bands in the spectrum are all displaced, slightly toward smaller frequencies, essentially because of the anharmonicity of the oscillational motion, so that the vibration frequencies themselves are only approximately given by the band centers. The constant α depends in a very critical manner upon the exact values of the frequencies so that the equations of Lechner do not, unfortunately, constitute a reliable method for determining this constant. Conversely the values f and d are very insensitive to the value of α. We have therefore determined the values of f and d from the equations of Lechner which are most consistent with the data of the three molecules H_2Se, HDSe and D_2Se entirely without regard to the value

[8] E. Lechner, Wien Bericht. **141**, 291 (1932).

TABLE X.

Force Constants in dynes/cm	Computed Frequencies			Measured Frequencies		
	H_2Se	D_2Se	HDSe	H_2Se	D_2Se	HDSe
$f = 3.12 \times 10^5$	$\nu_1 = 2300$ cm^{-1}	$\nu_1 = 1645$ cm^{-1}	$\nu_1 = 1639$ cm^{-1}	$\nu_1 = 2260$ cm^{-1}	$\nu_1 = 1630$ cm^{-1}	$\nu_1 = 1691$ cm^{-1}
$d = 3.17 \times 10^4$	$\nu_2 = 1060$ cm^{-1}	$\nu_2 = 745$ cm^{-1}	$\nu_2 = 914$ cm^{-1}	$\nu_2 = 1074$ cm^{-1}	$\nu_2 = 745$ cm^{-1}	$\nu_2 = 905$ cm^{-1}
	$\nu_3 = 2305$ cm^{-1}	$\nu_3 = 1652$ cm^{-1}	$\nu_3 = 2320$ cm^{-1}	$\nu_3 = 2350$ cm^{-1}	$\nu_3 = 1696$ cm^{-1}	$\nu_3 = 2352$ cm^{-1}

for the angle α. With these constants, f and d, so determined we have re-evaluated the frequencies ν_1, ν_2 and ν_3 from Lechner's equations, this time putting in for α the value 90°, the value which seems most consistent with the regularity of the rotational structure of ν_1 and ν_3.[9] The results of this recalculation of frequencies is given in Table X for comparison with the experimentally observed frequencies. The agreement seems to be satisfactory when one considers that no correction whatever has been made for the anharmonicity of the oscillational motion.

[9] These frequencies have been chosen as most indicative of what the bond angle really is since the molecule suffers less distortion when it is oscillating in these modes than when it is oscillating with the frequency ν_3.

NOVEMBER, 1939 JOURNAL OF CHEMICAL PHYSICS VOLUME 7

Line Absorption Spectra of Rare Earth Ions in Crystals

E. J. MEEHAN, AND G. C. NUTTING
Department of Chemistry, University of California, Berkeley, California

(Received August 10, 1939)

Absorption spectra of the sulfate octahydrates of Er^{+++}, Dy^{+++}, Ho^{+++} and Tm^{+++} have been obtained at temperatures ranging from 14°K to 300°K. From the study of the variation in intensity of the absorption lines with temperature, energy levels have been found, in Er^{+++}, at 19, 41 and 86 cm^{-1} above the normal state. Similar levels have been found in Dy^{+++} at 22 and 57 cm^{-1} above the lowest. No such low energy states have been found in Ho^{+++} and Tm^{+++}.

INTRODUCTION

NUMEROUS studies of the absorption spectra of rare earth ions have been made in the last few years, in the temperature interval 20°–300°K.[1] In this paper data are presented for the sulfate octahydrates of Er^{+++}, Dy^{+++}, Ho^{+++} and Tm^{+++} in the region 7000–3500A.

A great deal has been written about the absorption spectra of rare earth ions in crystals. It is sufficient here to say that these ions (excepting Ce^{+++} and Yb^{+++}) have absorption spectra containing numerous unusually sharp lines. From the absorption spectrum at a very low temperature we obtain an energy level diagram of the excited states, since the lines observed originate in the one lowest level. It is believed that, for the strong and sharp lines, the excited states as well as the normal state involve only $4f$ electrons which occupy a relatively sheltered position in the ion. Many of the observed terms are produced by crystal splitting of the terms of the free ion.

According to Van Vleck[2] the transitions between levels of the same $4f^z$ configuration, which would be forbidden as dipole radiation, may be quadrupole, magnetic dipole or electric dipole radiation induced by crystal fields. Probably the radiation contains some elements of the three types. Ewald,[1c] working with Nd^{+++}, showed that the strong and sharp lines are pure electron transitions but that anion and lattice vibrations are also concerned in producing the lines which are weaker and less sharp.

The normal states of these ions are important in determining magnetic susceptibilities and other low temperature thermal and magnetic

[1] (a) Ce^{+++}; S. Freed, Phys. Rev. **38**, 2122 (1931).
(b) Pr^{+++}; F. H. Spedding, J. P. Howe and W. H. Keller, J. Chem. Phys. **5**, 416 (1937); A. Merz, Ann. d. Physik [5] **28**, 569 (1937); P. Lehmann, Ann. d. Physik [5] **34**, 389 (1939).
(c) Nd^{+++}; F. H. Spedding, H. F. Hamlin and G. C. Nutting, J. Chem. Phys. **5**, 191 (1937); H. Ewald, Ann. d. Physik [5] **34**, 14 (1939).
(d) Sm^{+++}; S. Freed and J. G. Harwell, Proc. Acad. Sci. Amsterdam **35**, 979 (1932); F. H. Spedding and R. S. Bear, Phys. Rev. **46**, 308, 975 (1934).
(e) Gd^{+++}; G. C. Nutting and F. H. Spedding, J. Chem. Phys. **5**, 33 (1937).
(f) Eu^{+++}; E. J. Meehan, J. Chem. Phys. **3**, 621 (1935). (The conclusions advanced in this paper with respect to the spectrum of Eu^{+++} must be withdrawn. It has since been discovered that the sample contained sufficient impurities to account for many of the lines.) H. Lange, Ann. d. Physik **32**, 361 (1938).
(g) Yb^{+++}; S. Freed and R. Mesirow, J. Chem. Phys. **5**, 22 (1937).
(h) H. Gobrecht has studied many rare earth spectra. Most of his results are summarized in Ann. d. Physik [5] **31**, 755 (1938).

[2] J. H. Van Vleck, J. Phys. Chem. **41**, 67 (1937).

properties. From the behavior of the magnetic susceptibility at low temperatures it has been possible to deduce in some cases something about the energy levels close to the lowest one, and therefore indirectly to obtain information about the crystal field in the neighborhood of the rare earth ion. It is this field which determines the number and spacing of the energy levels which arise from a level single in the absence of a field. The field must be specified as to strength and symmetry.

Thus Kramers[3] found from the paramagnetic rotation that Ce^{+++} in tysonite (CeF_3) behaves as if its normal state were split into 3 states at 0, 113, and 489 cm^{-1} by a trigonal field. Becquerel and de Haas[4] postulate energy levels of Dy^{+++} at 0 and about 10 and 20 cm^{-1} in $Dy(C_2H_5SO_4)_3 \cdot 9H_2O$. A theoretical treatment by Penney and Schlapp[5] for $Pr_2(SO_4)_3 \cdot 8H_2O$ and $Nd_2(SO_4)_3 \cdot 8H_2O$, indicates that these salts must have crystal fields of cubic symmetry to agree with the magnetic data.[6]

The determination of crystal fields in this way presents some difficulties. The complete lattice structures are not known so that one must make the calculations for the most likely symmetries and choose that which best fits the magnetic data. Even with the most accurate magnetic data one can determine only the predominant kind of symmetry. Nothing in general can be said about weaker fields of lower symmetry.

By suitable spectroscopic methods it is possible to determine precisely the energy levels near the normal state. The procedure is as follows. One photographs the spectrum over a temperature range, for example, 14°–300°K. (One does not go much higher than 300°K because the lines become too diffuse and some crystals decompose.) In the spectrum at 14°K practically all the lines originate in the lowest level since there is no appreciable population in any level unless it is very close to the lowest one. Comparing the 14°K spectrum with that at 78°K one may find some lines enhanced in intensity. Such lines evidently originate in levels whose population has been increased by the rise in temperature. Obviously a requirement of this interpretation is that there should be certain often repeated constant energy differences between those lines intense at the low T and those whose intensity increased with T. These constant energy differences are the spacings of the low lying levels. This method is evidently limited to levels situated within about 300–400 cm^{-1} of the lowest, since to bring out lines from levels further removed, at ordinary T would require crystals of thickness too great for a usable exposure time.

It was thought that scattering of mercury radiation might serve to detect such higher levels and others of the lowest multiplet situated perhaps several thousand cm^{-1} above the normal state, since an electronic Raman effect in Ce^{+++} has been reported.[7] Attempts to obtain an electronic effect from Pr^{+++}, Nd^{+++}, Sm^{+++} and even Ce^{+++} failed, necessarily so since the subsequent discovery in the infra-red absorption spectrum[1h] of many of the frequencies sought for showed it to be impossible for the same frequencies to appear in a Raman spectrum.

In the present work of extending the study of rare earth salts to the second half of the group, the sulfate octahydrates were chosen, because magnetic measurements are most abundant for these salts and because they have most generally been used for similar studies of other rare earths.

In the sulfate octahydrates the crystal fields must be very nearly alike, for (excepting $Ce_2(SO_4)_3 \cdot 8H_2O$) they are isomorphous and the molecular volumes differ only slightly. The crystallographic symmetry is monoclinic but the internal structure is unknown. There are good reasons for believing that in these compounds, there are six oxygen atoms, contributed by water molecules and sulfate ions, placed at the corners of an octahedron about the rare earth ion, this octahedron being not much distorted, so as to give nearly cubic symmetry.[8]

Experimental Methods and Observations

The spectra were photographed on a 3-meter grating, the crystals being immersed in liquid

[3] H. A. Kramers, Proc. Acad. Sci. Amsterdam **35**, 1272 (1932).
[4] J. Becquerel and W. J. de Haas, Leiden Comm., Supplement 74a.
[5] W. G. Penney and R. Schlapp, Phys. Rev. **41**, 194 and **42**, 666 (1932).
[6] C. J. Gorter and W. J. de Haas, Leiden Comm. 218b.
[7] Brunetti and Ollano, Il nuovo cimento, **8**, 281 (1931); Zeits. f. Physik **75**, 415 (1932).
[8] C. J. Gorter, Phys. Rev. **42**, 427 (1932).

H_2 (14° or 20°K) N_2(78°K), C_2H_4(169°K) or being at room temperature (300°K). The apparatus has been described.[9]

Since the purity of the rare earth materials containing Er, Dy, Ho and Tm was not known the first problem was to determine the constituents of each sample and the lines belonging to each element. The samples available were "thulium," "dysprosium" and three samples of "erbium." They were converted into sulfate octahydrates and absorption spectra of single crystals 1–2 mm thick and of thicker conglomerates were photographed so as to bring out the strong and faint lines, respectively.

La^{+++}, Ce^{+++}, Gd^{+++}, Yb^{+++} and Lu^{+++} have no absorption in the region studied. Therefore contamination of the samples by any of these would introduce no spurious lines. To test for impurities of the colored ions, Pr^{+++}, Nd^{+++} and Sm^{+++}, 3 mm conglomerates of preparations of $Ce_2(SO_4)_3 \cdot 8H_2O$ containing 1–2 percent of these elements were photographed at 78°K. It was not at the time appreciated that the cerium salt is not isomorphous with the other sulfate octahydrates. The symmetry of the crystal fields acting on the metal ions in this lattice is quite different from that in the monoclinic crystals, for the spectra of Pr^{+++}, Nd^{+++} and Sm^{+++} in the mixtures with Ce^{+++} are notably different from the spectra in the pure compounds.

As an alternative procedure crystal sections 0.1–0.3 mm thick of the sulfates of Pr, Nd and Sm were photographed and then compared with the spectra of the impure "Er," "Dy" and "Tm." Eu and Tb remained to be tested for. The presence of Tb in rare earths is indicated by the brown color its oxide imparts to the oxides with which it is mixed. By far the largest concentration of Tb in any of our rare earths was present in a Gd sample, but no trace of the single band in the green characteristic of Tb^{+++} was evident even in a 5-mm conglomerate of $Gd_2(SO_4)_3 \cdot 8H_2O$ at 78°K. In this spectrum, however, the sharp lines of Eu^{+++} at 3960A and 5260A were clearly visible. The few lines due to the above five elements were discounted, leaving thus the spectra of Er, Dy, Ho and Tm.

Matching the spectrum of, let us say, "erbium" with that of "dysprosium," lines common to both were picked out and then both were compared with "thulium." Then the spectra of the several samples were compared with the abundant data on solutions.[10] Recognizing in a spectrum a characteristic region, for example the 14,500 cm^{-1} multiplet of Tm^{+++}, this could be assigned to the appropriate element. Then lines common to all the spectra in which the characteristic group appears evidently constitute the true spectrum, which of course must accord throughout with the best solution data.

Considering only the colored earths, it was found that (*a*) thulium was pure, (*b*) "dysprosium" contained also holmium but no others, (*c*) one sample of "erbium" contained Er, Ho, and Tm but no others, (*d*) the other two samples of erbium were identical with (*c*) except for traces of Nd and Pr. Subtracting the few lines of Tm from Er (*c*) left the spectra of Er+Ho. Matching this with the "Dy" gave the lines of Ho, leaving then those due to Er and to Dy.

Confirmation of these conclusions was obtained by means of the emission spectra in the region 2350–3250A, obtained on a Hilger E 185 quartz spectrograph. From the intensities of the arc lines a very rough estimate of the relative amounts of the constituents may be made, but a quantitative analysis is impossible without comparison with samples of known composition. The results of this analysis were (*a*) "Tm" was mainly Tm and Yb with very small amounts of Y and Lu, (*b*) "Dy" was mainly Dy and Ho with small amounts of Y, Gd and Lu, (*c*) "Er" was mainly Er with lesser amounts of Ho, Tm and Y.

The question arises whether the spectra of the elements in the mixtures we were forced to use are the same as those in the pure salts. Because of the near-identity of the lattices it is to be expected that the number of lines is the same in the pure salts as in the mixtures, but conceivably the positions may be somewhat different. A test of this point was made. About one percent of Nd^{+++} was introduced into a portion of $Er_2(SO_4)_3 \cdot 8H_2O$ and the spectrum of a 3.5-mm conglomerate was

[9] F. H. Spedding and G. C. Nutting, J. Chem. Phys. **2**, 422 (1934).

[10] Taken mainly from: L. F. Yntema, J. Am. Chem. Soc. **45**, 907 (1923); P. W. Selwood, *ibid.* **52**, 408 (1930); G. Urbain, Comptes rendus **142**, 785 (1906); J. H. Gardiner, J. Chem. Soc. 1518 (1926); W. Prandtl, Ber. **116**, 96 (1921); Prandtl and Scheiner, Zeits. f. anorg. Chemie **220**, 107 (1934).

photographed at 78°K. This procedure was repeated, substituting Sm^{+++} for Nd^{+++}. The lines were compared with those of pure Nd and Sm salts. It was found that there was indeed a slight effect. Nd^{+++} lines in the mixture were shifted to the red while the Sm^{+++} seemed to show no systematic shift, some being substantially unchanged. The amount of the shift was always very small. Nd (atomic number 60) and Sm (62) are much further removed from Er (68) than are Ho (67) and Tm (69) which were associated with Er in our samples. The already small differences in the Nd^{+++} and Sm^{+++} spectra would thus be expected to be much smaller if Tm and Ho were the contaminating elements in the Er. The frequencies reported later for Ho^{+++} are the averages of those measured in the "Er" and "Dy" samples. Differences of 1 cm^{-1} were rare and most differences were not much more than the error of measurement (about 0.3 cm^{-1}).

Concerning these spectra in general it appears that the intensity of absorption depends to a great extent on atomic number, being considerably less for the heavier elements. Quantitative measurements have not been made, but it appears that crystals of the Pr salt (Pr has atomic number 59) only 0.1 mm thick, and of Nd (60) only 0.3 mm thick, absorb with intensity comparable to that of 5-mm conglomerates containing the heavier ions Dy^{+++}, Ho^{+++}, Er^{+++} and Tm^{+++}. Even at 20°K a 2-mm crystal of $Pr_2(SO_4)_3 \cdot 8H_2O$ absorbs so strongly that the satellites of the strongest lines are so enhanced that many of the strong lines appear as diffuse as those of the heavier ions at a much higher temperature. The observed low level of absorption cannot be due to contamination by large amounts of colorless impurities. Determination of the average combining weight of the rare earths in the samples has ruled out the possibility of the presence of much Y^{+++} or Ce^{+++}. Colorless Yb^{+++} and Lu^{+++} are comparatively rare and cannot be present in any great amount.

In the following paragraphs, features of the spectra will be discussed in turn for Er, Dy, Ho and Tm. Fig. 1 is a plot of the spectra at 20°K.

$Er_2(SO_4)_3 \cdot 8H_2O$

Wave-lengths at 14°K and frequencies at five temperatures are given in Table I. Intensities are rough visual estimates. All the prominent lines are marked *L* or *H* according to whether they are relatively more intense at low or high temperatures. As usual, at low temperatures the lines are sharper and better resolved than at higher temperatures. The effect of temperature on ν is slight, much less than in Sm^{+++} (1*d*) and Gd^{+++} (1*e*) for which some shifts as large as 5–10 cm^{-1} to smaller ν occurred between 300° and 78°K. In Er^{+++}, the sharpest and most accurately measured lines are rarely shifted as much as 5 cm^{-1} between the extreme temperatures and the direction seems to be quite random.

In Table II is presented evidence for levels close to the lowest.* The values are 19.2 and 41.0 cm^{-1} at 20°K and 19.5, 41.1, and 85.7 cm^{-1} at 78°K. Fig. 2 shows the consistency of these levels in explaining the structure and intensity relations of a typical multiplet in the Er^{+++} spectrum.

Spedding[11] has used the method of Penney and Schlapp to calculate the effect of crystal fields on the normal state of Er^{+++}, $^4I_{15/2}$. He was able to show that our results agree with the assumption of a cubic field of the same strength as in Nd^{+++}(1*c*). A cubic field splits $^4I_{15/2}$ into five levels, and any field of lower symmetry, into eight. The five levels are assumed to be at 0, 19,

* In addition to the pairs of lines given in Table II (1) as evidence for a 19-cm^{-1} level there are several other doublets with the same separation which are distinctive in that both components are of comparable intensity at very low temperatures and the long wave-length component does not become much more prominent at higher temperatures at the expense of the short wave-length component. This is doubtless because of unusual disparity in the absorption coefficients for the two frequencies. Normally one expects approximately equal absorption per atom, whereupon intensity variation with temperature expresses changing population in the two levels according to Boltzmann's relation. The line pairs are listed below. Frequencies are averages of 14°K and 20°K measurements. Intensities are for 14°K.

ν_1	Int.	ν_2	Int.	$\Delta\nu$
15245.2	7	15225.7	5	19.5
15285.6	8	15266.2	6	19.4
15310.1	9	15290.6	8	19.5
15338.4	9	15318.7	8	19.7
19115.8	10	19096.0	9	19.8
19261.3	10	19241.7	10	19.6
20509.2	6	20489.6	5	19.6
20540.0	6	20520.6	6	19.4
22241.2	6	22221.4	5	19.8
26522.3	3	26502.3	4	20.0
27356.1	2	27335.5	2	20.6

Average = 19.7 cm^{-1}

[11] F. H. Spedding, J. Chem. Phys. **5**, 316 (1937).

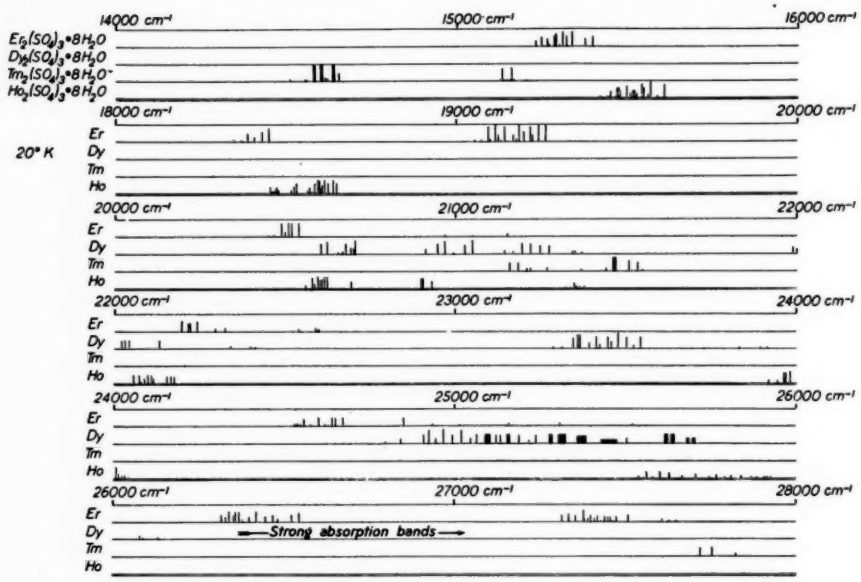

FIG. 1.

38, 85 and 87 cm^{-1} with statistical weights of 4, 4, 2, 4, and 2. If superposed on the dominant cubic field is a lesser field of lower symmetry the 0, 19 and 85 cm^{-1} levels should be split by an amound depending on the relative strengths of the two fields. Since in the spectra there is no evidence of any such effect, it is concluded that the distortion of the octahedral oxygen envelope about Er^{+++} is inappreciable even though the ErO_6 complex is in a lattice of low symmetry.[12]

The magnetic susceptibility of this substance is known,[13] and from it Jackson has postulated an excited level at about 40 cm^{-1}.

Using our spectroscopic levels and the predicted statistical weights, the electronic heat capacity of Er^{+++} in $Er_2(SO_4)_3 \cdot 8H_2O$ may be computed. The results are in Table III. Accurate measurements of the heat capacity of this substance combined with the data for the Gd salt, which has no such excited levels, would give this quantity experimentally as a check on the spectroscopic values. The contribution due to the low levels is quite appreciable, since at 10°K it should be about twice the ordinary heat capacity and at 15°K the two quantities should be approximately equal.

$Dy_2(SO_4)_3 \cdot 8H_2O$

Measurements are given in Table IV. In contrast to the case of Er^{+++}, the majority of the lines shift to lower ν by 2–4 cm^{-1} between 78°–20°K. The general features of the multiplets are similar to those of Er^{+++}. Thus the 22,000, 20,5000 and 23,500 cm^{-1} groups extend over about 70, 100 and 200 cm^{-1}, respectively. The higher multiplets are not so well resolved as these; seemingly the greater diffuseness of the corresponding higher levels indicates a less complete shielding.

Dy^{+++} also has low lying levels. In Table V is presented evidence for levels at 22.2 and 56.8 cm^{-1} at 20°K, and at 21.9 and 55.6 cm^{-1} at 78°K. It is possible that higher levels also exist but there is not sufficient evidence for a definite statement. Jackson[12] has made magnetic measurements for this substance but no analysis of the data to determine crystal splitting is reported. For the ethylsulfate measurements[14] indicate levels at about 10 and 20 cm^{-1} in this

[12] K. S. Krishnan and A. Mookerji (Proc. Roy. Soc. **A237**, 135 (1938)) have found paramagnetic anisotropies in the rare earth sulfate octahydrates, which indicates that the fields cannot be pure cubic.

[13] W. J. de Haas, E. C. Wiersma and W. H. Capel, Leiden Comm. 201b; S. Velayos, Anales soc. espan. fis. quim. **33**, 297 (1935); L. C. Jackson, Proc. Phys. Soc. **48**, 741 (1936).

[14] W. J. de Haas, J. van den Handel and C. J. Gorter, Phys. Rev. **43**, 81 (1933).

TABLE I. *Conglomerate absorption lines of* $Er_2(SO_4)_3 \cdot 8H_2O$. *Frequencies* (ν) *are in* cm^{-1}. *Intensities* (*Int.*) *have been estimated visually on the scale 0–10. The letters vd, d, nd, s, vs indicate increasing degrees of sharpness of the lines. D indicates that the line is probably double. L and H stand, respectively, for low temperature and high temperature lines.*

14°		20°		78°		169°	300°	
λ	ν	ν	Int.	ν	Int.	ν	ν	
6,566.11	15,225.5	15,225.8	3*vs*	15,226.2	3*vs*	15,225.1	15,229.0	*L*
57.70	245.0	245.3	5*vs*	244.7	6*s*	245.2	246.0	*L*
48.67	268.1	266.2	4*vs*	266.1	8*s*	267.7	267.6	*L*
47.37	269.1	269.1	1	268.8	5*s*			*H*
40.34	285.5	285.7	6*vs*	285.4	8*s*			*L*
38.15	290.6	290.6	7*vs*	290.7	8*s*	290.5	289.8	*L*
35.24	297.4	297.7	1	297.5	1			*H*
29.81	310.2	310.0	8*s*	309.8	9*nd*	309.2	305.5	*L*
26.07	318.8	318.6	6*s*	319.0	9*nd*	318.8	318.5	*L*
17.76	338.5	338.2	8*s*	338.0	9*nd*	336.9	335.0	*L*
				355.4	2*nd*	356.5		*H*
01.35	377.2	377.2	4*d*	376.2	2*d*	373.9	380.0	*L*
6,493.58	395.6	396.5	6*d*	395.7	8*d*	397.3		*L*
92.01	399.3						17,904	*H*
							18,181	*H*
							240	*H*
							290	*H*
				18,302.8	2*s*			*H*
5,448.87	18,347.3	18,347.3	1	346.9	4*vs*	18,347.6	346.7	*H*
				360.7	1	364.5		*H*
42.62	368.4	367.3	1	369.1	4*vs*	368.9	367.2	*H*
36.77	388.2	388.0	5*vs*	388.5	5*vs*	388.0	388.3	*L*
31.22	407.0	406.5	3*vs*	406.7	7*s*	406.3	400.9	*H*
24.79	428.8	428.8	5*s*	428.7	6*s*	428.7	422.8	*H*
19.03	448.4	448.3	9*s*	448.5	8*s*	447.5		*L*
							784	*H*
							957	*H*
						966	979	*H*
						998		*H*
						19,013.3		*H*
				19,029.4	4*nd*	033.3	19,035.4	*H*
5,246.03	19,056.7	19,057.7	0	055.7	3*nd*	057.6	057.0	*H*
41.17	074.4	074.2	1*s*	074.4	5*vs*	075.4	075.8	*H*
35.31	095.8	096.1	9*vs*	096.4	8*s*	098.3	098.1	*L*
33.72	101.6	101.0	1*vs*	101.5	8*s*			*H*
29.76	116.0	115.5	10*vs*	115.4	9*s*	116.2	118.5	*L*
27.85	123.0	122.2	3*vs*	122.6	5*vs*	122.1		*H*
		131.0	0	132.0	2	131.2		*H*
22.56	142.5	142.1	9*vs*	143.0	6*nd*	144.0	142.7	*L*
				155.8	2*nd*	160.6		*H*
15.78	167.3	166.8	4*vs*	167.3	5*vs*	168.2	168.2	*H*
13.25	176.6	176.8	2*s*	176.6	4*s*	177.7		*H*
10.45	186.9	186.6	10*vs*	186.5	9*s*	186.7	19,184.0	*L*
07.03	199.5	199.0	5*s*	200.1	9*s*	200.7	200.7	*H*
02.05	217.9	217.5	9*vs*	218.2	8*s*	219.9	220.0	*L*
00.77	222.6	222.3	4*vs*	221.1	7*s*			*H*
5,195.61	241.7	241.6	10*s*	241.9	9*s*	242.0	240.0	*L*
90.34	261.2	261.3	10*s*	261.1	9*s*	260.2	259.2	*L*
							20,252.4	*H*
							292.6	*H*
							374.0	*H*
				20,424.4	1		430.0	*H*
		20,450.4	0	20,455.3	1	20,451.9		*H*
		467.4	1*vs*	468.1	5*s*	469.3	471.9	*H*
4,879.18	20,489.6	489.5	8*vs*	490.3	7*s*	490.8		*L*
77.05	498.5	498.7	3*vs*	498.6	6*s*	499.1	494.2	*H*
74.55	509.0	509.3	8*vs*	509.2	7*s*	509.6		*L*
71.78	520.7	520.5	8*vs*	520.2	8*s*	521.0	524.4	*L*
67.22	539.9	540.1	8*vs*	540.1	8*s*	540.0	542.0	*L*
							842	
4,767.92	967.7	968.0	0	21,065	1	21,066		
49.43	21,049.3	21,049.0	0	078	2	081		
26.22	152.7	152.6	2			157.4		
							21,717	*H*
							842	*H*
							899	*H*
							959	*H*
				21,992.3	0			*H*
				22,015.0	1*nd*		22,015	*H*
4,504.03	22,196.1	22,196.6	6*vs*	196.7	6*s*	22,195.1	196.3	
				209.1	1	207.8		*H*
00.08	215.6	216.0	5*vs*	215.1	4*s*	215.8		*L*
4,498.93	221.3	221.4	5*vs*	221.7	6*s*	220.9	220.7	*L*
94.95	241.0	241.3	6*vs*	241.1	6*vs*	237.0	241.4	*L*
		297.0	2*d*	297.0	3*d*		305	
		326.0	2*d*	319.8	3*d*			
				520.5	2*nd*	519.0		
35.39	539.6	539.6	1*vs*	535.5	2*nd*	535.5		
				546.6	2*nd*	546.9	549.1	
29.53	559.4			569.2	2*nd*	570.1	573.0	

14°		20°		78°		169°	300°	
λ	ν	ν	Int.	ν	Int.	ν	ν	
27.90	577.8							
25.39	590.6	590.4	2*vs*	588.3	5*vs*	592.7		
		595.8	1	597.4	1*s*		597.5	
23.84	598.5	599.7	1					
4,278.12	23,368.2							
	881.4						23,717	
				23,875.9	1		23,855	
				897.5	1		24,184	*H*
							268	*H*
				24,423.6	1	24,422.9		*H*
				452.7	1			*H*
				470.7	1	478.9	477	*H*
				505.2	1	502.6		*H*
				514.8	3*s*	513.1	512.2	*H*
				521.0	2*s*		521.7	*H*
		24,528.0	1	528.5	1	528.9		*H*
4,074.47	24,536.2	536.2	1*vs*	537.3	5*s*	537.4	542.4	*H*
73.75	540.5	541.1	1*vs*					
72.56	547.7	548.0	1*nd*	546.8	2			
71.22	555.8	556.3	4*vs*	556.0	6*s*	555.9	555.1	*L*
		577.2	1*nd*	578.2	3*s*			*H*
64.14	598.5	598.5	5*vs*	597.2	4*s*	595.0	595.3	*L*
		618.9	1*nd*	617.9	1	614.1		*H*
		626.6	0	624.7	0			
				629.9	1	630.2		*H*
				637.1	4*s*			*L*
57.80	637.0	637.6	5*vs*	651.4	5*s*	651.3	649.2	*H, L*
55.39	651.6	652.1	5*vs*	670.8	5*s*	671.7	666.0	*L*
52.25	670.7	671.8	5*vs*	852.8	4*s*	855.8	856	
22.67	851.9	851.9	4*vs*	911.5	2*nd*	914.3		
12.26	916.6			935	2*d*			
09.0	937	934	0			949	946	
				956.7	2*nd*	956.6		
05.92	956.0							
04.04	967.7			969.9	1*s*			
3,998.16	25,004.5					25,004.3		
		25,017.0	0	25,020.0	0	017.1		
73.89	157.2	158.2	2*nd*	157.2	1*s*			
49.93	309.8	309.1	2*nd*	306.1	0		25,361	
		523.2	0	520.1	0			
							26,198	*H*
				26,271.0	2*s*	26,278.2		*H*
				286.7	1*s*			*H*
				296.7	0	297.9		
				303.2	0	306.5		
3,798.62	26,317.9	26,317.0	4*vs*	316.7	2*s*	316.8		*H, L*
96.76	330.8	330.0	3*vs*	328.9	2*s*	330.3		*H*
95.57	339.1	339.1	6*vs*	338.6	2*s*	339.0		*H, L*
93.73	351.8	352.2	4*vs*	355.4	2*d*	356.8		*H*
92.81	358.2	359.0	6*vs*					*L*
90.89	371.6	372.2	6*vs*				26,365	*L*
		378.7	1*s*	377.8	2*d*	376.4		*H*
86.88	399.5	399.9	3*vs*	400.3	2*s*	400.3		*H*
84.11	418.8	419.2	6*vs*	421.5	2*d*	420.4		*L*
80.12	446.7	447.3	3*vs*	446.5	1*s*	448.7		
77.11	467.8	467.6	5*s*	462.0	2*d*	464.7		
74.73	484.5	483.1	2*nd*	481.3	1	482.3		
72.13	502.7	501.9	5*nd*	500.8	2*nd*	502.2		
69.35	522.3	522.3	4*s*	522.7	2*nd*	522.1		
66.43	542.8	543.1	5*d*	541.5	2*d*	543.0	26,534	
3,660.07	27,314.1	27,314.9	4*s*	27,312.3	1*s*	27,318.5		
57.24	335.3	335.7	5*s*	334.2	1*s*	340.8		
54.45	356.1	356.0	4*s*	353.1	1*s*	357.7		
51.66	377.0	377.7	7*s*	377.7	1*s*	377.1		
50.5	386	384	0	389	1*s*			
49.60	392.5	392.4	2*vs*			393.4		
48.3	402	401	4*nd*	400	1			
47.0	412	411	3*nd*	410	0			
45.9	420	419	4*nd*	421	0	420		
		431	1*nd*	433	0	432		
43.16	440.9	440.7	3*s*			440.5		
41.77	451.4	452.4	3*nd*	451.5	1*s*	454.6		
41.04	456.9	457.4	3*nd*					
		463.0	0	464.	0			
39.:	472	474	3*d*	470	0	470		
38.44	476.5			477	0			
33.97	510.3	510.0	4*s*					
20.8	610	609	1					
18.3	629	629	1					
15.8	649	649	0					

hexagonal crystal. To detect spectroscopically an intensity change due to a 10 cm^{-1} level a temperature below 14°K is needed, but the presence of such a level would be indicated by a constant, frequently repeated separation of pairs of lines. Such a separation does not occur. Thus the lowest (spectroscopic) level in the monoclinic sulfate is higher than the lowest (magnetic) level in the hexagonal ethylsulfate. A similar situation exists in Sm^{+++}.

TABLE II. *Evidence for low-lying levels in* $Er_2(SO_4)_3 \cdot 8H_2O$. *The frequencies are averages of the 14°K and 20°K measurements.*

(1) 19 cm^{-1} LEVEL		
ν_A	ν_B	$\Delta\nu_{(1)}$
15,396.5	15,377.2	19.3
18,388.1	18,367.9	20.2
18,448.4	18,428.8	19.6
19,142.3	19,122.6	19.7
19,186.8	19,167.0	19.8
19,217.7	19,199.3	18.4
19,241.7	19,222.5	19.2
24,556.1	24,536.2	19.9
24,637.3	24,618.9	18.4
24,671.3	24,651.9	19.4
26,358.6	26,339.1	19.5
26,371.9	26,352.0	19.9
26,419.0	26,399.7	19.3
	Average =	19.2 cm^{-1}

(2) 41 cm^{-1} LEVEL		
ν_A	ν_B	$\Delta\nu_{(2)}$
15,310.1	15,269.1	41.0
15,338.4	15,297.6	40.8
15,395.7	15,355.4	40.3
18,388.1	18,347.3	40.8
18,448.4	18,406.8	41.6
19,115.8	19,074.3	41.5
19,142.3	19,101.4	40.9
19,217.7	19,177.7	40.0
20,509.2	20,467.4	41.8
24,556.0	24,514.8	41.2
24,670.8	24,629.9	40.9
26,358.6	26,317.5	41.1
26,371.9	26,330.4	41.5
26,419.0	26,378.7	40.3
	Average =	41.0 cm^{-1}

(3) 86 cm^{-1} LEVEL (THESE VALUES ARE FOR 78°K)		
ν_A	ν_B	$\Delta\nu_{(3)}$
18,388.5	18,302.8	85.3
18,448.5	18,360.7	87.8
19,115.4	19,029.4	86.0
19,143.0	19,055.7	87.3
19,218.2	19,132.0	86.2
19,241.9	19,155.8	86.1
20,509.2	20,424.4	84.8
20,540.1	20,455.3	84.8
24,556.0	24,470.7	85.3
26,355.4	26,271.0	84.4
26,371.9	26,286.7	85.2
	Average =	85.7 cm^{-1}

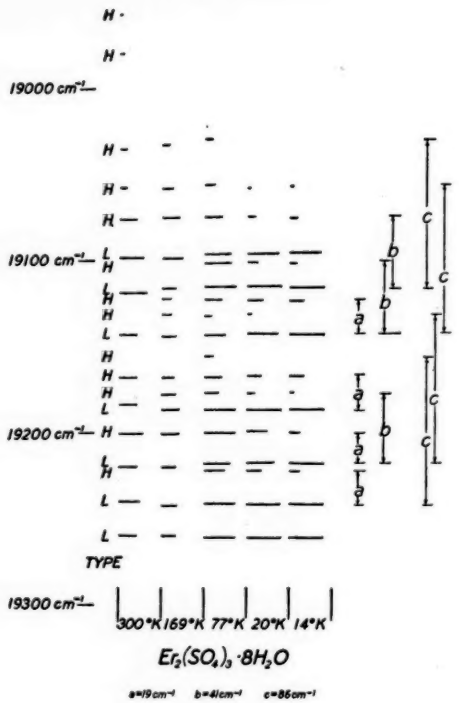

FIG. 2.

The normal state of Dy^{+++}, $^6H_{15/2}$, should split into two doubly-degenerate and three quadruply-degenerate levels in a cubic field. A treatment similar to that which proved successful for Er^{+++}[11] did not agree with our results for Dy^{+++}. It seems that the discrepancy may be due to the presence of an extra, perturbing level. Dy^{+++} is the analog of Sm^{+++}; the two ions have the same normal states but inverted. In Sm^{+++}

TABLE III. *Calculated electronic heat capacity of* Er^{+++} *in* $Er_2(SO_4)_3 \cdot 8H_2O$.

T.(°K)	C_v(CAL. PER G-ION)
0	0
5	0.24
10	0.94
20	1.04
25	1.02
50	0.86
75	.58
100	.38
150	.20
200	.12
250	.08
300	.06

more levels were found than could possibly arise from $^6H_{5/2}$. The "extra" levels in Sm^{+++} evidently have counterparts in Dy^{+++}.

$Ho_2(SO_4)_3 \cdot 8H_2O$

Data are in Table VI. Considering only the strongest lines, it cannot be said that there is any systematic shift with T. It is in this spectrum however that the largest temperature effects are found. Thus shifts of 5 cm^{-1} between 169°K and 20°K are by no means uncommon.

There seems to be no evidence of crystal splitting of the ground term, $^5I_8$, although some removal of the 17-fold degeneracy is to be expected. No new lines appear on warming the crystal from 14° to 300°K and no significant alterations in intensity occur. To rule out very low levels, which would not give rise to intensity variations, no small frequently repeated separations occur. It is not permissible from this work to say anything about levels much more than 200–300 cm^{-1} above the lowest.

TABLE IV. *Conglomerate absorption lines of* $Dy_2(SO_4)_3 \cdot 8H_2O$.

20°			78°		300°		20°			78°		300°	
λ	ν	INT.	ν	INT.	ν		λ	ν	INT.	ν	INT.	ν	
4,851.78	20,605.3	5*s*	20,604.2	5*nd*		*L*	4,269.26	416.7	7*nd*	417.1	4*nd*		*L*
47.83	622.1	7*s*	623.6	6*s*		*L*	67.32	427.3	3*nd*	428.2	4*d*	427.5	*H*
39.8	656.3	1	657.1	2*nd*		*H*	63.25	449.7	7*nd*	449.6	5*nd*		*L*
38.0	663.9	1					61.53	459.2	5*nd*	460.6	4*nd*	456.6	*L*
36.6	669.9	2	668.9	1*nd*		*H*	57.57	481.0	9*d*			483.6	*L*
34.57	678.4	6*nd*	678.6	5*d*		*L*	53.34	504.4	7*s*	504.1	3*nd*		*L*
31.26	692.8	4*d*	693.8	3*d*		*L*	49.78	524.0	2	526.5	3*d*	535.5	
29.64	699.7	3*nd*					45.85	545.8	7*nd*	546.1	3*d*		*L*
28.25	705.7	8*s*	707.7	8*s*		*L*						701.3	
					20,723.5	*H*	4,194.1	836.3	0			836.9	
			809.3	2*vd*	814.5	*H*	83.7	895.6	0	900.1	1	885.3	
			863.7	6*vd*	853.6	*H*	80.3	915.0	0	917.9	1		
			888.5	6*vd*		*H*				24,739.4	0	24,744.3	*H*
4,780.84	20,911.0	3*nd*	913.3	6*d*	924.3	*H*				776.8	1		*H*
72.83	946.1	6*nd*	947.5	6*d*		*L*, *H*	4,031.5	24,797.7	0	797.1	1		
67.83	968.1	8*nd*	967.4	6*d*		*L*				819.1	3d	813.1	
62.1	993.3	1	995.1	5*d*		*H*	24.31	842.0	3*s*	843.7	5*d*		
54.24	21,028.0	4*nd*	21,026.3	6*vd*		*H*	13.35	909.8	5*nd*				
49.22	050.2	8*nd*	050.0	7*vd*	21,041.0	*L*	11.45	921.6	8*nd*	915.8	6*vd*		
27.95	144.9	2*d*					07.69	945.0	3*s*				
22.4	169.8	2*vd*	171.6	4*vd*			04.16	967.0	8*d*	959.5	6*vd*		
17.03	193.9	6*vd*	198.0	4*vd*	181.4		3,999.92	993.5	5*vd*	996.1	2*d*		
10.89	221.5	6*s*	223.0	4*d*			95.62	25,020.6	8*vd*	25,022.6	2*d*		
04.45	250.5	5*vd*	253.3	6*vd*	257.1		91.56	045.8	3*d*				
4,698.98	275.3	5*vd*	274.6	6*vd*			88.4	065.6	5*d*	25,063.1			
83.36	346.2	2*vs*					85.5	083.9	5*d*		2*vd*		
82.0	352.4	2*vs*					82.1	105.3		25,100.3			
77.4	373.4	1	374.9	1			79.60	121.1	5*d*				
					21,802.7	*H*	77.2	136.2	5*vd*				
					858.5	*H*	75.1	149.5	5*vd*	25,145	2*vd*		
			888.2	1		*H*	72.4	166.1		165			
			941.5	5*vd*	924.7	*H*	69.6	184.4	5*d*			25,192	
			969.0	4*vd*	970.9	*H*	64.3	218	2*d*				
4,546.56	21,988.5	4*nd*	990.7	6*d*		*L*	61.1	238	5*vd*				
44.42	998.9	3*nd*	22,000.1	6*d*		*L*	55.9	272	5*vd*	25,269			
39.38	22,023.3	5*s*	020.3	5*d*		*L*	53.4	288			2*vd*	25,298	
37.32	033.3	5*s*	039	6*vd*		*L*	52.1	296	5*vd*				
35.07	044.2	5*nd*	045	6*vd*		*L*	46.4	332		25,330			
17.02	132.3	5*d*	132.9	6*vd*		*L*	43.2	353	4*vd*				
4,474.4	343.1	2*d*					37.2	392					
62.30	403.7	1*d*					32.5	422	2*vd*	25,442	4*vd*	25,446	
60.2	414.2	1*d*					23.1	483		482			
					23,059.5	*H*	19.8	504	3*d*	510	2*vd*	Intense	
			23,261.2	0			02.0	621	5*d*	626	2*vd*	diffuse	
4,292.7	23,288.8	0	291.7	5*d*	297.5	*H*	3,899.4	638	5*d*			absorption	
88.0	23,314.4	1	23,315.6	4*nd*		*H*	92.4	681	3*d*	25,681			
82.01	347.0	6*nd*	349.6	7*nd*	334.5	*L*	89.9	700	3*d*	712			
79.0	363.4	8*d*	362.8	8*d*		*L*	33.1	26,081	1*d*	Intense			
77.84	369.7	8*d*	371.0	8*d*	374.9	*L*	25.5	133	1*d*	diffuse			
73.38	394.1	4*nd*	396.3	7*nd*		*H*				absorption			

TABLE V. *Evidence for low-lying levels in* $Dy_2(SO_4)_3 \cdot 8H_2O$. *Frequencies are for 20°K.*

(1) 22 cm^{-1} LEVEL		
ν_A	ν_B	$\Delta\nu_{(1)}$
20,678.4	20,656.3	22.1
20,692.8	20,669.9	22.9
20,968.1	20,946.1	22.0
21,050.2	21,028.2	22.2
23,369.7	23,347.0	22.7
23,416.7	23,394.1	22.6
23,449.7	23,427.3	22.4
23,545.8	23,524.0	21.8
24,967.0	24,945.0	22.0
		Average = 22.2 cm^{-1}

(2) 57 cm^{-1} LEVEL		
ν_A	ν_B	$\Delta\nu_{(2)}$
20,968.1	20,911.0	57.1
21,050.2	20,993.3	56.9
23,369.7	23,314.4	55.3
24,797.1	24,739.4	57.7
		Average = 56.8 cm^{-1}

One reason why the anticipated crystal splitting was not detected may be that the absorbing layers were not thick enough.* No quantitative information is available as to the relative amounts of Ho, Dy, and Er in the samples. Since Ho is known to be relatively more scarce there was probably no more than 0.1 as much Ho as either of the others. However, transitions from excited levels of Dy^{+++} and Er^{+++} are easily detectable in the spectra of single crystals only 1 mm thick while they are not apparent for Ho^{+++} even in 7 mm conglomerates.

$Tm_2(SO_4)_3 \cdot 8H_2O$

Data are in Table VII. There is little change with T, so figures are given only for 20° and

* Especially at 14° and 20°K one is limited to reasonable exposure times.

TABLE VI. *Conglomerate absorption lines of* $Ho_2(SO_4)_3 \cdot 8H_2O$.

14°		20°		78°		169°	300°
λ	ν	ν	Int.	ν	Int.	ν	ν
		15,423.8	1	15,424.8	1		
		425.2	1				
		441.9	1	441.1	1		
6,470.43	15,450.7	449.1	2	445.6	2		
69.67	452.5 *D*	452.5	4*s*	452.4	5*d*	15,451.5	
63.15	468.1	467.9	0				
		472.5	6*s*	472.7	5*d*		15,471.5
60.56	474.3	475.2	6*s*			476.5	474.7
58.69	478.7	478.8	4*s*	478.8	5*d*		478.8
57.82	480.8	480.8	4*s*				
50.69	497.9	498.8	7*d*	499.0	6*d*	501.4	496
45.53	510.8	510.5	3*d*	510.6	5*d*		
43.20	516.0	516.8	4*nd*	516.0	4*d*	516.7	515
41.39	520.3	521.4	4*d*	521.2	3*d*		
		523.4	1				
38.14	528.2 *D*	528.4	3*d*	528.8	4*d*		534
33.18	540.1 *D*	540.3	8*d*	540.5	6*d*		
29.59	548.8	548.6	6*nd*	548.6	4*nd*		
24.85	560.3	562.3	4*d*				
20.90	569.8	570.4	10*nd*	570.2	8*nd*	15,568.6	15,568.4
13.2	589	587.8	2*d*	588.5	2*d*		
04.30	610.2	610.7	8*nd*	608.6	6*nd*	603.4	601.0
5,417.00	18,455.3	18,455.4	3*s*				
15.97	458.8	458.2	1	18,457.2	3*s*	18,461.3	
14.68	463.2	462.8	1				
13.42	467.5	467.6	2				
12.43	470.9	469.9	4*s*	470.7	6*s*	471.4	18,470
10.43	477.7	477.7	2	477.2	1	476.9	
5,398.77	517.6	518.1	2	518.6	2*s*		500
96.53	525.3	525.3	4*s*	525.4	3*s*	525.0	528
5,394.47	18,532.4	18,532.6	6*s*	18,532.9	4*s*	18,531.2	536
84.97	565.6	565.5	2*nd*	566.6	4*nd*		
82.71	572.6	572.2	4*nd*	573.0	4*nd*		
81.51	577.0	578.2	1*d*	579.4	2*nd*	577.0	578
79.54	583.8	583.6	6*nd*	584.8	6*nd*		
76.96	592.7	592.4	8*d*	593.1	6*d*	590.1	
75.75	596.9	597.2	7*nd*	597.8	6*d*	597.2	
74.66	600.7	600.8	3*nd*				
72.87	606.9	606.6	5*d*	607.3	4*d*	606.8	
70.32	615.7	615.3	8*d*	615.2	8*d*		612
67.72	624.7 *D*	624.5	6*nd*	625.3	8*nd*		
63.48	639.4	638.8	8*d*	639.1	6*d*	638.5	18,630
61.00	648.1	647.7	6*d*	648.2	3*d*	649.1	
4,862.27	20,560.8	20,560.8	2	20,559.9	1	20,561.9	
58.40	577.2	576.7	6*nd*	577.1	6*nd*	571.0	20,579
56.06	587.1	587.1	3*s*	586.7	2	582.3	
54.27	594.7	595.3	7*s*	596.4	6*nd*	592.4	
52.14	603.7	602.5	5*s*	601.6	4*nd*	598.3	603
51.02	608.5	608.5	5*s*	607.2	4*nd*	606.2	

14°		20°		78°		169°	300°
λ	ν	ν	Int.	ν	Int.	ν	ν
4,849.68	20,614.2	20,614.6	7*s*	20,615.2	5*s*		20,616
47.03	625.5	624.8	7*s*	624.6	6*s*	20,624.3	
30.63	695.5	694.3	4*nd*	694.6	3*d*		695
4,740.38	21,089.5	21,089.5	6*d*	21,089.0	7*nd*	21,089.9	
36.58	106.4	108.4	4*d*	106.3	7*nd*	104.4	21,105.4
30.81	132.1	132.1	4*nd*	131.2	5*d*	137.9	
		324.2	0	328.0	2*d*		21,330
4,684.98	338.9	338.6	0				
82.91	348.3	349.1	3*s*	348.7	4*d*		346
81.49	354.8 *D*	355.8	2*s*				
79.10	365.7 *D*	366.2	1*s*	365.4	2*s*		370
4,532.83	22,055.1	22,056.5	5*nd*	22,060.3	6*d*		
28.27	077.2	076.0	5*d*				
		079.7	1	079.9	6*d*	22,081.2	22,078
26.29	087.0	088.4	3*nd*	087.3	6*d*		
24.14	097.5	098.0	5*d*			092.6	
21.80	108.9	108.8	5*d*	107.3	6*d*	105.7	22,113
20.59	114.8	115.6	3	114.3	6*nd*		
12.24	155.7	155.6	4*d*	155.4	5*d*	156.1	22,147
09.93	167.1	167.5	4*s*	167.4	5*d*	166.9	
08.05	176.3	176.1	4*s*	177.0	5*d*	176.9	22,177
4,179.23	23,921.1	23,921.1	2	23,922.5	1		23,926
		946.8	1	947.2	2		
71.66	964.6	964.7	6*s*	965.0	6*s*	23,965.5	
70.14	973.3	973.0	6*s*	974.3	6*s*	973.2	23,978
68.38	983.4	983.2	7*nd*	983.9	8*nd*	990.3	
64.14	24,007.8	24,007.2	7*nd*	24,007.1	8*nd*	24,009.9	
		013.3	3	014.2	3	018.8	
		027.1	2	027.1	2	025.1	24,029.0
		033.4	2	032.8	2	041.1	
		046.2	1	046.9	1		
3,914.06	25,541.7	25,541.3	0	25,541.5	1		
10.72	563.5	563.5	4*ns*	563.1	4*s*		
07.96	581.6	581.1	1*ns*	580.7	1*s*		
04.70	602.9	602.0	4*ns*	602.8	4*s*		
01.07	626.8	627.7	4*ns*	627.1	4*s*	Diffuse	
3,895.45	663.7	666.4	1*nd*				
88.89	707.0	706.9	3*nd*	706.6	2*nd*	absorption	
		747.1	1	743.8	1		
79.92	766.5	766.8	2*nd*	767.2	1*nd*	bands	
		792.6	0	793.7	1		
72.9	813	812	2*nd*	815	2		
68.9	840	838	2*nd*	840	1		
		851	0	851	1		
64.6	869	868	1	865	1		
62.4	883	885	1	879	1		
59.2	905	908	1	904	1		
57.8	914	914	1	913	0		
56.8	921	924	1	922	0		

78°K. The spectrum of Tm^{+++} is remarkably simple. Perhaps this is because there is little chance of coupling between electronic and vibrational transitions, as suggested by Bethe and Spedding.[15] It seems that the complexity of the rare earth absorption is roughly symmetrical around the center of the group.

The spectrum of Tm^{+++} has been studied by Gobrecht[16] in absorption and also in emission in the infra-red. He has identified the excited states in terms of allowed states for $4f^{12}$ as was also done by Bethe and Spedding.[15] There is not complete agreement between the two term schemes.

There is no evidence for low electronic levels in Tm^{+++}. The normal state, $^3H_6$, should form six levels in a cubic field. Failure to observe them may be due to the use of insufficiently thick crystals, as with Ho^{+++}. Thus for Pr^{+++} (59) it was found that thicker layers were required to bring out lines from excited levels than required for Nd^{+++} (60) and Sm^{+++} (62). If this effect is characteristic for ions of odd atomic number, then failure to observe the expected crystal splitting in Ho^{+++} (67) and Tm^{+++} (69) becomes understandable.

[15] H. A. Bethe and F. H. Spedding, Phys. Rev. **52**, 454 (1937).

[16] H. Gobrecht, Ann. d. Physik [5] **31**, 600 (1938).

TABLE VII. *Absorption lines of a single crystal of* $Tm_2(SO_4)_3 \cdot 8H_2O$.

λ	20° ν	Int.	78° ν	Int.
6,888.7	14,512.5	1	14,511.7	1
69.0	554.2	1	554.4	1
65.8	560.9	1	560.5	1
61.0	571.1	10*vd*	570.1	6*vd*
52.2	589.8		589.4	
49.2	596.2	10*vd*	596.0	6*vd*
43.7	608.0		608.0	
40.83	614.1	2	615.0	1
38.71	618.6	2	621.2	1
33.0	630.8	10*vd*	630.0	5*vd*
24.7	648.6		649.8	
23.75	650.7	5	650.0	3*d*
6,607.8	15,129.5	1		
06.17	133.2	8*s*	15,132.8	7*s*
02.5	141.6	1	141.6	1
6,598.9	149.9	1	150.0	1
96.1	156.3	1	155.6	1
93.97	161.2	8*s*	161.1	8*s*
91.6	166.6	1	166.3	1*s*
74.1	207.0	1	206.5	1*s*
4,724.11	21,162.1	5*vs*	21,162.1	4*vs*
18.56	187.0	5*vs*	187.2	4*vs*
12.99	212.0	2*vs*	214.7	2*s*
09.71	226.8	2*vs*	226.5	2*s*
4,699.93	271.0	3*s*	272.5	2*s*
79.7	362.9	1	367.5	1
62.42	442.1	2*d*	440.5	2*vd*
59.0	457.8	8*vd*	461.0	5*d*
54.8	477.2		472.1	
47.12	512.7	6*nd*	512.5	6*d*
42.06	536.2	5*nd*	536.4	5*nd*
38.8	551.3	1	547.6	1
3,574.41	27,968.7	5*vs*	27,967.3	5*vs*
69.47	28,007.4	5*vs*	28,005.9	4*s*
60.63	076.9	2*d*	074.0	1

On the Ellipsoids of Polarization of Bonds and Octets

SHENG-NIEN WANG
Department of Chemistry, National Central University, Chungking, China

(Received May 24, 1939)

By using the method of Gunther Sachsse the transverse and longitudinal polarizabilities of bonds and octets occurring in simple organic molecules are calculated from the Kerr constants and the degrees of depolarization of compounds in the gaseous state. The results are more reliable and show more regularities than those calculated by Sachsse from his measurements on solutions.

THE ellipsoids of polarization of many molecules with some symmetrical elements in their ground states have been determined chiefly by Stuart and his co-workers.[1] They are based upon the measurements of Kerr constant, depolarization factor, and the index of refraction in the gaseous state at temperatures where the excited state of nuclear vibration is still not appreciable. Their bearing upon the molecular structure has been manifestly shown. Gunther Sachsse,[2] in studying the Kerr effect of chlorine derivatives of methane, ethane, and ethylene has gone a step further to ascribe longitudinal and transversal polarizabilities to C−H, C−C, C=C bonds and C−Cl octet. Suggestive as this work is, its value is greatly lessened for two reasons. First, the measurement of Kerr constant was carried out in the liquid solution where the theory is far from perfect. Secondly, the presence of more than one strongly interacting bond or octet in the compounds used robs them of much of their independent significance. In view of the theoretical importance of the polarizabilities of bonds and octets, it is deemed worth while to find values of several simple bonds and octets from experimental data of typically simple compounds where only one interactingly active bond or octet is present. In general, a polarization ellipsoid, i.e., a symmetrical polarization tensor, can be ascribed to a bond or an octet. In the case of bonds and octets with rotational symmetry where two of the three principal values are equal and one principal direction is along the axis of symmetry, we prefer the use of b_1^s and b_t^s to denote the longitudinal and transverse polarizabilities of the group s.

[1] H. A. Stuart, Erg. exakt. Naturwiss. **10**, 159–206 (1931). H. A. Stuart, *Molekülstruktur* (Julius Springer, 1934).

[2] Gunther Sachsse, Physik. Zeits. **36**, 357–67 (1935).

All the values of polarizabilities of molecules used in the calculation are taken from Stuart's works. They are listed in Table I.

DERIVATION

We start with methane and ethane in which the state of C−H bonds may be regarded as invariant. Taking into consideration their spatial configuration, we obtain the three relations

$$(8/3)b_t^{C-H}+(4/3)b_l^{C-H}=b^{CH_4}=26.1\cdot10^{-25}, \quad (1)$$

$$(16/3)b_t^{C-H}+(2/3)b_l^{C-H}+b_l^{C-C}=b_1^{C_2H_6}=56\cdot10^{-25}, \quad (2)$$

$$(10/3)b_t^{C-H}+(8/3)b_l^{C-H}+b_t^{C-C}=b_2^{C_2H_6}=40\cdot10^{-25}, \quad (3)$$

linking the four constants of C−H and C−C bonds. On simplification, we have

$$b_t^{C-H}=9.8\cdot10^{-25}-(1/2)b_1^{C-H}, \quad (4)$$

$$b_l^{C-C}=3.8\cdot10^{-25}+2b_l^{C-H}, \quad (5)$$

$$b_t^{C-C}=7.4\cdot10^{-25}-b_l^{C-H}. \quad (6)$$

In order to get their absolute values, one more relation is necessary. Fortunately, we can find one in the case of acetone. If we assume, as we

TABLE I.[3]

MOLECULE	$3\alpha\cdot10^{25}=(b_1+b_2+b_3)\cdot10^{25}$ CC	$b_1\cdot10^{25}$ CC	$b_2\cdot10^{25}$ CC	$b_3\cdot10^{25}$ CC
Cl_2	138.3	66.0	36.2	36.2
HCl	79.0	31.3	23.9	23.9
CO_2	79.5	41.0	19.3	19.3
CH_4	78.3	26.1	26.1	26.1
C_2H_6	135.9	56	40	40
C_2H_2	99.9	51.2	24.3	24.3
C_6H_6	309.6	63.5	123.1	123.1
CH_3Cl	137	54.2	41.4	41.4
CH_3Br	166.5	68.5	49	49
CH_3OCH_3	154.7	63.0	43.1	48.6 $\mu=\mu_3$, $b_2\perp$COC plane
CH_3COCH_3	190	71.0	48.2	70.8

[3] See Tables 45 and 59 in *Molekülstruktur*.

shall do, that the C−H bonds and C−C bonds are essentially in the same state in acetone as in methane and ethane, we have in the polarization ellipsoid of acetone only two additional unknowns, i.e., the longitudinal and transversal polarizabilities of the C=O octet. Since there are three distinct values of principal polarizabilities, we have one new relation which enables us to get the absolute values of the polarizabilities of C−H, C−C bonds and C=O octet.

The orientation of the principal directions is as in Fig. 1. We can easily obtain the following three relations:

$$b_l^{C=O}+2b_l^{CH_3-C}=b_2=48.2\cdot10^{-25}, \quad (7)$$

$$b_l^{C=O}+2b_l^{CH_3-C}\cos^2 55°+2b_l^{CH_3-C}\sin^2 55° = b_1=71\cdot10^{-25}, \quad (8)$$

$$b_l^{C=O}+2b_l^{CH_3-C}\sin^2 55°+2b_l^{CH_3-C}\cos^2 55° = b_3=70.8\cdot10^{-25}. \quad (9)$$

The longitudinal and transversal polarizabilities of the CH_3-C group can be expressed in terms of those of C−C, and C−H bonds. Solving these six equations, we get the following three sets of polarizabilities:

	$(C-H)_l$	$(C-H)_t$	$(C-C)_t$		
$b\cdot10^{25}$	7.2	6.2	18.2		
		$(C-C)_l$	$(C=O)_l$	$(C=O)_t$	
		0.2	19.4	8.0	cc.

Now by assuming the state of C−H bonds still unchanged in some simple compounds, the polarizabilities of many other bonds or octets can be found.

1. Polarizabilities of C−Cl and C−Br octets

From the ellipsoids of polarization of CH_3Cl and CH_3Br, with the use of tetrahedral models, their values can straightwardly be obtained.

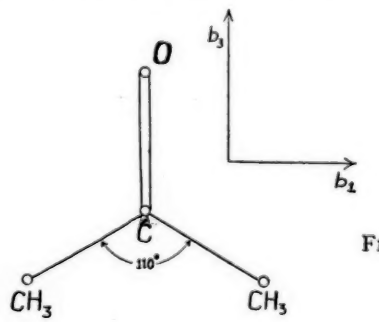

FIG. 1.

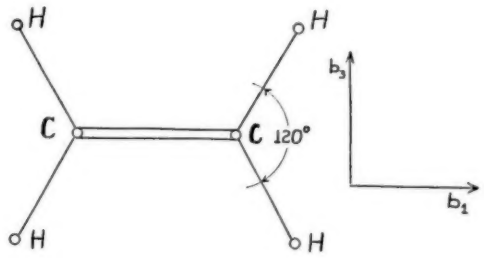

FIG. 2.

	$(C-Cl)_l$	$(C-Cl)_t$	$(C-Br)_l$	$(C-Br)_t$	
$b\cdot10^{25}$	35.3	21.5	49.6	29.1	cc.

2. Polarizabilities of carbon-carbon double and triple bonds

From the ellipsoid of polarization of acetylene we find

	$(C\equiv C)_l$	$(C\equiv C)_t$	
$b\cdot10^{25}$	36.8	11.9	cc.

For ethylene (Fig. 2), on symmetrical grounds, we know one of the three principal directions is along the double bond, and the other two perpendicular to the bond, one perpendicular to the plane of molecule and the other lying in the plane of the molecule. Obviously b_2 and b_3 cannot be equal. But because ethylene possesses no permanent moment, the Kerr constant yields no more information than the depolarization factor in this respect. Therefore the purely experimental results are not sufficient to fix the three principal values. It is perhaps for this reason that b_2 and b_3 are assumed equal in the calculation as stated in Stuart's book.

	100Δ	$(n_d-1)10^4$	$a\cdot10^{25}$
ethylene[3]	2.6	7.25	42.6
	$b_1\cdot10^{25}$	$b_2\cdot10^{25}=b_3\cdot10^{25}$	
	56.1	35.9.	

However, making use of the polarizabilities of C−H bond, we can express the three distinct values of its polarizabilities in terms of the longitudinal and transversal polarizabilities of the C=C bond which the two relations*

$$\frac{10\Delta}{6-7\Delta}=\frac{(b_1-b_2)^2+(b_2-b_3)^2+(b_3-b_1)^2}{(b_1+b_2+b_3)^2}.$$

$$b_1+b_2+b_3=3(n-1)/2\pi N$$

* In these equations Δ is the degree of depolarization, b_1, b_2, b_3 are the principal axes of the polarization ellipsoid. N is Avogadro's number and n, the refractive index.

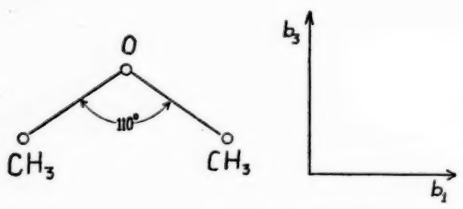

FIG. 3.

suffice to fix. On evaluation, we obtain

	$(C=C)_l$	$(C=C)_t$	
$b\cdot10^{25}$	30.2	9.6	cc.,

and in turn for the ellipsoid of polarization of ethylene

$b_1=56\cdot10^{-25}$cc $b_2=34.4\cdot10^{-25}$cc $b_3=37.4\cdot10^{-25}$cc.

3. Polarizabilities of aromatic carbon-carbon bond

On the assumption that the polarizabilities of $C_{ar}-H$ bond may be, to a good approximation, equated with those of $C_{ali}-H$ bond, we get immediately from the ellipsoid of polarization of benzene

	$(C_{ar}-C_{ar})_l$	$(C_{ar}-C_{ar})_t$	
$b\cdot10^{25}$	23.2	4.4	cc.

4. Polarization ellipsoid of oxygen octet in ether

We make use of the data of dimethyl ether (Fig. 3) in this calculation. The three principal directions of the ellipsoid of polarization of this octet are in coincidence with those of this symmetrical ether. The three values found are, namely,

$b_1=21.9\cdot10^{-25}$cc, $b_2=3.3\cdot10^{-25}$cc, and $b_3=12.1\cdot10^{-25}$cc.

DISCUSSION

It is certain that the assumptions introduced in our calculation can not be strictly correct. For instance, the C−H and C−C bonds which are influenced by the C=O bond in acetone cannot be exactly the same as the C−H and C−C bonds in methane and ethane; the state of C−H bond also can not be altered in passing from methane to ethylene and acetylene. However, the difference may be rather small to justify our procedure. In fact, crude as these values should be, we find many regularities which cannot but be due to their good approximation to correctness.

1.	H−H	C−H	C−C
$b_l\cdot10^{25}$	5.55(6.14)*	7.2	18.0 cc
$b_t\cdot10^{25}$	9.16(8.49)	6.2	0.2 cc

These three bonds are all composed of only single pair of covalence electrons. The hydrogen atom apparently favors a higher value of transversal polarizability while the carbon atom favors a higher value of longitudinal polarizability. In C−H linkage, the effect of H is more than counterbalanced by that of C atoms; hence the longitudinal polarizability is greater. The particularly small value of the transversal polarizability of C−C bond is of great interest. Is it a common property of covalence electron pair between atoms other than hydrogen? There is no information to enable us to test this point.

2.	H−Cl	C−Cl	Cl−Cl
$b_l\cdot10^{25}$	31.3	35.3	66.0 cc
$b_t\cdot10^{25}$	23.9	21.5	36.2 cc

In comparing H−Cl and C−Cl octets, we get a striking confirmation of the generalization in Section 1. The transversal polarizability of H−Cl is greater than that of C−Cl, while of the longitudinal polarizabilities H−Cl has the smaller one. In both H−Cl and C−Cl there are complete octets of electrons; in Cl−Cl, however, the valence electron pair is common to both atoms. Thus we may reasonably expect that the values of polarizabilities of Cl−Cl would be less than twice those of C−Cl and H−Cl. In the case of C−Cl this is found to be true. Nevertheless, we see that the longitudinal value of H−Cl is even less than half of that of Cl−Cl. This again sug-

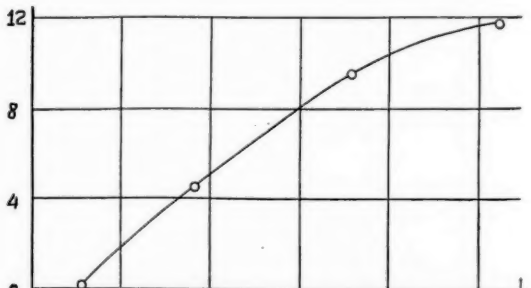

FIG. 4.

* The values in parenthesis are theoretically calculated by B. Mrowka, reference 4.

[4] B. Mrowka, Zeits. f. Physik **76**, 300 (1932); **84**, 448 (1933).

gests the particular property of hydrogen. Indeed, the uniqueness of hydrogen nucleus, as a free proton, is well known, and we find here only another instance of its characteristics.

3.	>C=O(carbonyl)	O=C=O	
$b_l \cdot 10^{25}$	19.4	41.0	cc
$b_t \cdot 10^{25}$	8.0	19.3	cc

We see here that both the longitudinal and transversal polarizabilities of CO_2 are approximately twice those of carbonyl group. This is remarkable in view of the interaction between the two >C=O in CO_2.

4.	C−C	$C_{ar}-C_{ar}$	C=C	C≡C
$b_l \cdot 10^{25}$	18.2	23.2	30.2	36.8 cc
$b_t \cdot 10^{25}$	0.2	4.4	9.6	11.9 cc

By plotting b_l as abscissa and b_t as ordinate, it is found that these four pairs fall on a smooth curve (Fig. 4). May it be possible that the pairs of different bond characters would all fall on a single smooth curve?

It is really unfortunate that the available data are too scanty to make possible a more thorough analysis. Pertinent experimental works in this field are seriously needed.

NOVEMBER, 1939 JOURNAL OF CHEMICAL PHYSICS VOLUME 7

The Thermal Decomposition of Diacetyl*

F. O. Rice and W. D. Walters†
The Johns Hopkins University, Baltimore, Maryland

(Received July 29, 1938)

The products formed in the decomposition of diacetyl indicate an over-all reaction, $CH_3COCOCH_3 \rightarrow CH_4+CO+CH_2=CO$, followed by some decomposition and polymerization of the ketene. The reaction, as measured by pressure change, is first order and is only slightly affected by a large increase in the surface-volume ratio of the reaction vessel. The decomposition has a surprisingly high frequency factor of the order of 10^{17}. A free radical scheme has been proposed for the decomposition but in its present form this scheme does not explain the high frequency factor.

1. Introduction

In the course of an investigation of the thermal decomposition of acetone and other organic compounds it was discovered that the decomposition of diacetyl showed certain effects that merited further study and which will be reported in this and subsequent papers. In this paper we shall give the results of a preliminary study of the pure substance.

The only previous work on the thermal decomposition of diacetyl was the determination by Hurd and Tallyn[1] of the yield of ketene when diacetyl was passed through a hot tube at 605–675°C. They suggest that ketene is produced according to the reaction $CH_3COCOCH_3 \rightarrow CH_2=CO+CO+CH_4$ which they preferred rather than another possibility represented by the equation $CH_3COCOCH_3 \rightarrow 2CH_2=CO+H_2$. Their yields of ketene varied from 11–15 percent at temperatures a little above 600°C, but fell to about 3 percent at 675°C. However, it seems probable that the yield of ketene depends essentially on the extent to which the diacetyl is decomposed and the low yields of ketene obtained by Hurd and Tallyn may be attributed to secondary reactions that occur when a large part of the diacetyl is decomposed.

2. Experimental

In the present study, the rate of decomposition of diacetyl was measured over the temperature range 424–470°C, using a static method in

* In part from a dissertation submitted by W. D. Walters to the Johns Hopkins University in partial fulfillment of the requirements for the degree Doctor of Philosophy.

† Wm. R. Warner Fellow in Chemistry 1934–1938. Present address, University of Rochester.

[1] Hurd and Tallyn, J. Am. Chem. Soc. **47**, 1779 (1925).

TABLE I. *Determination of ketene in the decomposition of diacetyl. 12-liter Pyrex bulb, ketene weighed as acetanilide.*

RUN	TEMP. °C	IN. PRESS. MM	FINAL PRESS.	MOLES KETENE RECOVERED PER MOLE DIACETYL DECOMPOSED
1	397	350	435	0.27
2	407	447	671	0.07
3	399	553	686	0.16

which the rate was followed manometrically. The reaction vessel used for most of the runs was a cylindrical Pyrex bulb 63×130 mm; for experiments with increased surface, a Pyrex bulb filled with thin wall Pyrex tubes was prepared having approximately the same free space as the unpacked bulb. The furnace was manually controlled to within ±1°C and the chromel-alumel thermocouple checked at the boiling point of sulfur to within ±1°C. The rest of the apparatus was substantially the same as that described in a previous paper,[2] except that in the runs at pressures of diacetyl greater than 40 mm, a heating device similar to that described by Steacie and Smith was used.[3] Before taking measurements with a new bulb, four preliminary runs were made and discarded; however the rate in new bulbs was approximately the same as with old bulbs.

In order to obtain samples of the reaction products for analysis, experiments were made in the apparatus described above and also in a 12-liter Pyrex reaction flask. A number of runs were made and at a certain point in the decomposition, the products were removed quickly by expansion into an evacuated bulb together with the use of a Toepler pump. In several runs with the large vessel the products were pumped out through small dry ice and liquid-air traps in order to be able to examine separately the diacetyl, ketene and permanent gas.

Two specimens of commercial diacetyl were purchased from different sources, dried, and carefully purified by several fractional distillations, in each of which only the middle two-thirds was retained. This diacetyl was then stored in a bulb at −80°C and protected from light.

[2] Rice and Polly, J. Chem. Phys. **6**, 273 (1938).
[3] Steacie and Smith, J. Chem. Phys. **4**, 504 (1936).

3. PRODUCTS FORMED

In Table I we give the results of three runs made in the 12-liter flask in which we measured the amount of diacetyl decomposed and the amount of ketene produced. The melting point of the recrystallized acetanilide was found to be 114±.5°C. The last column was obtained by assuming that three moles of products are formed from one mole of diacetyl, according to the equation $CH_3COCOCH_3 \rightarrow CH_4+CO+CH_2=CO$. Although our recovery of ketene was not quantitative, it seems clear that if this equation represents the over-all decomposition, an appreciable portion of the ketene produced is either decomposed or polymerized. We recovered and examined very carefully the liquid portions from these runs, but they seemed to consist only of diacetyl unaccompanied by any other liquid products, except a minute amount of a dark involatile liquid condensed in the cooler portion of the connective tubing. On distillation all the fractions had the correct refractive index for diacetyl and gave an oxime with almost exactly the correct M.P. for diacetyl di-oxime.

The analysis of the gaseous products which are given in Table II are the percentage compositions of the gases after removal of the ketene. There seems to be 4–5 percent of CO_2 formed in the decomposition, but we are somewhat uncertain of this because of the difficulty of proving the presence of this small amount mixed with a large excess of diacetyl and ketene.

Measurements of the final pressure in experiments at 450°C with an initial pressure of 39 mm gave a pressure increase of about 200 percent.

TABLE II. *Analysis of permanent gases formed in the decomposition of diacetyl. Ketene removed by treatment with aniline and aqueous* KOH. *High pressure runs made in 350* cc. *Pyrex reaction vessel, low pressure runs made in 12 l. Pyrex reaction vessel.* $\Delta P/2P_0$ *gives approximately the percent decomposition.*

TEMP. °C	INITIAL PRESS.	$\Delta P/2P_0$	CO	CH_4	C_2H_4	C_2H_6	H_2
424	428	17.5	56.1	33.7	4.7	2.3	0
424	376	24.5	57.3	36.5	3.1	1.5	1.6
436	378	37	57.5	33.9	4.7	2.0	0.3
436	336	51	54.4	30.8	5.6	5.1	1.6
470	227	88	54.0	35.2	6.5	3.5	1.3
406	39	12	50.9	36.4	7.6	3.1	1.7
407	39	16.5	56.6	36.0	5.2	1.2	1.0
451	39	97.5	52.4	33.5	12.0	2.3	0
450	38	99	51.3	32.2	11.8	3.7	0.5

The pressure increases in runs carried to completion, using initial pressures of 200 mm, at 470°, 460°, 450°, and 436°C were found to be 193 percent, 189 percent, 187 percent and 177 percent, respectively.

The products of the reaction together with the pressure increase observed, indicate an over-all reaction,

$$CH_3COCOCH_3 \rightarrow CH_4 + CO + CH_2{=}CO$$

followed by some decomposition and polymerization of the ketene.[4]

4. Kinetics

According to the pressure measurements, the reaction proceeds without any induction period. The summarized results are given in Table III, where $t_{12.5}$, t_{25}, and t_{50} are the times for the pressure to increase 12.5 25 and 50 percent, respectively; the actual percentage decomposed will be somewhat more than half of these percentage pressure increases.

The fractional times are constant (within our experimental error) with varying initial pressures, showing that the reaction is first order. For a given run, the first-order constant, calculated on the basis that the final pressure represents complete decomposition, begin to fall off appreciable after 30 percent decomposition, the reaction products apparently exerting an inhibiting influence. However, a retarding effect by unsaturated products such as ketene or ethylene is to be expected, and a falling off of first-order constants during a run cannot be taken as significant. Moreover, an apparent falling off of the constants might occur if more diacetyl had decomposed during the early stages of the reaction than would be indicated by a comparison of ΔP_t with ΔP_∞.

From Table III it will be seen that the rates of decomposition in the experiments carried out in the packed vessel were about 15 percent slower than those in the unpacked vessel, so that we may assume that ordinary surface catalysis is not present to an appreciable extent.

If it is assumed that the slight variation of final pressure with temperature is due to some slow reaction taking place subsequent to the initial decomposition of diacetyl, then the fractional times given in Table III, which are near the beginning of the reaction would represent equal percentages of decomposition at all temperatures. The activation energy for initial pressures of about 350 mm may then be obtained in the usual way by plotting logarithms of reciprocal fractional times against the reciprocal of the absolute temperature. The value for $t_{12.5}$ is 69.1 kcal. and the values for t_{25} and t_{50} are

[4] Williamson, J. Am. Chem. Soc. **56**, 2216 (1934); Muller and Peytral, Comptes rendus **196**, 279 (1933); and Hurd and Williams, J. Am. Chem. Soc. **58**, 962 (1936).

TABLE III. *Rate of decomposition of diacetyl. In most cases each result is the mean of at least three experiments.*

Temp. °C	P. mm	$t_{12.5}$ sec.	t_{25} sec.	t_{50} sec.
Unpacked Bulb				
470	40	32	68	159
470	196	36	74	165
470	253	35	72	167
470	322	35	73	171
470	352	35	74	172
470	382	38	77	178
460	40	65	134	318
460	244	65	139	325
460	265	73	154	359
460	289	70	148	350
460	327	73	152	373
460	405	71	149	364
460	428	69	148	368
450	40	133	288	686
450	201	133	287	714
450	253	131	287	691
450	317	139	307	776
450	342	142	299	743
450	402	137	295	743
450	458	140	300	751
436	40	384	789	1860
436	140	342	708	1650
436	144	333	711	1720
436	278	350	753	1860
436	320	334	730	1900
436	410	345	760	1960
436	487	336	744	1920
424	291	830	1790	—
424	315	780	1740	—
424	379	770	1730	—
424	405	805	1790	—
424	427	744	1720	—
Packed Bulb $(S/V)_{\text{PACKED}} \div (S/V)_{\text{UNPACKED}} = 25$				
450	246	156	348	838
450	296	169	352	855
450	336	152	352	886
450	340	156	343	832
450	362	158	344	833

slightly higher, but within our experimental error which we estimate to be ±3 kcal. At initial pressures of 40 mm a value of 74.6 kcal. was obtained, but the experimental error in these experiments is higher. The variation of $t_{12.5}$ with the temperature is given by the equation,

$$1/t_{12.5}=5.3\times10^{18}\times e^{-69,100/RT}\text{ sec.}^{-1}.$$

The first-order reaction constant calculated from the data at 450°C, assuming that 2.9 volumes of products are produced from each volume of diacetyl, is

$$k=0.0681/t_{12.5}=3.6\times10^{17}\times e^{-69,100/RT}\text{ sec.}^{-1}.$$

If, on the other hand, it is assumed that the variation of total pressure increase is due to a reaction occurring simultaneously with the decomposition, the activation energy, obtained from fractional times representing equal percentages of decomposition rather than equal percentages of pressure increase, would be 66.5±3 kcal. and the value of the reaction constant

$$k=6.0\times10^{16}\times e^{-66,500/RT}\text{ sec.}^{-1}.$$

5. Discussion

A general scheme for the free radical decomposition of organic compounds may be written as follows:

$$M_1\rightarrow 2R_1, \quad (1)$$

$$R_1+M_1\rightarrow R_1H+R_2, \quad (2)$$

$$R_2\rightarrow R_1+M_2, \quad (3)$$

$$R_1+R_2\rightarrow R_1-R_2, \quad (4)$$

in which an organic compound M_1 decomposes into two radicals R_1 which attack the substrate forming R_1H and the large radical R_2; the large radical decomposes into R_1 and the molecule M_2. In this particular scheme, the termination occurs by a cross combination of the chain radicals R_1 and R_2. It has already been shown[5] that a scheme of this kind gives an over-all unimolecular reaction rate.

The free radical decomposition of diacetyl may be represented as follows:

$$CH_3COCOCH_3\rightarrow 2CH_3CO \quad (5)$$

or

$$\rightarrow CH_3+COCOCH_3, \quad (5a)$$

$$CH_3CO\rightarrow CH_3+CO, \quad (6)$$

$$CH_3COCO\rightarrow CH_3+2CO, \quad (6a)$$

$$CH_3+CH_3COCOCH_3\rightarrow CH_4+CH_2COCOCH_3, \quad (7)$$

$$CH_2COCOCH_3\rightarrow CH_2=CO+CH_3CO, \quad (8)$$

$$CH_3CO\rightarrow CH_3+CO, \quad (9)$$

$$CH_3+CH_2COCOCH_3\rightarrow CH_3CH_2COCOCH_3. \quad (10)$$

In this scheme, reaction (5) corresponds to reaction (1), and we can probably neglect reaction (6) owing to the relative instability of the acetyl radical. Even if the primary break consists of separation into CH_3 and CH_3COCO, the same reasoning would be expected to apply. Reaction (7) should have a very low activation energy since the highly resonating radical $CH_2COCOCH_3$ is formed. On the other hand, the activation energy of (8) should be high and hence the chain ends by (10). We have neglected such reactions as

$$CH_3+CH_3COCOCH_3\rightarrow CH_3COCH_3+CH_3CO, \quad (11)$$

in which a radical attacks an exposed negative group, for reasons given in a previous paper.[6]

The reactions in the free radical decomposition of diacetyl therefore follow essentially the scheme shown in reactions (1) to (5) and hence a unimolecular decomposition of diacetyl would be expected on the basis of the free radical scheme. On the other hand, the free radical scheme in its present form offers no explanation of the high frequency factor of $\sim10^{17}$ and this question will be considered in another paper.[7] This surprising result makes it very desirable to measure directly the change of substrate concentration with time,[8] and one of us (W.D.W.) is preparing to do this.

[5] F. O. Rice and K. F. Herzfeld, J. Am. Chem. Soc. **56**, 284 (1934); F. O. Rice and K. K. Rice, *Aliphatic Free Radicals* (Johns Hopkins Press, Baltimore, 1935), p. 87.

[6] F. O. Rice and E. Teller, J. Chem. Phys. **6**, 489 (1938); **7**, 199 (1939).

[7] F. O. Rice and K. F. Herzfeld, this Journal.

[8] See Rice and Vollrath, Proc. Nat. Acad. Sci. **15**, 702 (1929).

Phase Transitions*

JOSEPH E. MAYER AND S. F. STREETER
Havemeyer Hall, Columbia University, New York, New York

(Received June 23, 1939)

H-T and *V-P* curves for various types of phase transitions are shown. In second-order transitions a discontinuity in the curvature of the free energy occurs. It appears to follow that some change in the system must be occurring in the phase of high heat capacity, and that this change is such that it has gone to completion at the transition, so that an extrapolation of the phase is meaningless. It is shown that it is extremely difficult uniquely to prove, by calorimetric or equation-of-state data alone, the presence of an anomalous first-order transition, in which heat capacity and compressibility approach infinity continuously as the transition is approached. This type of transition can be distinguished by obtaining two phases of differing density in equilibrium, or by sound velocity measurements.

A tentative discussion of phase transitions, based on a suggestion of Frenkel, is given. It is shown that the factors determining the type of transition can be partially unraveled. A positive surface free energy between the phases necessitates a simple first-order transition.

The relation of the Band and Frenkel developments, for an imperfect gas, to the method based on Ursell's development is discussed, and it is shown that the two methods are not identical.

INTRODUCTION

IF the heat content H of a macroscopic one component system is plotted against the temperature T, at constant pressure P, the slope, $(\partial H/\partial T)_p = C_p$, is always positive. If the plot is vertical at some temperature, C_p infinity, this temperature is that of a first-order phase transition. Correspondingly the plot of the volume V against P at constant T has always a negative slope, $-\beta V = (\partial V/\partial P)_T$, which is minus infinity as the pressure of a first-order phase transition.

The normal first-order transitions, to which the chemist is most accustomed, have almost normal specific heats, C_p, and compressibilities β, as the transition point is approached. That is, there is little evidence, in the behavior of the stable phase, of the approaching calamity, as the transition is neared.

It is, of course, thermodynamically possible that C_p and β (necessarily both if both heat content and volume change) approach infinity continuously as the transition point is neared. Such behavior one might refer to as an anomalous first-order transition.

Columns I and II of Fig. 1 show plots of these functions for these two cases.

If the heat content rises abruptly, and the volume decreases rapidly, in a small temperature pressure range, but the changes are of such a nature that C_p and β, although showing abnormally high values, remain finite, the region may be referred to as one in which the system undergoes a diffuse transition. The plots of the functions for a diffuse transition are shown in column III of Fig. 1. Rutgers[1] has shown that if such transitions occur in sufficiently small temperature pressure ranges the line of the transition, in the $P-T$ diagram, is determined by certain ΔH and ΔV values with exactly the same equations as the first-order transition.

The second-order transition, named by Ehrenfest,[2] is characterized by a break in the slope of the H and V curves, without a discontinuity in their values, column V, Fig. 1. The thermo-

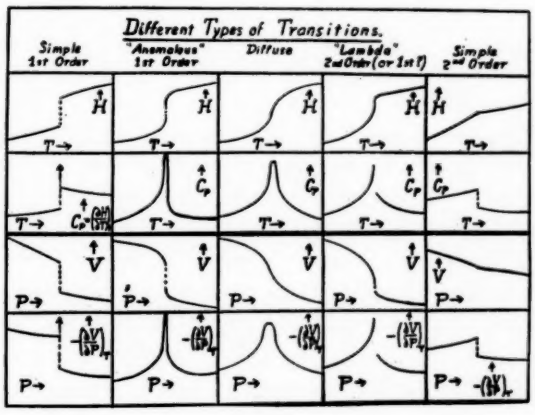

FIG. 1.

* Contribution from the Chemical Laboratory of The Johns Hopkins University.

[1] A. J. Rutgers and A. Wouthuysen, Physica **4**, 515 (1937).
[2] P. Ehrenfest, Leiden Comm. Suppl. 75b (1933).

dynamics of these transitions have been discussed by Ehrenfest.

The second-order transitions are probably always of the type indicated in column IV, in which an abnormal rise in H, and decrease in V, precedes the transition on the low temperature side.

It is obvious from a study of the plots that various intermediate cases are possible, and that a sharp experimental distinction between some of these cases would be difficult.

Second-Order Transitions

One peculiarity of the second-order transitions has been remarked,[3] and has led to some scepticism about their existence.[4] The second-order transition is characterized by a discontinuity in $C_p = -T(\partial^2 F/\partial T^2)_p$, a discontinuity in the curvature of the free energy. The extrapolation of the Gibbs' free energy F of the phase with the *higher* heat capacity C_p always lies *lower* than that of the other phase on *both* sides of the transition point.

It has been common to explain first-order transitions by the fact that the free energy curves of the two phases cross, the phase having the lower free energy being always the stable phase. In the case of the second-order transition there must be some reason why the extrapolation of the free energy of the phase of higher heat capacity is meaningless,[5] since otherwise, if the extrapolation of the phase were conceivable, the extrapolated phase would necessarily be stable. The difficulty is not obviated by assuming that the specific heat has actually no discontinuity, but only a *sharp* break in slope.[4]

In short, one must assume that in all second-order transitions there is some natural reason why the phase of high heat capacity can have no extrapolated existence beyond the transition point. This can be clearly understood if one assumes that this phase consists of essentially a mixture of two phases, the fraction of the high temperature phase growing rapidly with temperature accounts for the high heat capacity. The transition point corresponds to the attainment of complete conversion. Stated more generally, the abnormal heat capacity of this phase is due to some change, which, by its very nature, cannot proceed indefinitely. After the change has occurred completely, the heat capacity drops abruptly to a lower value. In a later section we shall endeavor to show a more formal representation of this case.

In those cases for which the explanation of the second-order transitions are at least partially understood, it is clear that this situation exists. In the transition from the low temperature to the high temperature modification of liquid helium presumably the translational degeneracy of the molecules is lifted. The abnormal heat capacity of helium II[6] is due to the increasing numbers of molecules entering the normal momentum states. When the lowest state is emptied the abnormal heat capacity ceases; an extrapolation to less than zero numbers of molecules in this lowest state has no meaning.

Similarly, in the order-disorder transitions of alloys the transition point occurs when one hundred percent disorder is attained. The transition to free rotation must also belong to the point where complete free rotation is attained, in the cases for which a second-order transition is observed.

Experimental Criterion of an Anomalous First-Order Transition

One purpose of this paper is to emphasize the experimental difficulties in distinguishing clearly between the three cases of columns II, III, and IV of Fig. 1: the anomalous first order, the diffuse, and the lambda-transition. Calorimetric and equation of state measurements always serve, essentially, only to give isolated experimental points on an H-T or V-P curve. It is true that the points may be obtained relatively close together, but the derivatives, C_p and $-(\partial V/\partial P)_T$, are not directly measured, except as finite differences, $\Delta H/\Delta T$ and $-\Delta V/\Delta P$.

It is, of course, clear that certain transitions are diffuse, and not anomalous first order. Others appear to be definitely second order, and are at least certainly not first order, since C_p is assuredly

[3] W. H. Keesom and Miss A. P. Keesom, Physica **1**, 161 (1934).
[4] E. Justi and M. v. Laue Zeits. f. tech. Physik **15**, 521 (1934).
[5] W. H. Keesom, Leiden Comm. Suppl. 80b, p. 7 (1936).
[6] F. London, J. Phys. Chem. **43**, 49 (1939).

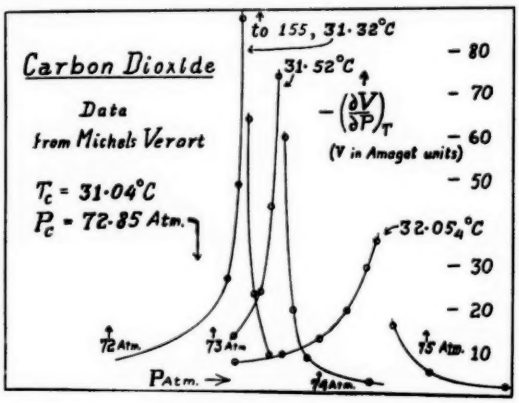

FIG. 2.

everywhere finite. No transition of the anomalous first-order type has been described as such from experimental data, except the explanation given by one of us[7] of certain anomalies just above the critical point.

It appears, however, that the possibilities of such an anomalous first-order transition occurring as that sketched in column II, Fig. 1, or a lambda-transition of column IV which is truly first order, have been somewhat neglected.

The simple first-order transitions, column I, are readily detectable. Even if the material investigated contains an impurity, in which case the H and V curves at the transition are not truly vertical, the sharp discontinuity in slope is readily distinguished from the experimental points. However, the most convincing demonstration of the existence of the transition is in the possibility of obtaining, and maintaining, the two separate phases of demonstrably differing densities and heat content in equilibrium with each other.

The anomalous first-order transition (column II) is scarcely distinguishable from an abrupt diffuse transition (column III), or even from a lambda-type transition (column III), in which the specific heat is abnormally high at the transition point. By plotting the observed experimental points of H against T, or of V against P, on a sufficiently large scale, it is always possible to draw a smooth curve through the points, the derivatives of which are all continuous. The difficulty of distinguishing is increased by the fact that in all real systems the presence of impurities always means that the H and V curves are not exactly vertical, even if a true anomalous first-order transition is present (column II). In this case (of a two component system) the transition is characterized by an abnormal rise in C_p (or β), and a discontinuity, at the initial P-T values of the transition in the slope of the C_p or β curve. Thus one must distinguish in the H-T or V-P curve drawn through the experimental points a discontinuity in the *second* derivative, a task which is almost impossible, even with the best data.

The existence of a "latent heat" is not a distinguishing mark, since the integral under the region of abnormal heat capacity plays *exactly* the same thermodynamic role as a latent heat (see Rutgers).

The difficulty of deciding from equation-of-state data is illustrated in Fig. 2. The data used are the excellent P-V data on CO_2 in the critical region obtained by Michels Verart.[8] It is seen from the figure that one can scarcely believe the compressibility curve to be continuous at 0.28° and 0.48° above the critical point. Even at 1° above T_c the curve certainly does not appear to be continuous, although here it also does not appear to go to infinity. By choosing the pressure axis scale tenfold greater, however, one could draw a reasonable appearing curve through these points.

On the other hand the points of these curves are themselves the differences of the two experimental points, $\Delta V/\Delta P$ and this method of choosing the slopes of finite chords of the true curve always leads to a smoother set of points than the true slopes would give. It is altogether doubtful whether, even with data as good as this, one can actually distinguish between an anomalous first-order or a diffuse transition.

It may be objected, in this case, that the classical theory, which assumes a diffuse transition, requires an enormously steep V-P curve so close to the critical point. Fig. 3 demonstrates the very considerable difference between the observed P-V points and the simplest classical equation: the van der Waals curve. The experimental point at $V/V_c=1.12$ shows about one-

[7] S. F. Harrison and Joseph E. Mayer, J. Chem. Phys. **6**, 101 (1938).

[8] A. Michels, B. Blaisse and C. Michels, Proc. Roy. Soc. London **A160**, 358 (1937).

fifth of the deviation from horizontal that is predicted by the van der Waals equation for the same temperature.

It appears to be clear, that whereas the experimental data of Michels Verart do not show horizontal P-V curves above the critical point, they nevertheless can be explained by assuming very small traces of impurities, and a true anomalous first-order transition. There is considerable difficulty in fitting the points to a smooth curve with continuous derivatives. The experimenters[9] have remarked that different virial coefficients are required to fit the data above and below the critical densities.

In particular, the heat content may be calculated at any pressure and temperature from the known heat content curve of the perfect gas, and the P-V data. It makes no essential difference in the calculated value if the P-V curve is assumed to be *exactly* horizontal in a short volume range, or very nearly so as given by the experimental points. The argument of an absence of "latent heat" is wholly fallacious.

Having attempted to demonstrate that equation of state data, and also calorimetric data, cannot uniquely decide between a diffuse and anomalous first-order transition in this case, we might well enquire whether any experimental procedure can so decide. Two methods, at least, appear to be available.

The first of these is the method so successfully employed by Maass[10] and his co-workers, who have shown that two phases of differing density to coexist at the same temperature and pressure above the critical point.

This method is not without difficulty. Since the $(\partial P/\partial V)_T$ curve is continuous for the anomalous first-order transition, as distinct from the simple first-order case, the extrapolated density and free energy of either phase does not differ from that of the equilibrium mixture of both phases. An isothermal compression will, consequently, always result in a uniform change of density throughout the system, instead of a separation into two macroscopic regions of differing density, as in the simple transition. It

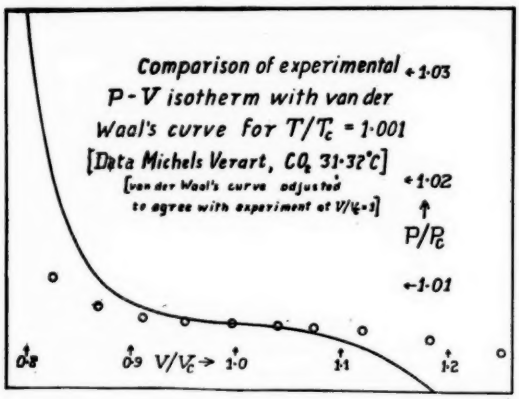

FIG. 3.

is therefore necessary to resort to a trick to obtain the two differing phases in different macroscopic parts of the system. Maass accomplishes this by heating the material at constant volume, approximately the critical volume, through the critical point.

The plots of density against height which are obtained are equivalent to plots of density against an almost linear, but enormously extended, pressure scale. Marked discontinuities are observed. The possibility of inadequate mixing of impurities appears to be answered by maintaining these density differences for as long as six hours without observable change, in spite of gentle stirring.

Certain peculiarities in the dependence of the system upon history are ingeniously explained by Pall.[11] The authors feel that these experiments conclusively demonstrate the existence of an anomalous first-order transition in these cases.

A second method of approach appears to be capable of distinguishing between these various types of transitions. This is the measurement of sound velocity, which determines $(\partial P/\partial V)_S$. Since a derivative (at low sound intensities) is directly measured, one may expect, from a plot of the experimental points, to distinguish discontinuities in the slope.

An anomalous first-order transition should show a marked decrease in sound velocity plotted against volume as the transition point is approached. At the limiting volume of the phase the plot should become (discontinuously) horizontal, and then show a discontinuous increase in

[9] A. Michels and Mrs. C. Michels, Proc. Roy. Soc. **A160**, 348 (1937).

[10] J. S. Tapp, E. W. R. Steacie and O. Maass, Can. J. Research **9**, 217 (1933); C. A. Winkler and O. Maas, *ibid.* **9**, 613 (1933); O. Maas, Chem. Rev. **23**, 17 (1938).

[11] David Pall, dissertation, McGill University (1939).

slope upwards as the volume of the second phase is reached. The presence of impurities would not alter the discontinuities of slope, but would only result in a not exactly horizontal range in the volume range of the transition. A discontinuity in the value of the sound velocity itself would indicate a second-order transition.

A Tentative Theory of Phase Transition

It appears to be possible to present a half-thermodynamic, half-statistical, theory of phase transitions which gives some insight into the factors determining which type of transition will occur in a special instance.

We shall adopt a method proposed independently by Band[12] and by Frenkel,[13] and identified, somewhat erroneously we believe, by these authors with a method previously employed by one of us.[14]

We treat a system, the molecules of which are primarily in a certain phase, say the phase a, but at a temperature and pressure near the transition line to a second phase b. It will be assumed that some division of the phase space for the molecules can be drawn which would enable us to say that in a certain region of the phase space, l molecules formed a cluster which existed as the phase b. We shall not enquire further how such a division should be made, but assume its conceivability.

The formation of a cluster of l molecules in phase b, as an island in the molecules of phase a, will be accompanied by some standard change in free energy $\Delta F(l)$, which will be positive, for large values of l at least, in the temperature pressure region for which the phase a is stable.

Now the ratio of the numbers of molecules N_{lb} existing in such clusters of l molecules each as phase b, to the number of molecules N_a existing as phase a will be proportional to the exponential of $-\Delta F(l)/kT$, and the ratio of all the molecules, N_b, in phase b, to all those in phase a, N_a, will be the sum of this ratio over all values of l,

$$\frac{N_b}{N_a}=\sum_l B(l)e^{-\Delta F(l)/kT}. \tag{1}$$

In this $B(l)$ is a function depending on l only as some small power of l. When this ratio is zero only phase a exists. When the ratio is infinity only phase b is present.

The change in free energy $\Delta F(l)$ for l molecules going from phase a into a cluster of l molecules of phase b will be proportional to l for sufficiently large values of l. If ϕ is defined by the equation:

$$\phi=\lim_{l\to\infty}\left\{\frac{1}{l}\Delta F(l)\right\}, \tag{2}$$

and $\theta(l)$ as

$$\theta(l)=\Delta F(l)-l\phi, \tag{3}$$

then (1) may be written as

$$\frac{N_b}{N_a}=\sum B(l)e^{-\theta(l)/kT}(e^{-\phi/kT})^l, \tag{4}$$

or

$$\frac{N_b}{N_a}=\sum f(l)\zeta^l, \tag{4'}$$

where

$$f(l)=B(l)e^{-\theta(l)/kT}, \quad \lim_{l\to\infty}\left\{\frac{1}{l}\ln F(l)\right\}=0, \tag{5}$$

$$\zeta=e^{-\phi/kT}. \tag{6}$$

The function $f(l)$ has been defined in such a a way that the sum (4'), N_b/N_a, is finite if $\zeta<1$, and infinite if $\zeta>1$, since all the terms of the sum are necessarily positive. The apparent lack of symmetry, that N_b/N_a is finite, but not necessarily zero, for $\zeta<1$, $\phi>0$, whereas this ratio is infinite if $\zeta>1$, $\phi<0$, comes about because the possibility of islands of molecules of phase a within the large clusters of phase b has been neglected.

The neglect of this possibility is arbitrary, but is merely included here in the definition of what is meant by phase b. We define any region enclosed by molecules of this phase as belonging completely to that phase. Since it is desired, at present, to discuss the behavior of the system in the pressure temperature range for which ϕ is positive or zero, the arbitrariness of this procedure will not concern us.

The behavior of the ratio N_b/N_a as the transition point $\phi=0$, $\zeta=1$ is approached (from the side for which $\phi>0$, $\zeta<1$) partially determines the character of the phase transition, and this behavior is fully determined by the character of the function $f(l)$.

[12] William Band, J. Chem. Phys. **7**, 324 (1939).
[13] J. Frenkel, J. Chem. Phys. **7**, 538 (1939).
[14] Joseph E. Mayer, J. Chem. Phys. **5**, 67 (1937).

If the sum $\Sigma f(l)$ converges, the ratio N_b/N_a approaches a finite value, the value of this sum, as the pressure and temperature for which $\phi=0$ is approached. In the succeeding infinitesimal change of temperature or pressure for which ϕ becomes negative, this ratio, N_b/N_a becomes infinite. The transition is then first order. If the sum $\Sigma f(l)$ diverges, the ratio N_b/N_a approaches infinity continuously as the temperature and pressure is approached for which $\phi=0$, $\zeta=1$. In this case the transition will not be first order.

The nth derivative of this ratio, N_b/N_a, with respect to T or P contains an additive term $\Sigma l^n f(l)\zeta^l$ multiplied by the nth power of the logarithmic derivative of ζ with respect to T or P. If all sums $\Sigma l^n f(l)$ are finite, then all the finite derivatives of the thermodynamic functions of the system remain finite as the transition point is approached. This is the case of the usual simple first-order transition.

If, on the other hand, the sum $\Sigma f(l)$ converges, but $\Sigma l f(l)$ diverges, the ratio N_b/N_a remains finite as the transition is reached, but its rate of change with T or P is infinite. The heat capacity C_p and compressibility β approach infinite values continuously at the transition. This is the case of the anomalous first-order transition.

Let us now return to Eqs. (5) and (3) which define the function $f(l)$. One would normally expect $f(l)$ to contain an additive term $l^{\frac{2}{3}}\sigma$ proportional to $l^{\frac{2}{3}}$, the interfacial free energy of the surface between the two phases a and b. The function $f(l)$ then contains the factor $(e^{-\sigma/kT})^{l^{\frac{2}{3}}}$, which will be its most important factor at large values of l. In this case, if σ is *positive*, all sums $\Sigma l^n f(l)$ will converge for finite n, and the transition will be a normal first-order transition, with all derivatives of the thermodynamic functions approaching finite values as the transition is approached.

If the surface free energy were negative the clusters would seek a geometrical shape such as to increase their surface (two-dimensional or one-dimensional string-like or octopus-like structures) and the surface would be no longer proportional to the $\frac{2}{3}$ power of the numbers of molecules, l, but to the first power of l. In this case the term $l^{\frac{2}{3}}\sigma$ would be missing in $\theta(l)$. The function $f(l)$ would then be determined by second-order combinatory factors entering into the exact statistical analysis, and would be expected to vary more like some power, ν, of l, as l becomes large.

The behavior of the system as the transition point is approached from the side of stable phase a depends, then, on this power ν of l which gives the dependence of $f(l)$ on l at high l values. For instance, one finds that if $-2\leq\nu<-1$ an anomalous first-order transition will occur, since $\Sigma f(l)$ converges and $\Sigma l f(l)$ diverges. If $-1\leq\nu<0$ the heat capacity approaches infinity at the transition, but the heat content curve is not vertical over a finite range of its values.

The description given so far is incomplete, insofar as the formation of phase a within the larger clusters of phase b have been neglected. The inclusion of this possibility, with equations which will be symmetrical to those already used, permits one to depict the nature of the approach to the transition from the side of stable phase b. If, in the absence of a surface energy term, the two functions $f(l)$ for clusters of phase b in a, and clusters of phase a in b, do not have the same analytical form, the transition will not be symmetrical as approached from the two sides.

This description of the phase transitions appears to offer some explanation of the different behavior in different cases. The presence of a positive surface energy between the two phases necessitates a simple first-order transition. In the absence of this term the type of transition is determined by certain combinatory terms, of no especial importance when the surface energy is present, which determine the relative weights of the large and small clusters.

Relation of the Band-Frenkel Approach to the Ursell Development

Both Frenkel and Band have implied that an approach somewhat similar to, but more detailed than, that given here, to the formation of clusters of molecules in the imperfect gas, was identical to the approach used by us, and based on Ursell's development, in treating the statistical mechanics of condensing systems. There is, however, an important difference between the two methods. The difference can best be illustrated by stating the difference between the definition of the numbers of clusters of certain sizes in each

case. Frenkel and Band both define the total number of pairs of molecules which are close enough together to interact as the number of clusters of two molecules each in the gas. It is obvious that this number depends on the exact choice of the limiting distance at which interaction is said to be appreciable, and is, consequently, arbitrary. In the statistical development certain numbers, m_l^*, were introduced, which were called the numbers of clusters of l molecules each, in the equilibrium distribution. These numbers, however, expressed *excesses* over random expectations. That is, m_2^* is the number of pairs of molecules close together *in excess* of that expected from the given density m_1^*/V of single molecules. Thus m_2^* can be a negative number, as it is at temperatures higher than the Boyle point.

Similarly, the cluster integrals Vb_l, introduced by us, are not simply the factor in the configuration integral due to the l molecules close together, but an integrated excess contribution due to the mutual potential of the molecules, over the extrapolated contribution obtained when any of the molecules are far from the others in the cluster. It is only by this trick that it is possible to state exactly the volume dependence of these integrals at large volumes, namely that Vb_l is proportional to volume, and b_l independent of volume.

The contribution, as a factor in the configuration integral, of one of the clusters defined by Band or Frenkel is *not* exactly proportional to V, since a portion of the volume space of the system is occupied by the other clusters and free molecules, and is not available to the cluster considered. In this case the factor might be more nearly approximated as $V-(N-l)b$, where b is the volume excluded by one molecule. The excluded volume, however, is not the same for one cluster of two molecules as for two single molecules, and is volume dependent. This method, then, although possessing certain advantages in the simplicity of its treatment, does not have the formal accuracy of the method based on Ursell's development.

NOVEMBER, 1939 JOURNAL OF CHEMICAL PHYSICS VOLUME 7

The Statistical Mechanics of Condensing Systems

VI. The Treatment of a System of Constant Energy

S. F. Streeter† and Joseph E. Mayer
Chemical Laboratory, The Johns Hopkins University, Baltimore, Maryland

(Received June 23, 1939)

The equations for the thermodynamic functions of an imperfect gas up to and including the pressure of condensation, are calculated for a one-component system consisting of chemically saturated molecules. The method starts with the calculation of the phase volume available to a system below a given energy. The thermodynamic functions are expressed in terms of integrals over the configuration space of a few molecules, the integrands involving the mutual potentials. The equations derived are formally equivalent to those derived in the previous papers of this series, using the Gibbs method.

1. Introduction

THERE are two common procedures available for the application of statistical methods to the calculation of the macroscopic thermodynamic properties of a mechanical system. These are, firstly, the method of Gibbs, in which the system considered is assumed to be kept at constant temperature, and, secondly, by the calculation of the total number, Ω, of quantum states available to a system of known energy.

The first method treats a system in equilibrium with an infinite heat reservoir of fixed tempera-

† Part of a dissertation submitted in partial fulfillment of the degree of Doctor of Philosophy at The Johns Hopkins University.

ture, which may (or may not) be taken to be a canonical ensemble of systems identical to that treated. The probability that the system considered be in a single (nondegenerate) quantum state n, of energy E_n is then proportional to the exponential of $-E_n/kT$. If the system can be treated classically, its properties are completely determined by the value of the Gibbs phase integral for the system.

In the previous papers of this series,[1] which will occasionally be referred to by Roman numerals, the development of Ursell[2] has been extended to enable calculation of the phase integral for a comparatively general system. The resulting equations for the thermodynamic properties of the system involve certain integrals which have been called cluster integrals, b_l, and irreducible integrals, $\beta_\mathbf{k}$. These are integrals over the configuration space of l and $\mathbf{k}+1$ particles, respectively. The integrand of these integrals are sums of products of functions of the distances r_{ij} between the molecule pairs i and j. The particular function $s(r_{ij})$, entering, is $e^{-u(r_{ij})/kT}-1$ in which $u(r_{ij})$ is the mutual potential energy of the pair of molecules i and j.

The cluster integral b_l involves the sum of all products occurring in β_{l-1}, and others besides, so that the cluster integrals may be written as sums of products of the irreducible integrals $\beta_\mathbf{k}$.

In this paper the alternative attack will be used. The number of quantum states, Ω, available to a system of given energy, E, will be calculated by determination of the classical phase volume W in the γ-space. Ω is (asymptotically) equal to W divided by h to the power of the number of degrees of freedom, and by the factorial of the number of particles. The logarithm of Ω, multiplied by Boltzmann's constant k gives the entropy S of the system, as a function of its energy E. By appropriate thermodynamic manipulation all other properties of the system may be determined.

The resulting equations are found to depend on certain integrals $a_{l\nu}$ and $\alpha_{\mathbf{k}\mu}$ which are also referred to as cluster integrals and irreducible integrals, respectively. These are integrals over the configuration space of l and $\mathbf{k}+1$ molecules, as are the b_l's and $\beta_\mathbf{k}$'s. The integrand is again a sum of products of functions of the distances between molecule pairs. The functions now, however, are simply the negative potentials, $-u(r_{ij})$. These integrals $a_{l\nu}$ and $\alpha_{\mathbf{k}\mu}$ are then temperature independent, and are (as are also the b_l's and $\beta_\mathbf{k}$'s) also volume independent, for volumes of the system greater than that of the condensed phase.

It will be shown that the integrals b_l, used in the previous papers, and also the $\beta_\mathbf{k}$'s, may be expressed simply in terms of these integrals $a_{l\nu}$ and $\alpha_{\mathbf{k}\mu}$, respectively, Eqs. (87) and (88). With these relationships the equations derived in this paper are formally identical to those arrived at previously.

2. Assumptions and Method

For the sake of simplicity the calculations will be restricted to a system which is defined so as to represent an idealization of a one component system composed of identical, monatomic, chemically saturated atoms.

It will be assumed that the mass of the molecules, and the total energy, are sufficiently large to permit the use of the classical equations. A system will be considered which is composed of N identical, spherically symmetrical molecules, each of mass m, with no internal degrees of freedom, moving in a three-dimensional space of volume V. It will be assumed that the total potential energy, U, is a sum,

$$U=\sum_{N\geq i>j\geq 1} u(r_{ij})=\sum_{ij} u_{ij}, \tag{1}$$

of the mutual potentials u_{ij} of the $\frac{1}{2}N(N-1)$ pairs of molecules, i and j. The mutual potentials are functions only of the distances r_{ij} between the centers of the molecules, and are assumed to approach zero asymptotically, more rapidly than r_{ij}^{-3} as r_{ij} approaches infinity. These assumptions concerning the nature of the system treated are the same as those used previously in the development for one component systems, I, II, III.

The method pursued here is as follows. The $6N$-dimensional phase volume W available to

[1] I, Joseph E. Mayer, J. Chem. Phys. **5**, 67 (1937); II, Joseph E. Mayer and Philip G. Ackermann, *ibid.* **5**, 74 (1937); III, Joseph E. Mayer and S. F. Harrison, *ibid.* **6**, 87 (1938); IV, S. F. Harrison and Joseph E. Mayer, *ibid.* **6**, 101 (1938); V. Joseph E. Mayer, J. Phys. Chem. **43**, 71 (1939).

[2] Ursell, Proc. Camb. Phil. Soc. **23**, 685 (1927).

the system below an energy E is evaluated. The entropy is determined by W through the equation,

$$S=k \ln \Omega=k \ln \frac{W}{h^{3N} N!}. \quad (2)$$

The phase volume W is composed of two factors: the $3N$-dimensional volume W_P of the momentum space, and the $3N$-dimensional volume of the configuration (coordinate) space.

The volume W_P contributed as a factor by the momentum space is just the volume of a $3N$-dimensional sphere, the radius squared, R^2, of which, is the sum of the squares of the $3N$ momenta. The sum of the momenta squared is $2m$ times the total kinetic energy, which is $2m$ times the total energy E minus the potential energy U of Eq. (1). The potential U depends on the position of the particles in the configuration space. One has, then

$$R^2=\sum_{n=1}^{n=3N} p_n{}^2=2m(E-U)=2m[E-\sum_{ij} u_{ij}]. \quad (3)$$

The volume W_P of the $3N$-dimensional sphere of radius R is proportional to R^{3N}, and this volume must be integrated over the $3N$-dimensional configuration space, in order to calculate the total available phase volume W.

One is confronted, therefore, with the problem of integrating $[E-\sum u_{ij}]^{3N/2}$ over the configuration space. If the power is expanded, the integral can be represented as a sum of terms, the integrand of each term being a product involving the ν_{ij} power of the negative potential $-u_{ij}$ between the pairs of molecules i and j. Zero values of ν_{ij} occur. Clusters of molecules are defined in such a way that in a particular product no terms u_{ij} (with nonzero power ν_{ij}) occur between molecules i and j which are in different clusters. The integral of the term, then, is simply the product of the integrals over the individual clusters. Molecules which occur nowhere as a subscript to a potential u_{ij} in the term are said to be in a cluster consisting of a single molecule, and the integral over the space of these molecules contributes the factor V to the integral of this term. Since the potentials between molecules which are in one cluster drop rapidly to zero for large distances of separation, the integral over all but the last molecule of the cluster contributes a volume independent factor, and the integral over the last molecule contributes the factor V, to the whole integral of the term.

By defining cluster integrals $a_{l\nu}$, Eq. (12), which are volume and temperature independent, the logarithm of the total number of quantum states, Ω, can be represented as the logarithm of a sum of products of the cluster integrals, Eq. (15). The algebraic details of these steps are shown in Section 3.

Equation (15), however, does not lead to an expression for the entropy which is convenient for purposes of numerical calculation, or even of formal mathematical manipulation. It is desirable to seek such an asymptotic expression for $N^{-1} \ln \Omega$ as N approaches infinity, that would lead to a manageable expression for the entropy per molecule.

Two procedures may be followed. The first of these is only rigorous if all the terms of the sum expression (15) for $\ln \Omega$ are positive. It is, however, extremely simple, and is shown in Section 4. The second, more general method is based on that used by Kahn and Uhlenbeck,[3] and by Born and Fuchs,[4] and is followed in Section 7.

The simple method employed in Section 4 is to equate the logarithm of the sum in Eq. (15) to the logarithm of the largest term in the sum. This method is rigorous if all the terms are positive, since the logarithm of the total number of terms does not increase linearly with N, whereas the logarithm of the largest term does. The largest term must be determined subject to certain conditions, and the method of undetermined multipliers is used. This procedure, which is carried out in Section 4 results in an expression for $\ln \Omega$, the essential part of which is a power series in these undetermined multipliers, Z and Y, Eq. (28). The coefficient of $Z^l Y^\nu$ in this series is proportional to the cluster integral $a_{l\nu}$.

The parameters Y and Z are determined by two conditions (29) and (30) on two other power series, the coefficients of which are $\nu a_{l\nu}$ and $l a_{l\nu}$, respectively. Although these equations are

[3] B. Kahn and G. E. Uhlenbeck, Physica **5**, 399 (1938).
[4] Max Born and Klaus Fuchs, Proc. Roy. Soc. London **A166**, 391 (1938).

not explicit equations for the parameters Z and Y themselves, they permit the unambiguous determination of the derivatives of the entropy S with respect to volume and energy. The derivative of S with respect to E, at constant V is the reciprocal of the temperature; that with respect to V at constant E is P/T. The pressure and temperature are thus introduced. These differentiations are carried out in Section 5, and serve to identify the parameters Z and Y with physical quantities. It is found that Y is just $1/kT$, and Z is the fugacity: the density in molecules per unit volume of a perfect gas having the same Gibbs' free energy as the system in question. This Z, then, is the same quantity as the parameter Z introduced in the previous papers of this series.

In Section 5, then, the equations for the thermodynamic properties of the system are obtained as functions of $Y=1/kT$ and Z, the fugacity, with formulae involving the cluster integrals $a_{l,v}$.

Since temperature is more readily measured than energy, it is entirely satisfactory that one finds the equations for the thermodynamic properties explicitly as functions of temperature rather than of energy. It is less satisfactory, however, to find that these equations are explicit functions of fugacity, Z rather than of the volume per molecule, v. The next chore, then, is to solve Eq. (38) for Z, and to use this solution in the equations for the system, so as to obtain expressions which are functions of the temperature and volume.

This could be carried out in a manner which involves no advanced mathematical treatment, but which would use a rather tedious algebraic manipulation. Thus, the following method will lead to the Eq. (77) which is explicit for the fugacity Z in terms of v and T. One expresses Z as an inverse power series in v and T, with undetermined coefficients, and by the usual method of successive equating of coefficients, solves for these from Eq. (38). If the coefficients are expressed in terms of the irreducible integrals $\alpha_{k,\mu}$, instead of the cluster integrals $a_{l,v}$, the resulting expansion is seen to be the same as that of Eq. (77) for Z. The method is, at best, only rigorous to the number of terms calculated, and is laborious. Instead, recourse will be taken to a procedure involving more advanced mathematical methods.

Before undertaking this calculation, the equation for the cluster integrals $a_{l,v}$ in terms of the irreducible integrals $\alpha_{k,\mu}$ is derived in Section 6. This equation is identical to that for the cluster integrals b_l in terms of the β_k, derived in previous articles. It is consequently possible to entirely avoid the very involved discussion of the combinatory problem, by merely demonstrating the essential identity of the present problem with that previously solved.

The formal calculations of Sections 7 and 8 are sufficient to prove rigorously Eqs. (77) to (80) of Section 9, which give, finally, the thermodynamic properties of the system as explicit functions of temperature and volume per molecule. The method discussed in Sections 7 and 8 is actually pure mathematics, and does not lead to any greater understanding of the physical equations than is obtained from their perusal alone.

With the equations of Section 9 the problem has been essentially solved. There remains, however, one point to discuss. This concerns a neglect made in determining the phase volume.

In the original integration over the configuration space of the integrand, $(E-\sum u_{ij})^{3N/2}$, no specific mention was made of the possible case that regions of the configuration space could exist for which $E-\sum u_{ij}$ becomes negative. For molecules having high repulsive potentials at short mutual distances this would be the case. Actually, it appears, from the identity of the equations derived by this method with those obtained from the Gibbs' integral, that this neglect is not serious, as long as it is assumed that u_{ij} is nowhere infinite; however, the method of attack is open to serious objection. If, instead, a system is treated for which the mutual potential $u(r_{ij})$ between pairs becomes strictly infinite for all values of r_{ij} less than some distance r_0, then $E-\sum u_{ij}$ is negative if any pair of molecules i and j are closer together than r_0. If u_{ij} is negative for all values of r_{ij} greater than r_0 the function $E-\sum u_{ij}$ is everywhere else positive. It is shown in Section 10 that a system with such mutual potentials can be readily, and rigorously, handled with this method by using a slightly altered

definition of the integrals $a_{l\nu}$ and $\alpha_{k\mu}$, Eqs. (85) and (86).

In Section 11 it is shown that the equations of this method are formally identical to those derived previously using the Gibbs' integral.

3. The Integral of the Phase Volume

The expression for the volume, W_P, of a $3N$-dimensional sphere of radius R is (for even N),

$$W_P=\frac{\pi^{3N/2}}{(3N/2)!}R^{3N}. \tag{4}$$

If Eq. (3) is used for R, $R=E-U$, W_P gives the contribution to the total phase volume W due to the $3N$ momenta, as a function of the configurational coordinates. The number Ω of quantum states available to the system is

$$\Omega=\frac{W}{h^{3N}N!}=\frac{(2\pi m)^{3N/2}}{h^{3N}N!(3N/2)!}\int\cdots \times\int\Big[E-\sum_{N\geq i>j\geq 1}u_{ij}\Big]^{3N/2}d\tau_1\cdots d\tau_N, \tag{5}$$

where $d\tau_i=dx_i dy_i dz_i$. Using the Stirling approximation,

$$\ln P!=P(\ln P-1) \tag{6}$$

and introducing the energy ϵ per molecule,

$$\epsilon=E/N, \tag{7}$$

one may write

$$\ln\Omega=N\ln\left(\frac{4\pi m\epsilon e}{3h^2}\right)^{3/2}+\ln\Theta, \tag{8}$$

in which Θ is defined as

$$\Theta=\frac{1}{N!}\int\cdots\int\left[1+\sum_{N\geq i>j\geq 1}\frac{-u_{ij}}{N\epsilon}\right]^{3N/2}d\tau_1\cdots d\tau_N. \tag{9}$$

If the mutual potentials u_{ij} between the molecule pairs i and j are identically zero, the integrand in (9) is unity, and one finds

$$\left.\begin{aligned}\ln\Theta&=\ln\frac{V^N}{N!}=N\ln ve &(9')\\ \ln\Omega&=N\ln\left(\frac{4\pi m\epsilon}{3h^2}\right)^{3/2}ve^{5/2} &(8')\end{aligned}\right\}(u_{ij}\equiv 0),$$

in which $v=V/N$ is the volume per molecule. Eq. (8′) is the usual expression for a classical perfect monatomic gas.

In order to obtain a general expression for Θ from Eq. (9) we shall, at first, avoid difficulties which arise when $E-U$ becomes negative by treating only systems of positive energy, E, and by tacitly assuming that $-u_{ij}$ is everywhere positive.

On expanding the power in the integrand of (9) one may write

$$\Theta=\sum_{M=0}^{3N/2}\frac{(3N/2)!}{[(3N/2)-M]!(N\epsilon)^M}\Theta_M, \tag{10}$$

with

$$\begin{aligned}\Theta_M&=\frac{1}{N!M!}\int\cdots\int\Big[\sum_{N\geq i>j\geq 1}-u_{ij}\Big]^M d\tau_1\cdots d\tau_N\\ &=\frac{1}{N!}\int\cdots\int\sum_{\substack{\nu_{ij}\\ \Sigma\nu_{ij}=M}}\prod_{i,j}\frac{(-u_{ij})^{\nu_{ij}}}{\nu_{ij}!}d\tau_1\cdots d\tau_N.\end{aligned} \tag{11}$$

As discussed in Section 2 the same method of division of the molecules in the individual terms of the sum (11) into clusters is used, that was employed in the previous papers, I, III. A cluster integral, $a_{l\nu}$, of l molecules with ν "bonds" is defined as

$$a_{l\nu}=\frac{1}{1!V}\int\cdots\int\sum_{\substack{\nu_{ij}\\ \Sigma\nu_{ij}=\nu}}\prod_{l\geq i>j\geq 1}\frac{(-u_{ij})^{\nu_{ij}}}{\nu_{ij}!}d\tau_1\cdots d\tau_N \tag{12}$$

(all products at least singly connected).

For $l=1$ only the term $\nu=0$ exists, and $a_{1,0}\equiv 1$.

The cluster integrals $a_{l\nu}$ are temperature independent, and for moderate volumes and small l values, are also volume independent. As is the case for the cluster integrals b_l, the volume at which the $a_{l\nu}$ of high l values become (appreciably) volume dependent is found to be the volume of the condensed phase.

With these integrals one may express Θ_M as

$$\Theta_M=\sum_{\substack{m_{l\nu}\\ \Sigma\nu m_{l\nu}=M,\\ \Sigma l m_{l\nu}=N}}\prod_{l,\nu}\frac{(Nva_{l\nu})^{m_{l\nu}}}{m_{l\nu}!}. \tag{13}$$

This equation strongly resembles that for the

configuration integral Q_τ in terms of the b_l's,

$$Q_\tau=\sum_{\substack{m_l \\ \Sigma l m_l=N}} \prod_l \frac{(Nvb_l)^{m_l}}{m_l!}, \tag{14}$$

differing only in the extra condition $\sum \nu m_{l\nu}=M$ imposed on the allowed products of (13).

Using (13) in (10) and (10) in (8), one finds

$$\ln \Omega=N \ln \left(\frac{4\pi m\epsilon\epsilon}{3h^2}\right)^{3/2}$$

$$+\ln \sum_{M=1}^{3N/2} \frac{(3N/2)!}{[(3N/2)-M]!(N\epsilon)^M} \sum_{\substack{m_{l\nu} \\ \Sigma \nu m_{l\nu}=M \\ \Sigma l m_{l\nu}=N}} \prod_{l,\nu} \frac{(Nva_{l\nu})^{m_{l\nu}}}{m_{l\nu}!}. \tag{15}$$

4. Evaluation by the Logarithm of the Largest Term

Equation (15) gives $\ln \Omega$ as the logarithm of a sum of products of cluster integrals. The logarithm of one of the terms $T(m_{l\nu})$ of the sum Θ_M, Eq. (13) is

$$\ln T(m_{l\nu})=\sum_{l,\nu} m_{l\nu}[\ln Nva_{l\nu}-\ln m_{l\nu}+1], \tag{16}$$

if the Stirling approximation (6) is used for $m_{l\nu}!$.

The values of the powers $m_{l\nu}$ for which this expression is a maximum, $m_{l\nu}^*$, are to be determined subject to the conditions that

$$\sum_{l,\nu} \nu m_{l\nu}=M, \tag{17}$$

$$\sum_{l,\nu} l m_{l\nu}=N, \tag{18}$$

which is done by adding $\ln Y$ times (17) and $\ln Z$ times (18) to (16), and setting the differential of the sum with respect to any $m_{l\nu}$ equal to zero.

One obtains

$$\ln Nva_{l\nu}-\ln m_{l\nu}^*+\nu \ln Y+l \ln Z=0 \tag{19}$$

$$m_{l\nu}^*=Nva_{l\nu}Z^lY^\nu.$$

The two conditions (17) and (18) serve to determine the two parameters Y and Z by the equations

$$\sum_{l,\nu} \nu va_{l\nu}Z^lY^\nu=\frac{M}{N}=m, \tag{20}$$

$$\sum_{l,\nu} lva_{l\nu}Z^lY^\nu=1. \tag{21}$$

Eq. (20) defines the new symbol m.

The values (19) of the powers $m_{l\nu}^*$ for which the term $T(m_{l\nu}^*)$ is the largest in the sum Θ_M, may be used in (16), giving directly the asymptotic value of $\ln \Theta_M$ for large values of the number of molecules N, as

$$\ln \Theta_M=\sum_{l,\nu} m_{l\nu}^*[1-\nu \ln Y-l \ln Z].$$

With (20) and (21) this leads to the expression

$$\ln \Theta_M=N\{\sum_{l,\nu} va_{l\nu}Z^lY^\nu-m \ln Y-\ln Z\}. \tag{22}$$

It will be found convenient to abbreviate the sum occurring in this expression, and we shall use the symbols $G_{\lambda n}$ for the sums defined by

$$G_{\lambda n}(va, Z, Y)=\sum_{l,\nu} l^\lambda \nu^n va_{l\nu}Z^lY^\nu. \tag{23}$$

It is seen that

$$dG_{\lambda n}(va, Z, Y)=G_{\lambda, n}\frac{dv}{v}+G_{\lambda+1, n}\frac{dZ}{Z}$$

$$+G_{\lambda, n+1}\frac{dY}{Y}. \tag{24}$$

The expression for $\ln \Theta_M$ is then

$$\ln \Theta_M=N\{G_{00}(va, Z, Y)-m \ln Y-\ln Z\}. \tag{22'}$$

Equation (10) for Θ is also a sum of terms, and, using $m=M/N$ the Stirling approximation (6), and Eq. (22'), one finds for the logarithm of the term T_M involving Θ_M the value

$$\ln T_M=N[\tfrac{3}{2} \ln \tfrac{3}{2}+G_{00}-\ln Z$$

$$-(\tfrac{3}{2}-m) \ln (\tfrac{3}{2}-m)-m(\ln \epsilon Y-1)]. \tag{25}$$

To find the value m^* of m for which T_M is a maximum this expression is differentiated with respect to m and equated to zero, obtaining

$$\ln (\tfrac{3}{2}-m^*)-\ln \epsilon Y=0, \quad m^*=\tfrac{3}{2}-\epsilon Y. \tag{26}$$

Inserting this value of m^* in (25) to obtain the logarithm of the largest term, $\ln T_M^*$, which is asymptotically equal to $\ln \Theta$ for large values of N, one obtains

$$\ln \Theta=N\left[-\frac{3}{2}+\epsilon Y+G_{00}-\ln Z+\frac{3}{2} \ln \frac{3}{2\epsilon Y}\right]. \tag{27}$$

The use of (27) in (8) yields

$$\ln \Omega = N\left[\ln\left(\frac{2\pi m}{h^2 Y}\right)^{3/2} + \epsilon Y + G_{00} - \ln Z\right] \quad (28)$$

for $\ln \Omega$. Since now the value of $m=m^*$, Eq. (26), for which the sum (10) of Θ is a maximum has been determined, Eqs. (20) and (21) which determine Y and Z are

$$G_{01}(va, Z, Y) = \tfrac{3}{2} - \epsilon Y, \quad (29)$$

$$G_{10}(va, Z, Y) = 1. \quad (30)$$

5. Thermodynamic Properties as Functions of $a_{l\nu}$, T, and Z

The thermodynamic temperature of the system is defined by the equation

$$\frac{1}{T} = \left(\frac{\partial S}{\partial E}\right)_v = \frac{1}{N}\left(\frac{\partial S}{\partial \epsilon}\right)_v = \frac{k}{N}\left(\frac{\partial \ln \Omega}{\partial \epsilon}\right)_v. \quad (31)$$

Using (28) for $\ln \Omega$ one finds

$$\frac{1}{T} = k\left\{Y + \frac{1}{Y}[G_{01} - (\tfrac{3}{2} - \epsilon Y)]\left(\frac{\partial Y}{\partial \epsilon}\right)_v + \frac{1}{Z}[G_{10} - 1]\left(\frac{\partial Z}{\partial \epsilon}\right)_v\right\},$$

which, in view of (29) and (30), reduces to

$$1/T = kY; \qquad Y = 1/kT, \quad (32)$$

the parameter Y is just $1/kT$!

Equation (29) may now profitably be inverted, and used to determine the energy, $E=N\epsilon$, as a function of temperature,

$$E = NkT\left\{\frac{3}{2} - G_{01}\left(va, Z, \frac{1}{kT}\right)\right\} = NkT\left\{\frac{3}{2} - \sum_{l,\nu} \nu v a_{l\nu} \frac{Z^l}{(kT)^\nu}\right\}. \quad (33)$$

Introducing $1/kT$ for Y in (28), and using (33), one may write for the entropy $S=k \ln \Omega$,

$$S = kN\left\{\ln\left(\frac{2\pi mkT}{h^2}\right)^{3/2} \frac{1}{Z} + \frac{3}{2} - G_{01} + G_{00}\right\} = kN\left\{\ln\left(\frac{2\pi mkT}{h^2}\right)^{3/2} \frac{e^{3/2}}{Z} - \sum_{l,\nu} (\nu - 1) v a_{l\nu} \frac{Z^l}{(kT)^\nu}\right\}. \quad (34)$$

The pressure is determined by the thermodynamic equation

$$\frac{P}{T} = \left(\frac{\partial S}{\partial V}\right)_E = \frac{1}{N}\left(\frac{\partial S}{\partial v}\right)_\epsilon = \frac{k}{N}\left(\frac{\partial \ln \Omega}{\partial v}\right)_\epsilon, \quad (35)$$

which is applied to (28) to give

$$\frac{P}{T} = k\left\{\frac{1}{v} - G_{00} + \frac{1}{Y}[G_{01} - (\tfrac{3}{2} - \epsilon Y)]\left(\frac{\partial Y}{\partial v}\right)_\epsilon + \frac{1}{Z}[G_{10} - 1]\left(\frac{\partial Z}{\partial v}\right)_\epsilon\right\}$$

with (24). Using (29) and (30) one finds

$$P = \frac{kT}{v} G_{00}\left(va, Z, \frac{1}{kT}\right) = \frac{kT}{v} \sum_{l,\nu} v a_{l\nu} \frac{Z^l}{(kT)^\nu}. \quad (36)$$

The Gibbs' free energy is $F=E-TS+PV$ which, with (33), (34), and (36) leads to

$$F = kNT \ln\left(\frac{h^2}{2\pi mkT}\right)^{3/2} Z. \quad (37)$$

Comparing this with the equation for a perfect gas,

$$F = kNT \ln\left(\frac{h^2}{2\pi mkT}\right)^{3/2} \frac{1}{v}, \quad (u_{ij} \equiv 0). \quad (37')$$

It is seen that Z is the fugacity of the system: the density in molecules per unit volume of a monatomic perfect gas of the same molecular weight having the same Gibbs' free energy as the system.

The parameter Z is consequently the same as the parameter Z introduced in the previous papers of this series.

The substitution of $Y=1/kT$ in (30) gives the equation by which this fugacity Z is determined as

$$G_{10}\left(va, Z, \frac{1}{kT}\right) = \sum_{l,\nu} l v a_{l\nu} \frac{Z^l}{(kT)^\nu} = 1. \quad (38)$$

6. The Expression for the Cluster Integrals $a_{l\nu}$ in Terms of the Irreducible Integrals $\alpha_{k\mu}$

The integrand of the expression (12) for $a_{l\nu}$ is a sum of products. Each product may be

represented as a graph of l vertices and ν lines, and the sum of all the terms corresponding to all the possible *connected* graphs of l points and ν lines forms the integrand of (12).

If the graph corresponding to one product consists of two parts, singly connected at one point only, the integral of this product is a product of two integrals (see the discussion in paper I of this series). In this way the integral (12) may be written as a sum of products of simpler integrals. The irreducible integral, $\alpha_{\mathbf{k}\mu}$, defined by

$$\alpha_{\mathbf{k}\mu}=\frac{1}{k!V}\int\cdots\int\sum_{\substack{\nu_{ij}\\ \Sigma\nu_{ij}=\mu}}\prod_{\mathbf{k}+1\geq i>j\geq 1}\frac{(-u_{ij})^{\nu_{ij}}}{\nu_{ij}!}\times d\tau_1\cdots d\tau_{k+1}, \quad (39)$$

(*products more than singly connected*).

differs from $a_{\mathbf{k}+1,\nu}$ only in that all the terms of the cluster integral which can be represented by a product of integrals are excluded; that is the graphs corresponding to the products of (39) cannot be broken up into singly connected parts.

It is clear that the cluster integrals $a_{l\nu}$ can be represented as a sum of products of the $\alpha_{\mathbf{k}\mu}$'s raised to powers $n_{\mathbf{k}\mu}$, subject to the conditions

$$\sum_{\mathbf{k},\mu}\mathbf{k}n_{\mathbf{k}\mu}=l-1, \quad (40)$$

$$\sum_{\mathbf{k},\mu}\mu n_{\mathbf{k}\mu}=\nu. \quad (41)$$

It is necessary, however to determine the coefficient of the product

$$\prod_{\mathbf{k},\mu}\alpha_{\mathbf{k}\mu}{}^{n_{\mathbf{k}\mu}}$$

in $a_{l\nu}$. Fortunately it is not difficult to ascertain that this coefficient is exactly the same as the coefficient of

$$\prod_{\mathbf{k}}\beta_{\mathbf{k}}{}^{n_{\mathbf{k}}}$$

in b_l, so that

$$l^2a_{l\nu}=\sum_{\substack{n_{\mathbf{k}\mu}\\ \Sigma\mu n_{\mathbf{k}\mu}=\nu\\ \Sigma\mathbf{k}n_{\mathbf{k}\mu}=l-1}}\prod_{\mathbf{k},\mu}\frac{(l\alpha_{\mathbf{k}\mu})^{n_{\mathbf{k}\mu}}}{n_{\mathbf{k}\mu}!}, \quad (42)$$

which is the same as the expression for l^2b_l

$$l^2b_l=\sum_{\substack{n_{\mathbf{k}}\\ \Sigma\mathbf{k}n_{\mathbf{k}}=l-1}}\prod_{\mathbf{k}}\frac{(l\beta_{\mathbf{k}})^{n_{\mathbf{k}}}}{n_{\mathbf{k}}!}, \quad (43)$$

Eq. (19) paper III, except for the extra condition $\sum\mu n_{\mathbf{k}\mu}=\nu$ in (42).

The demonstration that the coefficient of the $\alpha_{\mathbf{k}\mu}$ product in $a_{l\nu}$ is the same as that of the corresponding $\beta_{\mathbf{k}}$ product in b_l is fairly obvious, although awkward to express. The integrand of the expression (39) for $\alpha_{\mathbf{k}\mu}$ is symmetrical in all the $\mathbf{k}+1$ molecules. The total number of products in the integrand of (12) which would lead to the result

$$\prod_{\mathbf{k},\mu}\alpha_{\mathbf{k}\mu}{}^{n_{\mathbf{k}\mu}}$$

is $l!$ times the number of ways in which $n_{\mathbf{k}\mu}$ unnumbered frames of type $\mathbf{k},\mu$ with $\mathbf{k}+1$ symmetrically situated holes can be bolted together with $\sum\mathbf{k}n_{\mathbf{k}\mu}=l-1$ numbered bolts (the molecules) so as to fill every hole and to singly connect the frames.

This is the identical combinatory problem that was solved previously, and which led to Eq. (43), except that previously only one type of frame with $\mathbf{k}+1$ holes existed. The fact that we now have different types, μ, of frames with the same number of holes does not fundamentally alter the problem. The only proof of Eq. (43) which exists in the literature is that given by Born and Fuchs.[4] An alternate type of proof is implicit in article V of this series, where a similar problem is solved for frames having $\mathbf{k}$ square and κ round holes.

7. The Method of Complex Functions

An alternative method for deriving Eq. (28) from (15) will now be given; a method which is rigorous even if some of the $a_{l\nu}$'s are negative.

The logarithm of the complicated sum occurring in (15) may be transformed, by the use of the Stirling approximation (6), into

$$\ln\sum_{M=1}^{3N/2}\frac{(3N/2)!}{[(3N/2-M]!(N\epsilon)^M}\sum_{\substack{m_{l\nu}\\ \Sigma\nu m_{l\nu}=M,\\ \Sigma l m_{l\nu}=N}}\prod_{l,\nu}\frac{(Nva_{l\nu})^{m_{l\nu}}}{m_{l\nu}!}$$

$$=N\ln\frac{3}{2(e\epsilon)^{3/2}}+\ln\sum_{\substack{m_{l\nu}\\ \Sigma l m_{l\nu}=N}}\frac{(N\epsilon)^{(3N/2)-\Sigma\nu m_{l\nu}}}{[(3N/2)-\Sigma\nu m_{l\nu}]!}\prod_{l,\nu}\frac{(Nva_{l\nu})^{m_{l\nu}}}{m_{l\nu}!}. \quad (44)$$

The function F, defined by

$$F(N, L, va) = -\frac{1}{4\pi^2}\oint\oint \frac{e^{2L\epsilon y+NG_{00}(va,\, z,\, y)}}{z^N y^{3L}}\frac{dz}{z}\frac{dy}{y}, \quad (45)$$

in which the paths of integration enclose the origins $y=0$ and $z=0$, and no other singularities of the integrand, is the coefficient of $y^{3L}z^N$ in the exponent of $2L\epsilon y+NG_{00}(va, z, y)$.

If this exponential is expanded as

$$e^{2L\epsilon y+NG_{00}} = \sum_{p\geq 0}\sum_{q\geq 0}\frac{(2L\epsilon y)^p}{p!}\frac{(NG_{00})^q}{q!}$$

$$= \sum_{p\geq 0}\sum_{m_{l\nu}\geq 0}\frac{(2L\epsilon)^p}{p!}\prod_{l,\,\nu}\frac{(Nva_{l\nu})^{m_{l\nu}}}{m_{l\nu}!}z^{\Sigma l m_{l\nu}}y^{p+\Sigma\nu m_{l\nu}},$$

the coefficient of $z^N y^{3L}$, when $L=\frac{1}{2}N$, $p=3N/2-\sum\nu m_{l\nu}$, is seen to be the sum whose logarithm occurs in (44). It follows, therefore, from (15) and (44) that one may write

$$\ln\,\Omega = N\ln\left(\frac{2\pi m}{h^2}\right)^{3/2} + \ln F(N, \tfrac{1}{2}N, va), \quad (46)$$

in which F is defined by Eq. (45).

In order to determine the limit as N approaches infinity of $N^{-1}\ln F$ we define a new function H as

$$H(va, r, t) = \sum_{N\geq 0}\sum_{L\geq 0} F(N, L, va)r^N t^L. \quad (47)$$

Since the functions F are all real and positive the first singularity of H lies on the real positive axes of r and t, and the knowledge of the associated values r_0, t_0 for which H becomes singular will be found sufficient to determine the limit $N^{-1}\ln F$.

If (45) for F is used in (47), and the integration performed over paths for which always

$$\left|\frac{e^{2\epsilon y}}{y^3}t\right| < 1, \quad (48)$$

$$\left|\frac{e^{G_{00}}}{z}r\right| < 1, \quad (49)$$

the order of integration and summation may be inverted and H written as

$$H = -\frac{1}{4\pi^2}\oint\oint \frac{dz}{z-re^{G_{00}}}\frac{dy}{y-(te^{2\epsilon y}/y^2)}. \quad (50)$$

Integrating first over y, the pole at $y=y_0$ determined by

$$t = y_0^3 e^{-2\epsilon y_0} \quad (51)$$

is enclosed by the path of integration. The residue at the pole is determined by inserting the derivative of the denominator at the pole, for the denominator of the function. One obtains

$$H = \frac{1}{2\pi_i}\oint \frac{1}{3-2\epsilon y_0}\frac{dz}{z-re^{G_{00}}}, \quad (52)$$

in which G_{00} is now a function of z, and of y_0 determined by (51).

The path of integration over z encloses the pole at $z=z_0$, determined by

$$r = z_0 e^{-G_{00}(va,\, z_0,\, y_0)}. \quad (53)$$

The residue is determined as before, obtaining

$$H(va, r, t) = \frac{1}{3-2\epsilon y_0}\frac{1}{1-G_{10}(va, z_0, y_0)}. \quad (54)$$

Noting from Eqs. (51) and (53) that $t=0$ corresponds to $y_0=0$, and $r=0$ to $z_0=0$, and that the real positive axes of t and r correspond to real positive values of y_0 and z_0, one also sees from (54) that H is regular for all positive values of z_0 and y_0 satisfying all three of the conditions:

$$\begin{aligned} &\text{(a)} \quad G_{10}(va, z_0, y_0) < 1, \\ &\text{(b)} \quad G_{10}(va, z_0, y_0) \text{ regular}, \\ &\text{(c)} \quad y_0 < 3/2\epsilon. \end{aligned} \quad (55)$$

It is clear that H becomes singular if condition (a) or (c) is violated, and that the function *may* become singular if condition (b) is violated. Whether H actually becomes singular if condition (b) is violated will be discussed at the end of Section 8. This condition corresponds to condensation in the system. For the present we shall be concerned with such values of v, z_0 and y_0 that a slight increase in the values of z_0 and y_0 violates condition (a) only.

We are concerned with the determination of the value of the function φ defined as

$$\ln\,\varphi(x, va) = \lim_{N\to\infty}[1/N\ln F(N, xN, va)] \quad (56)$$

for the special value of $x=\frac{1}{2}$. From the definitions

(47) of H, and (56) of $\ln \varphi$, it follows that for all positive values of r and t for which H is regular, the inequality

$$\ln \varphi(x, va) \leq -\ln r - x \ln t, \tag{57}$$

holds, whereas for any positive pair of associated values r_0 and t_0 for which H becomes singular, there is some x for which Eq. (57) is an equality.

The function f is defined as

$$\ln f(x, z, y) = 2\epsilon xy + G_{00}(va, z, y) - 3x \ln y - \ln z, \tag{58}$$

and from (51) and (53) it is seen that

$$\ln f(x, z, y) = -\ln r - x \ln t \tag{58'}$$

for the values of r and t defined by these equations as functions of z and y. The derivative of f is, at constant x,

$$df = -(3x - 2\epsilon xy - G_{01})dy/y - (1 - G_{10})dz/z, \tag{59}$$

so that an absolute minimum of f is obtained, when $x = \frac{1}{2}$, at the values $z = Z$, $y = Y$, determined by

$$G_{10}(va, Z, Y) = 1, \tag{60}$$

$$G_{01}(va, Z, Y) = \tfrac{3}{2} - \epsilon Y. \tag{61}$$

From Eqs. (58'), (58), and (57) one can now set an upper bound on $\varphi(\frac{1}{2}, va)$

$$\ln \varphi(\tfrac{1}{2}, va) \leq \epsilon Y + G_{00}(va, Z, Y) - \tfrac{3}{2} \ln Y - \ln Z. \tag{62}$$

Since Eq. (60) violates condition (55a), these values of Z and Y correspond to a definite pair r_0 and t_0 of associated radii of convergence of the function H. It follows that for some value of x the equality

$$\ln \varphi(x, va) = \ln f(x, Z, Y) \tag{62'}$$

holds. For all *other* values of x than $x = \frac{1}{2}$, however, $\ln f$ has a minimum at *other* values of z and y than Z and Y. Consequently the equality (62') can only be fulfilled at $x = \frac{1}{2}$. This serves finally to permit us to write

$$\ln \varphi(\tfrac{1}{2}, va) = \epsilon Y + G_{00}(va, Z, Y) - \tfrac{3}{2} \ln Y - \ln Z. \tag{62''}$$

From the definition (56) of φ, and Eq. (46) for $\ln \Omega$ one finally evaluates $\ln \Omega$ as

$$\ln \Omega = N\left[\ln \left(\frac{2\pi m}{h^2 Y}\right)^{3/2} \frac{1}{Z} + \epsilon Y + G_{00}(va, Z, Y)\right], \tag{63}$$

which is the same as Eq. (28). The Eqs. (60) and (61) determining Z and Y are the same as (29) and (30).

One thus proves the equations of the preceding sections to be correct, even if the $a_{l\nu}$'s be negative, provided the conditions (b) and (c) of Eq. (55) are not violated by these values Z and Y.

8. Use of Complex Functions to Determine the Sums $G_{\lambda n}(va, Z, Y)$

The function Φ defined as

$$\Phi(l, \nu, \alpha) = -\frac{1}{4\pi^2} \oint \oint \exp \frac{[lG_{00}(\alpha, \zeta, \eta)]}{\zeta^l \eta^\nu} \frac{d\eta}{\eta} d\zeta \tag{64}$$

with G_{00} defined by (23), and in which the paths of integration enclose the origins, $\zeta = 0$, $\eta = 0$, and no other singularities, is the coefficient of $\zeta^{l-1}\eta^\nu$ in the expansion of the exponent of $lG_{00}(\alpha, \zeta, \eta)$. By inspection this coefficient is seen to be the same as Eq. (42) for $l^2 a_{l\nu}$.

It follows that the sum defined as

$$H(\alpha, Z, Y) = \sum_{l \geq 1} \sum_{\nu \geq 0} \Phi(l, \nu, \alpha) Z^l Y^\nu \tag{65}$$

is also equal to the sum $G_{20}(Q, Z, Y)$,

$$H(\alpha, Z, Y) = (1/v) G_{20}(va, Z, Y). \tag{65'}$$

We shall use the same method as that employed in the previous section to evaluate H from Eqs. (65) and (64).

By limiting ourselves to paths of integration for which

$$|Ze^{G_{00}(\alpha, \zeta, \eta)}/\zeta| < 1, \tag{66}$$

and

$$|\eta| > Y, \tag{67}$$

we may invert the order of integration and summation, finding

$$H = -\frac{1}{4\pi^2} \oint \oint \frac{1}{Z} \frac{d\zeta}{(\zeta e^{-G_{00}} - Z)} \frac{d\eta}{(\eta - Y)}. \tag{68}$$

Integrating first over η the pole at $\eta = Y$, which is enclosed by the path of integration is seen to

have a residue unity, so that

$$H=\frac{1}{2\pi i}\frac{1}{Z}\oint\frac{d\zeta}{\zeta e^{-G_{00}(\alpha,\,\zeta,\,Y)}-Z}. \tag{69}$$

The pole at $\zeta=\rho$,

$$\rho e^{-G_{00}(\alpha,\,\rho,\,Y)}=Z, \tag{70}$$

is enclosed by the path of integration. The residue is again determined by inserting the derivative of the denominator at the pole, for the denominator of the residue, so that one obtains

$$H=\rho/(1-G_{10}(\alpha,\,\rho,\,Y))$$

or, with (65′),

$$G_{20}(va,\,Z,\,Y)=v\rho/(1-G_{10}(\alpha,\,\rho,\,Y)), \tag{71}$$

where ρ is determined by (70).

From the definition, Eq. (23) of the functions $G_{\lambda n}$, and the differentiation given in (24) it is seen that

$$G_{10}(va,\,Z,\,Y)=\int_0^Z G_{20}(va,\,Z',\,Y)\frac{dZ'}{Z'}. \tag{72}$$

From (70) one finds that

$$\frac{dZ'}{Z'}=[1-G_{10}(\alpha,\,\rho',\,Y)]\frac{d\rho'}{\rho'}. \tag{73}$$

If this is used in (72) with (71) one obtains

$$G_{10}(va,\,Z,\,Y)=v\rho. \tag{74}$$

Repeating the integration,

$$G_{00}(va,\,Z,\,Y)=\int_0^Z G_{10}(va,\,Z',\,Y)\frac{dZ'}{Z'}$$

$$=\int_0^\rho v[1-G_{10}(\alpha,\,\rho',\,Y)]d\rho',$$

one obtains

$$G_{00}(va,\,Z,\,Y)=v\rho\left[1-\sum_{\mathbf{k},\,\mu}\frac{\mathbf{k}}{\mathbf{k}+1}\alpha_{\mathbf{k}\mu}\rho^{\mathbf{k}}Y^{\mu}\right]. \tag{75}$$

Equations (74) and (75) of this section are valid only if the two conditions (55b) and (55c) are satisfied. These two conditions will be fulfilled if the three conditions on the $\alpha_{\mathbf{k}\mu}$ sums,

(α) $G_{10}[\alpha,\,v^{-1},\,(kT)^{-1}]<1$,

(β) $G_{10}[\alpha,\,v^{-1},\,(kT)^{-1}]$ regular,

(γ) $\sum_{\mathbf{k}\mu}\frac{\mathbf{k}\mu}{\mathbf{k}+1}\alpha_{\mathbf{k}\mu}v^{-\mathbf{k}}(kT)^{-\mu}>0$,

are satisfied. That these conditions are sufficient may be seen as follows: If $G_{10}(va,\,Z,\,Y)$ is to be regular, so must $G_{20}(va,\,Z,\,Y)$, and from (71) it is then seen that if α and β are satisfied, then (55b) is satisfied. By comparing Eqs. (61) and (75) with condition (55c) it is seen that this condition is equivalent to γ.

Although it is clear that the Eqs. (74) and (75) are valid if all these conditions are satisfied, we have not completed the proof that if (55b), or if α or β are violated that these equations are no longer correct.

In order to complete this proof it would be necessary to show that the determinant $\partial(Z,\,Y)/\partial(r,\,t)$ is nonzero when (55b) is violated, so that then $H(va,\,r,\,t)$ must become singular. Similarly to show that if (β) is violated (55b) is also violated one must prove $\partial(\rho,\,Y)/\partial(Z,\,Y)$ to be nonzero at this singularity. This requires considerable algebraic juggling, which is not difficult, but tedious, and will be avoided here. Since in Section 11 it is shown that these equations are all formally identical to those derived by the previous treatment, and the conditions β and (55b) are those previously found for condensation[4] it appears to be unnecessary to burden the article with the proof.

9. The Thermodynamic Equations as Explicit Functions of Volume and Temperature

The parameters Y and Z are determined by the two Eqs. (60) and (61). In view of (60) it is seen from Eq. (74) that

$$v\rho=1, \quad \rho=v^{-1}. \tag{76}$$

Using this, and $Y=1/kT$ in Eq. (70), we obtain an explicit equation for the fugacity Z as a

function of volume and temperature, namely

$$Z=\frac{1}{v}\exp\left[-G_{00}(\alpha, v^{-1}(kT)^{-1})\right], \qquad (77)$$
$$=\frac{1}{v}\exp\left[-\sum\alpha_{k\mu}v^{-k}(kT)^{-\mu}\right].$$

With (37) for the Gibbs' free energy one then obtains

$$F=kNT\left[\ln\left(\frac{h^2}{2\pi mkT}\right)^{3/2}\frac{1}{v} - \sum_{\mathbf{k}\mu}\alpha_{\mathbf{k}\mu}\frac{1}{v^{\mathbf{k}}}\frac{1}{(kT)^{\mu}}\right]. \qquad (78)$$

The pressure, from (36) and (75), is

$$P=\frac{kT}{v}\left[1-\sum_{\mathbf{k},\mu}\frac{\mathbf{k}}{\mathbf{k}+1}\alpha_{\mathbf{k}\mu}\frac{1}{v^{\mathbf{k}}}\frac{1}{(kT)^{\mu}}\right]. \qquad (79)$$

Since

$$G_{01}(va, Z, Y)=Y\frac{\partial}{\partial Y}G_{00}(va, Z, Y),$$

one finds from (75) and (33) the equation for the energy to be

$$E=NkT\left[\frac{3}{2}-\sum_{\mathbf{k}\mu}\frac{\mathbf{k}\mu}{\mathbf{k}+1}\alpha_{\mathbf{k}\mu}\frac{1}{v^{\mathbf{k}}}\frac{1}{(kT)^{\mu}}\right]. \qquad (80)$$

10. Repulsion

The region of the configuration space for which the kinetic energy, $E-\sum u_{ij}$, is negative, is not available to the system, and should properly be excluded from the integral (5). If (5) is integrated over the whole configuration space this portion is not excluded, and will contribute to the integral an amount, the sign of which depends on the value of N, and the magnitude of which one can scarcely limit rigorously. It is, however, to be expected, that if the mutual potentials u_{ij} are everywhere finite, and not many magnitudes greater than kT in the repulsive region where they are positive, that this false contribution which is calculated by (5) will be insignificant, since such a small volume of the configuration space corresponds to a region where many molecules are repelling.

It is also to be expected that the properties of a system of molecules for which the mutual potentials u_{ij} became, say $100kT$, or $1000kT$, in the region of repulsion, and not infinity, would be the same as those of a system of real molecules. It is therefore not surprising, that in spite of the neglect which has been made, we are able to show in the succeeding section, that the equations derived so far are in agreement with those previously derived from the Gibbs' integral, provided u_{ij} is nowhere infinite. This point, nevertheless, leaves a considerable flaw in the logic of the argument.

One may, however, derive equations for a system for which the mutual potential between molecule pairs differs in the other extreme from those of real molecules, namely a system for which u_{ij} is infinite for all distances r_{ij} less than r_0, and negative for all values of r_{ij} greater than r_0. This system also will be expected to show properties almost identical with those of a real system, since actual repulsive potentials are so steep.

For such a system $E-\sum u_{ij}$ is negative if any distance r_{ij} is less than r_0. The integral (5) must be limited to such regions for which all mutual distances r_{ij} exceed r_0. This may be done by integrating over the complete configuration space, but multiplying the integrand by a function which is identically zero if any r_{ij} is less than r_0. Such a function is

$$\prod_{ij}(1+h_{ij}),$$

where

$$h_{ij}=h(r_{ij})=-1, \quad r_{ij}<r_0, \qquad (81)$$
$$=0, \quad r_{ij}\geq r_0.$$

Equation (5) is then rewritten as

$$\Omega=\frac{(2\pi m)^{3N/2}}{h^{3N}N!\,(3N/2)!}\int\cdots\int\prod_{ij}(1+h_{ij}) \times(E-\sum u_{ij})^{3N/2}d\tau_1\cdots d\tau_N, \qquad (82)$$

$$\ln\Omega=N\ln\left(\frac{4\pi m\epsilon e}{3h^2}\right)^{3/2}+\ln\Theta,$$

with

$$\Theta=\frac{1}{N!}\int\cdots\int\prod_{i,j}(1+h_{ij})\times\left(1+\sum_{ij}-\frac{u_{ij}}{N\epsilon}\right)^{3N/2}d\tau_1\cdots d\tau_N. \quad (83)$$

Since

$$\prod_{ij}(1+h_{ij})=\sum_{\substack{\mu_{ij}\\ \mu_{ij}=0\text{ or }1}}\prod_{ij}(h_{ij})^{\mu_{ij}}, \quad (84)$$

it is seen that by defining the cluster integrals $a_{l\nu}$ as

$$a_{l\nu}=\frac{1}{1!V}\int\cdots\int\sum_{\substack{\nu_{ij},\,\mu_{ij}\\ \Sigma\nu_{ij}=\nu\\ \mu_{ij}=0\text{ or }1}}\prod_{l\geq i>j\geq 1}h_{ij}^{\mu_{ij}}\times\frac{(-u_{ij})^{\nu_{ij}}}{\nu_{ij}!}d\tau_1\cdots d\tau_N \quad (85)$$

(all products at least singly connected).

instead of by Eq. (12), the complete argument of c may be repeated, resulting in the same final Eq. (15) for $\ln\Omega$.

In (85) the sum is to be extended only over those products for which the corresponding graph of $\nu+\sum\mu_{ij}$ lines and l vertices is a connected graph.

Similarly the argument of Section 6 can be exactly repeated if only the definition of the irreducible integrals $\alpha_{k\mu}$, Eq. (39), is altered to

$$\alpha_{k\mu}=\frac{1}{k!V}\int\cdots\int\sum_{\substack{\nu_{ij},\,\mu_{ij}\\ \Sigma\nu_{ij}=\mu\\ \mu_{ij}=0\text{ or }1}}\prod_{k+1\geq i>j\geq 1}h_{ij}^{\mu_{ij}}\times\frac{(-u_{ij})^{\nu_{ij}}}{\nu_{ij}!}d\tau_1\cdots d\tau_N. \quad (86)$$

(all products more than singly connected).

In this way the arguments of the preceding sections become completely rigorous for a system of this type of mutual potential u_{ij}.

Since the integrand of (82) contains the factor $\Pi(1+h_{ij})$ which is identically zero for all values of r_{ij} less than r_0 it is immaterial what the value of the other factor $(E-\sum u_{ij})^{3N/2}$ is, in this region. The simplest choice is to assume u_{ij} to be zero for all values of r_{ij} less than r_0. In this case all terms in (85) and (86) for which $\mu_{ij}=1$, $\nu_{ij}\neq 0$ lead to zero integrals, since the integrand is everywhere zero. This affords an appreciable simplification in the consideration of these integrals.

11. Comparison with the Previous Method

The equations of Section 5, and of Section 9, become identical to those derived formerly if the substitutions

$$b_l=\sum_\nu a_{l\nu}\frac{1}{(kT)^\nu} \quad (87)$$

and

$$\beta_k=\sum_\mu\alpha_{k\mu}\frac{1}{(kT)^\mu} \quad (88)$$

are introduced.

The cluster integrals b_l and irreducible integrals β_k were defined previously by the equations

$$b_l=\frac{1}{Vl!}\int\cdots\int\sum\prod_{l\geq i>j\geq 1}(e^{-u_{ij}/kT}-1)d\tau_1\cdots d\tau_1 \quad (89)$$

(sum over all products at least singly connected)

and

$$\beta_k=\frac{1}{Vk!}\int\cdots\int\sum_{k+1\geq i>j\geq 1}\prod(e^{-\mu_{ij}/kT}-1)d\tau_1\cdots d\tau_{k+1} \quad (90)$$

(sum over all products more than singly connected).

As long as it is assumed that the potentials u_{ij} are everywhere finite the exponentials can be developed, and one obtains

$$b_l=\frac{1}{Vl!}\int\cdots\int\sum_{\nu_{ij}}\prod_{l\geq i>j\geq 1}\frac{(-u_{ij})^{\nu_{ij}}}{\nu_{ij}!}\times(kT)^{-\Sigma\nu_{ij}}d\tau_1\cdots d\tau_l \quad (89')$$

(sum over all products at least singly connected).

and

$$\beta_k=\frac{1}{Vk!}\int\cdots\int\sum_{\nu_{ij}}\prod_{k\geq i>j\geq 1}\frac{(-u_{ij})^{\nu_{ij}}}{\nu_{ij}!}\times(kT)^{-\Sigma\nu_{ij}}d\tau_1\cdots d\tau_{k+1} \quad (90')$$

(sum over all products more than singly connected).

By comparison with the definitions (12) and (39) of $a_{l\nu}$ and $\alpha_{\mathbf{k}\mu}$ it is seen that Eqs. (89′) and (90′) are equivalent to (87) and (88), respectively.

In Section 10 a system composed of molecules for which the mutual potentials u_{ij} were infinity if $r_{ij}<r_0$ and negative for $r_{ij}\geq r_0$ was considered. In this case the exponential cannot be expanded. One may, however, write

$$e^{-u(r_{ij})/kT}-1=h(r_{ij})+\sum_{\nu_{ij}=1}^{\infty}\frac{[-u'(r_{ij})]^{\nu_{ij}}}{\nu_{ij}!(kT)^{\nu_{ij}}},$$

in which the function $h(r_{ij})$ is defined by Eq. (81). It is obvious, then, that if Eqs. (85) and (86) are used for $a_{l\nu}$ and $\alpha_{\mathbf{k}\mu}$, respectively, one arrives at Eqs. (87) and (88).

Professor Norbert Wiener has reported to the mathematical society meeting in New York in February a method of treating the imperfect gas by considering the solutions of the equations of motion. His results appear to be equivalent to those derived in this paper. The authors are greatly indebted to Dr. Maria Goeppert-Mayer, who originally demonstrated to them the feasibility of using the method employed here.

Glossary

The symbols used for the thermodynamic properties and parameters are: E, energy; $\epsilon=E/N$; S, entropy; F, Gibbs' free energy; N, number of molecules; V, total volume; $v=V/N$; P, pressure; T, temperature. In addition we use: k, Boltzmann's constant; h, Planck's constant; W, phase volume in γ-space; W_p factor of W in momentum part of γ-space; Ω, total number of quantum states of system below energy E, $\Omega=W/h^{3N}N!$; and U the total potential energy of the system as a function of the coordinates.

The running indices i, j, refer to numbered molecules:

r_{ij}, the distance between the molecule pair i, j;
$u_{ij}=u(r_{ij})$, the mutual potential energy of the pair;
$f_{ij}=f(r_{ij})=e^{-u_{ij}/kT}-1$;
$h_{ij}=h(r_{ij})$ a function defined by Eq. (81);
$d\tau_i=dx_i dy_i dz_i$.

The following integrals enter the equations:

$a_{l\nu}$ cluster integral of l particles and ν bonds, defined by (12) or (85) and related to b_l by (87);

$\alpha_{\mathbf{k}\mu}$ irreducible integral of $\mathbf{k}+1$ particles and μ bonds, defined by (39) or (86) and related to $\beta_{\mathbf{k}}$ by (88);

b_l cluster integrals of l particles in Gibbs' method, defined by (89);

$\beta_{\mathbf{k}}$ irreducible integral $\mathbf{k}+1$ particles in Gibbs' method, defined by (90).

The parameter Z, introduced in Section 4 as an undetermined multiplier, is identified with the fugacity, Eq. (37). In Section 7 Z is introduced as a special value of z_0, which is a special value of the (complex) variable of integration z.

The parameter Y, introduced in Section 4 as an undetermined multiplier, is identified with $1/kT$, Eq. (32). In Section 7 Y is introduced as a special value of y_0 which is a special value of the (complex) variable of integration y. In Section 8, Y is a special value of the (complex) variable of integration η.

The parameter ρ, identified with $1/v$ in (76), is a special value of the (complex) variable of integration ζ (Section 8).

The variable r and t are (complex) independent variables of the function H of Eq. (47), which function becomes singular for the (real) associated radii of convergence r_0, t_0.

In addition the following functions which enter are defined by the equations: Θ, Eq. (9); Θ_M Eq. (11); R, Eq. (3); $G_{\lambda n}$ Eq. (23); F, (N, L, va) Eq. (45); $H(va, r, t)$ Eq. (47); $\phi(x, va)$ Eq. (56); $f(x, y, z)$ Eq. (58); $\Phi(l, \nu, \alpha)$ Eq. (64); and $H(\alpha, Z, Y)$ Eq. (65).

A Differential Method Applied to the Surface Ionization of Sodium Halides on Tungsten

A. A. JOHNSON AND T. E. PHIPPS
Department of Chemistry, University of Illinois, Urbana, Illinois

(Received August 2, 1939)

A differential molecular-beam method for the study of the surface ionization of salts was developed. A reference filament and a working filament were placed in the paths of molecular beams emitted from the same furnace orifice; and the ratios of the positive ion currents collected from the two surfaces were measured with a center-tap galvanometer for different temperatures of the working filament. This method was applied to the study of the ionization of sodium halides on tungsten and tungsten-oxygen surfaces. The results were not in close agreement with the simple theory of the ionization of a gaseous sodium atom at a tungsten surface. The energy quantity, $(I-\Phi)\epsilon$, (I being the ionization potential of the alkali atom, and Φ, the work function of the surface) was about 0.3 v.e. less than that demanded by theory. To explain this defect an extension was made of the simple theory, in which it was assumed that a small fraction of the surface was covered with halogen atoms even to high temperatures. The experimental results could then be explained upon the assumption that from two to four percent of the tungsten surface (the exact value depending upon the particular halide and tungsten surface involved) held adsorbed halogen atoms up to 2600°K.

INTRODUCTION

THE surface ionization of the alkali metals on tungsten and tungsten-oxygen surfaces (hereafter referred to as W and W−O surfaces, respectively) has been studied by several investigators.[1] Recently Hendricks, Phipps and Copley[2] reported upon the ionization of potassium halides on W and on W−O surfaces by a molecular beam method. In that experiment beams of potassium halides were directed in high vacuum against a filament, and the positive ion currents to a collector cylinder were measured at different surface temperatures. Degrees of ionization on W surfaces were calculated upon the assumption that each halide molecule produced one positive ion on striking a W−O surface. The results on W surfaces at high temperatures (1800–2400°K) were interpreted as indicating surface dissociation of the potassium halide molecule, followed by partial ionization of the potassium atom and by escape of the halogen as an atom. Below 1800°K a surface of work function intermediate between that of W and W−O was observed, which was thought to be a tungsten-halogen (W−X) surface.

The high temperature data were treated by the Saha-Langmuir[3] equation,

$$\frac{i_+}{i_a}=\frac{\omega_+(1-r_+)}{\omega_a(1-r_a)}\exp\left[\frac{(\Phi-I)\epsilon}{kT}\right], \qquad (1)$$

in which i_+/i_a is the equilibrium ratio of ion to atom at zero field; ω_+/ω_a, the statistical weight ratio of ion to atom; r_+ and r_a, the reflection coefficients, respectively, of ion and atom from the surface; Φ the Richardson "work function" of the surface; I, the ionization potential of the alkali atom; and ϵ, k and T have their usual significances. The ratio, ω_+/ω_a, is $\frac{1}{2}$ for alkali atoms; and the coefficients r_+ and r_a are thought to be negligibly small.[4] Eq. (1) was then written in the form,

$$\log_{10}\frac{i_+}{i_a}=-0.301+\frac{(\Phi-I)\epsilon}{2.303\,kT}. \qquad (2)$$

At temperatures above 1800°K the data for the potassium halides, when treated according to (2), gave a value for Φ of 4.54 volts, which is in fair agreement with the values in the literature for clean tungsten determined by other methods. The intercept, however, was approximately −0.1 instead of −0.301. It had been suggested by Becker[5] that Φ may have a temperature de-

[1] A brief bibliography is given in reference 6.
[2] Hendricks, Phipps and Copley, J. Chem. Phys. **5**, 868 (1937).
[3] Langmuir and Kingdon, Proc. Roy. Soc. **107A**, 61 (1925).
[4] Taylor and I. Langmuir, Phys. Rev. **44**, 423 (1933).
[5] Becker, Phys. Rev. **45**, 694 (1934).

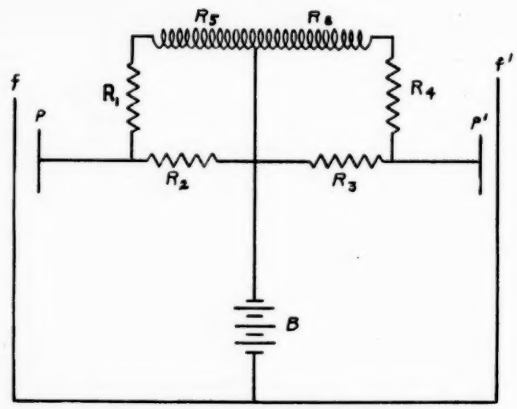

FIG. 1. Simplified electrical circuit used in surface ionization measurements. f and f' are the operating and the reference filaments, respectively. R_5 and R_6 are the half-coils of the center-tap galvanometer.

pendence of the form $\Phi=\Phi_0+\alpha T$. This suggestion was tentatively accepted, and (2) was modified to give

$$\log_{10}\frac{i_+}{i_a}=-0.301+\frac{\alpha\epsilon}{2.303\,k}+\frac{(\Phi_0-I)\epsilon}{2.303\,kT}. \quad (3)$$

A value of α was calculated from the experimental intercept.

In the present work the molecular beam method has been improved and extended to a study of the ionization of the sodium halides on tungsten, where a low degree of ionization was expected since the quantity $(\Phi-I)$ is negative for the process of ionization of a sodium atom on tungsten.

EXPERIMENTAL

Theory of the differential method

The accuracy of the experimental method previously employed in the study of surface ionization of potassium[6] and potassium halides[2] on tungsten was limited by the constancy of the molecular beam which was allowed to strike the tungsten surface. During the present investigation a differential method was developed, which improved the accuracy of the measurements without necessitating improvement in the constancy of the beam. In this method two molecular beams originating at the same furnace opening were allowed to strike separate tungsten surfaces each of which was surrounded by a collecting cylinder. One of the filaments, which will be designated as the reference filament, was kept at a constant temperature while the temperature of the other filament, which will be designated as the working filament, was varied. Under conditions of molecular streaming[7] from the furnace orifice the ratio of the intensities of the two beams remained constant with changes in total beam intensity and hence remained constant with time.

A schematic diagram of the electrical circuit which was used to measure the positive ion currents is shown in Fig. 1. Here R_1, R_2, R_3 and R_4 are variable resistances and R_5 and R_6 are the resistances of the half-coils of a center-tap galvanometer. A negative potential is applied to plates p and p', which collect positive ions from f and f', respectively. If the half-coils of the galvanometer are identical, the current through R_5 is equal to the current through R_6 when the galvanometer is at zero. f' is the reference filament which is kept at a constant temperature.

Assume that filament f is now set at T_0, at which temperature the ion current from f is i_0. The current from f' will be designated by i. R_1 and R_2 are then adjusted until the galvanometer is at zero. The following relation is then satisfied:

$$i_0\frac{R_2}{R_1+R_2+R_5}=i\frac{R_3^0}{R_3^0+R_4^0+R_6}, \quad (4)$$

or

$$\frac{1}{i}\frac{R_2}{R_1+R_2+R_5}=\frac{1}{i_0}\frac{R_3^0}{R_3^0+R_4^0+R_6}, \quad (5)$$

where R_3^0 and R_4^0 are the resistances of R_3 and R_4, respectively, during this balance at T_0. Assume now that the temperature of the working filament is changed to T_1 at which temperature the ion current is i_1. R_3 and R_4 are then adjusted, *keeping their sum constant*, until the galvanometer is again at zero. Let their values at this new balance be represented by R_3' and R_4'. The following relation is then satisfied:

$$i_1\frac{R_2}{R_1+R_2+R_5}=i\frac{R_3'}{R_3'+R_4'+R_6}, \quad (6)$$

or

$$\frac{1}{i}\frac{R_2}{R_1+R_2+R_5}=\frac{1}{i_1}\frac{R_3'}{R_3'+R_4'+R_6}. \quad (7)$$

[6] Copley and Phipps, Phys. Rev. **48**, 960 (1935).

[7] R. G. J. Fraser, *Molecular Beams* (Chemical Publishing Company of New York, Inc., 1938), p. 4.

By combining (5) and (7) we obtain

$$\frac{1}{i_0}\frac{R_3^0}{R_3^0+R_4^0+R_6}=\frac{1}{i_1}\frac{R_3'}{R_3'+R_4'+R_6}. \quad (8)$$

Since the sum of the resistances of R_3 and R_4 was kept constant,

$$R_3'+R_4'+R_6=R_3^0+R_4^0+R_6, \quad (9)$$

and hence

$$i_1/i_0=R_3'/R_3^0. \quad (10)$$

If the degree of ionization at T_0 is known to be K_0, then the degree of ionization K_1 at T_1 will be given by

$$K_1=K_0R_3'/R_3^0. \quad (11)$$

The ion-atom ratio $(i_+/i_a)_{T_1}$ is given by

$$(i_+/i_a)_{T_1}=K_0R_3'/(R_3^0-K_0R_3'). \quad (12)$$

If the initial balance at T_0 is made with the working filament oxygen-coated, K_0 may be assumed to be unity and

$$K_1=R_3'/R_3^0. \quad (13)$$

The ion-atom ratio at T_1 is then given by

$$(i_+/i_a)_{T_1}=R_3'/(R_3^0-R_3'). \quad (14)$$

The center-tap galvanometer

The center-tap galvanometer had to be constructed, since such an instrument could not be purchased. A coil with a center tap was constructed which had the same dimensions as the coil in a galvanometer of high current sensitivity.[8] Two parallel strands of No. 46 B. and S. gauge iron-free enameled copper wire of high purity[9] were wound on a collapsible form and the unsupported sections of the coil were treated with alcoholic shellac and dried. The form was then removed and the remaining sections of the coil were shellacked and dried. The ends of the two coils obtained in this manner were then connected to give one coil with a center tap.

A thin piece of copper sheet to which was soldered a small brass collar was attached to the top of the coil by means of chip shellac. The phosphor-bronze suspension, which served as the lead-out for the center tap, was connected to this collar. Two thin pieces of copper sheet were attached in the same way to the bottom of the coil. Narrow strips of gold leaf about 0.2 cm wide and 2 cm long served as leads from coil to binding posts.

At 25°C the resistance of each half-coil was approximately 3100 ohms and the sensitivity was 7.1×10^{-11} amp.-mm^{-1} with the scale at 5.6 meters and with 20,000 ohms damping resistance in parallel. Each half-coil was measured separately with the other disconnected. The condition necessary for critical damping for this coil was investigated. The results are shown in Fig. 2. As in Fig. 1 (R_1+R_2) is the resistance in parallel with one half-coil and (R_3+R_4) is the resistance in parallel with the other, when the coil is critically damped.

The galvanometer was surrounded by a double-walled galvanized iron case which had rock wool between the walls. This case served to keep the galvanometer at the same temperature throughout, thereby preventing thermoelectric currents from arising in the galvanometer.

The experimental cell

The details of the experimental cell are shown in Fig. 3. A quartz capsule *1* containing the salt *2* and provided with a small hole *3* is surrounded by a closely wound 16-mil tungsten spiral *4*, which is

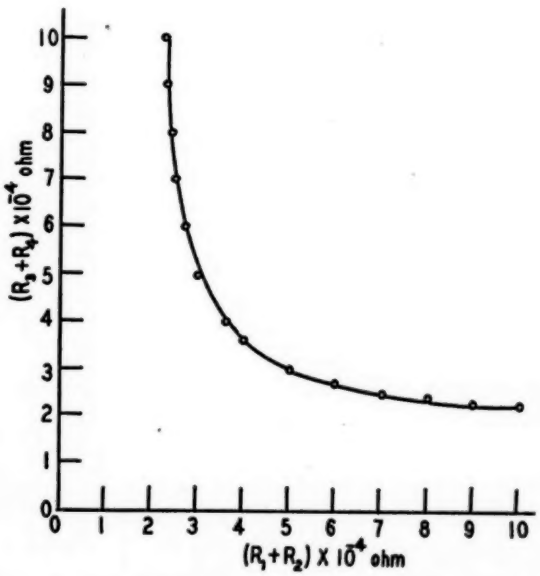

FIG. 2. Critical damping resistances for center-tap galvanometer.

[8] G-M Laboratories, Inc., Galvanometer No. 2551A.
[9] Obtained from Leeds and Northrup Company through the courtesy of Mr. H. J. W. Nethery of the Technical Sales Division.

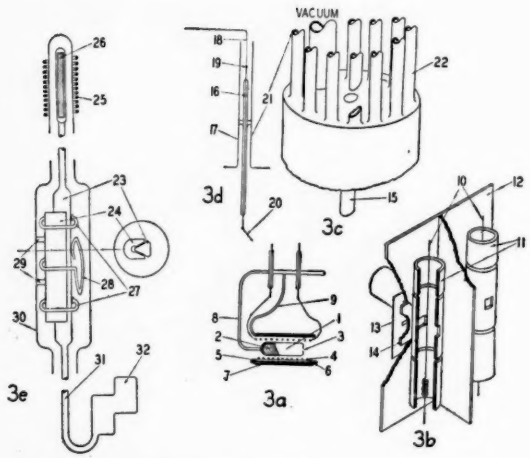

FIG. 3. Essential features of the experimental cell.

supported by two small quartz rods *5*. These rods are sealed to the ends of the quartz tube *6* around which is slipped a thin reflecting nickel cylinder *7*, which serves as a radiation shield. The capsule is supported by a quartz rod *8*; and the quartz tube, by a quartz rod *9*.

The 2-mil tungsten filaments *10* which constituted the ionizing surfaces were each surrounded by collecting cylinders *11*. These cylinders were made from sections of Pyrex tubing which were platinized according to the method of Taylor.[10] The two end cylinders around each filament functioned as guard rings. These guard rings were necessary since at high filament temperatures (2400–2600°K) the salt which had collected on the 6-mil tungsten spring and upper end of the filament during bake-out of the cell slowly evaporated,—partially as ions. The large platinized Pyrex shield *12* separated the collecting cylinders and prevented ions originating on one filament from reaching the other collector. A shield of thin tantalum sheet *13* was kept at a positive potential and prevented ions which originated on the furnace coils from reaching the collecting cylinders. The shutter *14*, which is described later, permitted interruption of either, neither or both of the beams at will.

The entire assembly 3b was supported by a heavy Pyrex rod *15* which was sealed to the head of the cell, Fig. 3c. Ten 40-mil tungsten lead-in wires were constructed as shown in 3d. A section of Pyrex encased 40-mil tungsten *16* was sealed inside of a Pyrex tube *17*. A flexible stranded nickel wire *18* was joined to the top of the tungsten wire by means of silver solder *19*; and a small flexible platinum wire *20* was melted onto the lower end of the tungsten wire. These ten lead-in units were sealed at *21* into ten tubes *22*, which had been sealed around the circumference of the head of the cell. The small platinum wires *20* were then joined by welding in the oxyhydrogen flame to similar small platinum wires (not shown) which had been previously welded to the various leads of the assembly 3b. The lead-in wires were constructed in this way to facilitate replacement. The construction sketched in 3b and 3c permitted removal of the entire assembly 3b by cutting the small platinum wires and sealing off the supporting Pyrex rod *15*, thus leaving the head 3c of the cell intact. The entire assembly 3b was enclosed in a 65-mm diameter Pyrex tube which could be cracked off from the head 3c by means of a hot wire and resealed with an oxyhydrogen flame and an auxiliary ring burner.

The all-glass shutter mechanism is shown in Fig. 3e. A Pyrex shaft *23*, ground to a triangular cross-sectional shape, moved in a track ground in a large piece of Pyrex capillary tubing *24*. The shaft was moved by the action of a solenoid *25* on a glass-enclosed iron nail *26*. The two guides *27* held the shaft to a sliding fit, and the tension was supplied by a glass spring *28*. The stationary track *24* was supported by two glass rods *29* which were sealed to the Pyrex mantle *30*. A Pyrex rod *31* which carried the shutter *32* was joined to the lower end of the shaft. The shaft moved easily in the track, but would remain in any position.

Procedure

The cell was baked out in an electrically heated oven for 24–30 hours above 460°C, and the vacuum line back to the first diffusion pump was heavily torched for 2–3 hours. The cell was evacuated by two mercury diffusion pumps supported by a Cenco Hyvac pump. Other accessories included two protective liquid-air traps, a mercury cut-off and a McLeod gauge. The entire cell was immersed in liquid air while the measurements were being made. Observations on the constancy of the electron emission from the filaments with time indicated that the

[10] G. F. Taylor, J. Opt. Soc. Am. **18**, 138 (1929).

partial pressure of oxidizing gases was less than 10^{-10} mm Hg.

After a satisfactory vacuum had been attained the furnace temperature was increased until a molecular beam of the desired intensity was observed. The reference filament was kept at a constant temperature, usually 2075°K. The working filament was heated to some "standard" temperature T_0 (usually also 2075°K) and an initial balance made by adjusting R_1 and R_2. The working filament was then heated to different temperatures and R_3 and R_4 were adjusted, keeping their sum constant, until a balance was again obtained at each temperature.

The degree of ionization at T_0 was obtained as follows. The mercury cut-off was closed and oxygen was allowed to enter the system by means of an oxygen valve[11] until the pressure was approximately 10^{-4} mm Hg. The filament was given several flashes at 2300°K and was then held at 1450°K for 15 minutes. The oxygen was then pumped out and the cell was immersed in liquid air. The ion current was measured before and after flashing off the oxygen layer. The degree of ionization at T_0 on clean tungsten was then calculated on the assumption that each sodium halide molecule furnished one positive ion upon striking a W−O surface.

The ion-atom ratio was found to increase with increasing field, and a brief study was made of the effect of field. The ion current at constant temperature was determined as a function of field, and a linear extrapolation was made to zero field on a plot of $\log_{10}(i_+/i_a)$ against E.

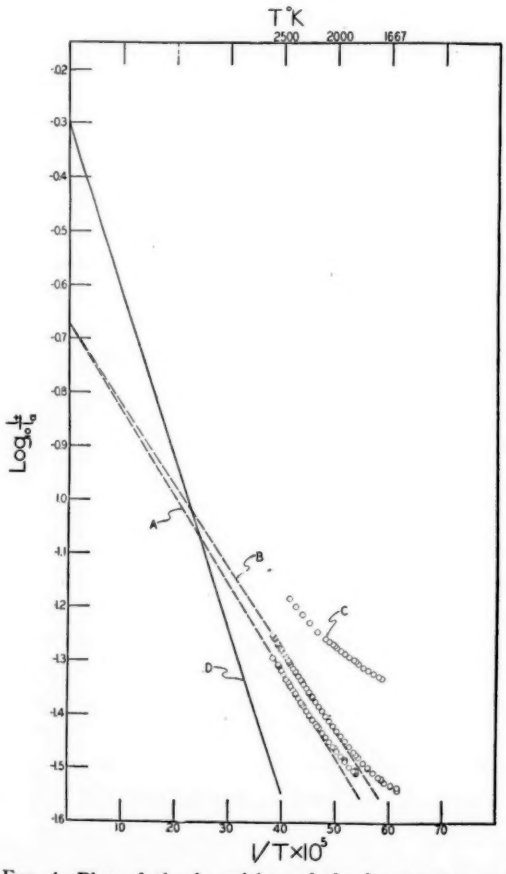

FIG. 4. Plot of the logarithm of the ion-to-atom ratio against the reciprocal of the absolute temperature. *A*, NaCl; *B*, NaBr; *C*, NaI; *D*, theory for sodium atom on clean tungsten.

[11] J. B. Taylor, Rev. Sci. Inst. **6**, 243 (1935).

RESULTS

Figure 4 is a plot of the logarithm of the ratio i_+/i_a against $1/T\times10^5$ for the data on oxygen-free surfaces. The data for NaI are not as complete or as accurate as those for NaCl and NaBr. An attempt was made to study NaF, but it was found that the salt reacted with the quartz capsule even when dry and in a high vacuum. A gaseous product of the reaction was observed, which was thought to be SiF_4. The value of i_a (the fraction of molecules evaporating without ionization) was calculated from the relation $i_a=(1-i_+)$. The calculation of i_+ and i_a was made upon the assumption that each sodium halide molecule furnishes one positive ion upon striking a W−O surface. The ion current from a W−O surface was found to be independent of both temperature and applied field in the region from 1250–1500°K. This observation was taken as evidence for 100 percent ionization. The curves for sodium halides on W−O surfaces have been omitted here, since they were similar to those which have already been given for potassium halides.[2] The ion current from a W−O surface decreased below 1250°K, probably due to the formation of a low work function surface such as W−O−Na. The ion current also decreased above 1500°K due to the stripping of the oxygen from the W−O surface.

The theoretical line for Na ($I=5.12$ volts) on W ($\Phi=4.50$ volts) is line *D* in Fig. 4. The equation for this line may be written as

$$\log_{10}(i_+/i_a)=-3124/T-0.301. \qquad (15)$$

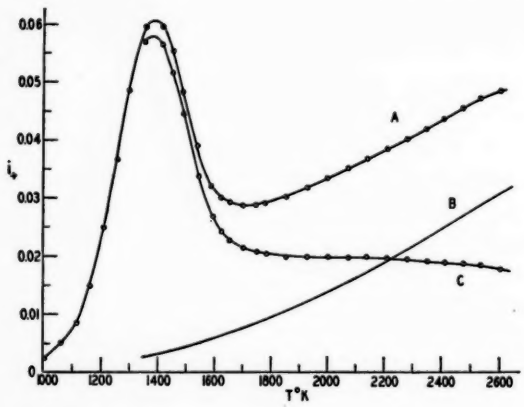

FIG. 5. Plot of the degree of ionization (i_+) against the temperature for NaCl on W. A. The experimental degree of ionization of NaCl on W. B. The theoretical degree of ionization of Na on W. C. *A* minus *B*.

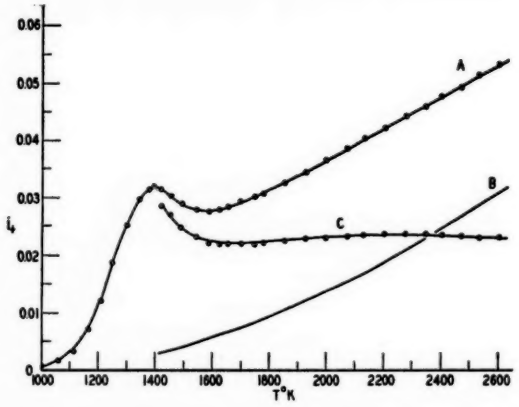

FIG. 6. Plot of the degree of ionization (i_+) against the temperature for NaBr on W. A. The experimental degree of ionization of NaBr on W. B. The theoretical degree of ionization of Na on W. C. *A* minus *B*.

The equation for line *A* in Fig. 4, which represents the data for NaCl above 2200°K and at zero field, is

$$\log_{10}(i_+/i_a) = -1616/T - 0.670; \qquad (16)$$

and the equation for line *B* in Fig. 4, which represents the data for NaBr above 2100°K and at zero field, is

$$\log_{10}(i_+/i_a) = -1514/T - 0.670. \qquad (17)$$

If we assume that Φ depends upon temperature and apply Eq. (3) we obtain a value for α of -7.3×10^{-5} volt-deg.$^{-1}$. This result conflicts even as to sign with the values of α calculated from results on potassium metal[6] ($\alpha=4.2\times10^{-5}$ volt-deg.$^{-1}$) and on potassium halides[2] ($\alpha=5.6\times10^{-5}$ volt-deg.$^{-1}$). It would appear from this, then, that the divergence of experiment from theory, at least in the sodium halide case, cannot be accounted for by the existence of a temperature coefficient of Φ.

The quantity $(I-\Phi)$, for the NaCl case, calculated from (16) is 0.32 volt; $(I-\Phi)$ for the NaBr case, calculated from (17) is 0.30 volt. For the process,

$$\mathrm{Na}(g)+W=\mathrm{Na}^+(g)+(E^-\text{ in W}), \qquad (18)$$

the quantity $(I-\Phi)$ should be 0.62 volt according to theory. No ionization process suggests itself for which the ionization potential is less than that for the ionization of the sodium atom;[12] namely, 5.12 volts. In the following treatment it will be assumed that the ionization of a gaseous atom is involved, and that the defect of the experimental $(I-\Phi)$ from 0.62 volt is to be imputed to the existence, under the conditions of the experiment, of a surface of work function greater than that of clean tungsten.

A well-aged tungsten filament is known to have active areas which are capable of holding adsorbed atoms very tenaciously.[4] Presumably these active areas are located "at any re-entrant angle between crystal planes or at irregularities in the lattice." Under the conditions of the present experiment, in which there is a continuous supply of halogen atoms to the surface, it is possible that these active areas would retain adsorbed halogen atoms even to high temperatures. The work function of a tungsten surface covered with halogen atoms is not known exactly, but a W−I surface is known to have a work function of approximately 5.5 volts,[13] which is high enough to ionize sodium atoms almost 100 percent. In the following treatment we shall assume (1) that active areas exist which consist of tungsten covered with halogen, (2) that the sodium halide molecules striking these active areas are 100 percent ionized, and (3) that the

[12] It has been pointed out recently to one of the authors by indirect correspondence that an unpublished thesis research by B. Toybes, University of California 1926, under the direction of Professor G. K. Rollefson, established the fact that if alkali halides are heated on a tungsten filament the corresponding positive ions of the alkali metals are formed.

[13] R. W. Spence and M. J. Copley, unpublished data, University of Illinois, Department of Chemistry, 1939.

deviation of the experimental results from theory is entirely due to this cause.

We consider 1 cm² of tungsten surface and let x be the area in cm² which is in an active condition; then $(1-x)$ is the area of the clean tungsten. Let n be the number of molecules striking 1 cm² per second. Then nx is the number per second which strike active areas and $n(1-x)$ is the number per second which strike clean tungsten. On the basis of the assumption that the molecules which strike active areas are 100 percent ionized and those which strike clean tungsten are ionized to the extent predicted by theory, we can write

$$nx+n(1-x)K=n_1, \tag{19}$$

where K is the degree of ionization on clean tungsten predicted by theory, and n_1 is the total number of ions evaporating per second from 1 cm². We can solve (19) for x and obtain

$$x=(n_1-Kn)/(n-Kn), \tag{20}$$

or

$$x=[(n_1/n)-K]/(1-K). \tag{21}$$

In (21) x represents the fraction of the surface covered by active areas and n_1/n is the ratio of the number of ions evaporating to the number of molecules striking. This ratio is equal to i_+, the degree of ionization. Making this substitution we write

$$x=(i_+-K)/(1-K). \tag{22}$$

Figures 5, 6, and 7 are plots of i_+ against T for NaCl, NaBr, and NaI, respectively. Curve A is the experimental degree of ionization (i_+) and

TABLE I. *The fraction of the tungsten surface at different temperatures which behaved as "active area" of high work function for the halides of sodium.**

T°K	x (NaCl)	x (NaBr)	x (NaI)
2607	0.0183	0.0231	
2478	0.0191	0.0232	
2347	0.0195	0.0236	0.0376
2214	0.0197	0.0235	0.0375
2075	0.0200	0.0232	0.0375
1931	0.0199	0.0228	0.0378
1782	0.0205	0.0221	0.0376
1705	0.0215	0.0222	0.0376
1625	0.0242	0.0221	0.0385
1545	0.0339	0.0232	0.0383
1492	0.0446	0.0250	
1456	0.0518	0.0269	0.0375
1418	0.0566	0.0285	

* The data for NaCl and NaBr were taken with the same filament. A different filament, but with the same aging schedule, was used for the NaI data.

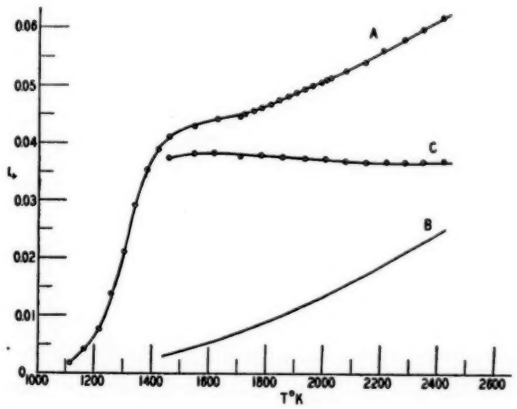

FIG. 7. Plot of the degree of ionization (i_+) against the temperature for NaI on W. A. The experimental degree of ionization of NaI on W. B. The theoretical degree of ionization of Na on W. C. A minus B.

B is the theoretical degree of ionization (K). Curve C is constructed by plotting (i_+-K) against T. Since K is small compared to unity, the value of (i_+-K) (Eq. (22)) is nearly equal to x.

Table I gives values of x calculated by (22) for the sodium halides. It was observed that the degree of ionization for a particular halide was not exactly the same on different filaments even though they had been given the same aging treatment. If NaI had been studied upon the same filament as NaCl and NaBr the agreement in x would possibly have been better.

Inspection of Table I shows that the fraction of the surface covered with halogen atoms is fairly constant above 1800°K. Below 1800°K, x increases, reaching a maximum at approximately 1400°K probably owing to an extension of the halogen layer from the active spots to other parts of the surface in this temperature range. It was found that below 1800°K the degree of ionization depended upon the rate of arrival of molecules at the surface. A study was made of the effect of arrival rate upon the degree of ionization of NaCl and NaBr below 1800°K. The results for NaCl are shown in Fig. 8. In the region from 1400 to 1800°K the degree of ionization varies directly with the rate of arrival, indicating that at a given temperature a greater fraction of the surface is covered with halogen atoms at the higher rate of arrival. Below 1400°K the degree of ionization at any temperature varies inversely with the rate of arrival, indi-

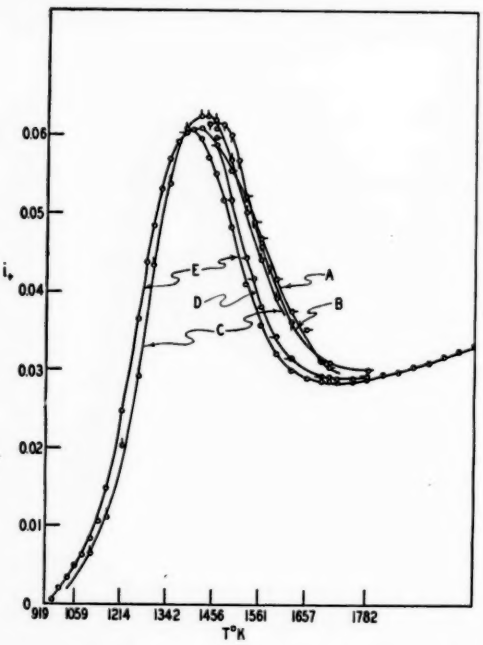

FIG. 8. The effect of rate of arrival of molecules at the tungsten surface upon the degree of ionization of NaCl at temperatures below 1782°K. Rates of arrival (molecules cm^{-2} $sec.^{-1}) \times 10^{-14}$: *A*, 25; *B*, 9.2; *C*, 6.6; *D*, 4.6; *E*, 3.5.

acting that a greater fraction of the surface is covered with a low work-function layer (W−X−Na or W−Na) at the higher rate of arrival. The same general behavior was observed in the case of NaBr except that the degree of ionization was not so large at the maximum.

Experiments on KCl and KI below 1800°K also showed that the degree of ionization depended upon the rate of arrival, which indicates that the surface was not completely covered with halogen atoms in the experiment of Hendricks, Phipps and Copley,[2] a fact which is in disagreement with their assumption that the W−X surface was complete. It is, therefore, apparent that their calculation of the work function of W−X layers is not valid.

Hendricks, Phipps and Copley[2] observed that the degree of ionization for the potassium halides was slightly greater than the degree of ionization of metallic potassium at the same temperature. In the case of the potassium halides the presence of a small percent of active area would hardly be noticed, because the potassium halides are about 80 percent ionized on the clean surface at high temperatures. A calculation using (22) shows that if 2 percent of the surface were covered by active spots of high work function the degree of ionization would be increased only from 0.800 to 0.804. This change is of the order of the experimental error. The potassium case is then a very unfavorable one in which to become aware of the existence of a small number of active spots of high work function. Only in cases such as that of the sodium halides, in which the degree of ionization on the clean surface is very small, do the active areas of high work function play an important role.

ACKNOWLEDGMENT

The authors wish to express their thanks to Dr. R. L. Seifert for his suggestion of the differential method and for preliminary calculations regarding its use.

A Method of Obtaining the Expanded Secular Equation for the Vibration Frequencies of a Molecule

E. BRIGHT WILSON, JR.
Mallinckrodt Chemical Laboratory, Harvard University, Cambridge, Massachusetts

(Received July 24, 1939)

A method is described for obtaining the secular equation for the vibration frequencies of a molecule directly in expanded form, i.e. as an algebraic rather than a determinantal equation. The force constants occur literally and the masses may occur either literally or numerically, as desired. The symmetry may be employed as usual to factor the secular equation. Several methods of obtaining approximate roots are described for which the expanded form is particularly suitable. Finally, an example, the nonlinear general triatomic molecule, is worked out algebraically.

THE usual procedure for calculating the vibration frequencies of a polyatomic molecule with a given set of force constants involves the solution of a secular or determinantal equation.[1] Since this frequently is of a high degree, its solution is one of the most troublesome steps in the treatment of this problem. Consequently a method which leads directly to an algebraic equation in expanded form rather than a determinantal equation should be of use. Such a method will be described below and some of its advantages and disadvantages listed.

SECULAR EQUATION IN TERMS OF INTERNAL COORDINATES

The potential energy of vibration of a molecule is most conveniently described in terms of some set of "internal" coordinates, such as changes in interatomic distances and angles between bonds, since force constants in terms of these coordinates have a more easily visualized physical meaning than others. In addition these force constants appear in certain cases at least to carry over from one similar molecule to another. Cartesian displacement coordinates x_i are more convenient, however, for expressing the kinetic energy. In terms of these, the kinetic energy is

$$2T=\sum_{i=1}^{3n} m_i\dot{x}_i^2, \tag{1}$$

where n is the number of atoms and m_i is the mass associated with x_i. Suppose that the internal coordinates R_k are given in terms of the Cartesians x_i by the linear relations

$$R_k=\sum_{i=1}^{3n} B_{ki}x_i, \quad (k=1, 2, \cdots, 3n-6), \tag{2}$$

or in matrix-vector notation, $R=Bx$. Then a useful set of quantities may be defined as follows

$$G_{kl}=\sum_{i=1}^{3n} B_{ki}B_{li}/m_i, \quad (k, l=1, 2, \cdots 3n-6). \tag{3}$$

It is shown in the appendix that the kinetic energy in terms of the velocities $\dot{R}_k$ is

$$2T=\sum_{k,\,l=1}^{3n-6}(G^{-1})_{kl}\dot{R}_k\dot{R}_l=\dot{R}'G^{-1}\dot{R}, \tag{4}$$

where G^{-1} is the matrix inverse to $G=\|G_{kl}\|$, $\dot{R}$ is the column matrix $\|\dot{R}_k\|$, and $\dot{R}'$ is the transpose of $\dot{R}$.

The potential energy is given by the expression

$$2V=\sum_{k,\,l=1}^{3n-6} F_{kl}R_kR_l=R'FR, \tag{5}$$

in which F_{kl} is one of the force constants.

The secular equation therefore has the form

$$|F-G\lambda| = \begin{vmatrix} F_{11}-(G^{-1})_{11}\lambda & F_{12}-(G^{-1})_{12}\lambda & \cdots \\ F_{21}-(G^{-1})_{21}\lambda & F_{22}-(G^{-1})_{22}\lambda & \cdots \\ \cdots & \cdots & \cdots \end{vmatrix} = 0, \tag{6}$$

in which $\lambda=4\pi^2\nu^2$, ν being a vibration frequency.

[1] See, for example, D. M. Dennison, Rev. Mod. Phys. **3**, 280 (1931).

Expansion of Secular Equation

By multiplying the secular equation of Eq. (6) by the determinant formed from the quantities G_{kl} of Eq. (3), a new secular equation is obtained, namely,[2]

$$|GF-E\lambda| = \begin{vmatrix} \sum_{i=1}^{3n-6} G_{1i}F_{i1}-\lambda & \sum_j G_{1j}F_{j2} & \cdots \\ \sum_i G_{2i}F_{i1} & \sum_j G_{2j}F_{j2}-\lambda & \cdots \\ \cdots & \cdots & \cdots \end{vmatrix} = 0. \quad (7)$$

Here E is the unit matrix. This form is convenient for expansion as an algebraic equation in λ. The highest power of λ is $(-\lambda)^{3n-6}$ and the lowest is λ^0, which has as a coefficient the determinant of Eq. (7) with $\lambda=0$. The whole equation has the form[3]

$$\sum_{s=0}^{3n-6}(-\lambda)^{3n-6-s} \times \sum_{k<l<\cdots} \begin{vmatrix} \sum_{i=1}^{3n-6} G_{ki}F_{ik} & \sum_{j=1}^{3n-6} G_{kj}F_{jl} & \cdots \\ \sum_i G_{li}F_{ik} & \sum_j G_{lj}F_{jl} & \cdots \\ \cdots & \cdots & \cdots \end{vmatrix}, \quad (8)$$

in which the determinant is an s-rowed principal minor of the determinant GF and the inner sum is over all such s-rowed minors, i.e., minors whose diagonal elements are selected from the diagonal elements of $|GF|$. But

$$\begin{vmatrix} \sum_i G_{ki}F_{ik} & \sum_j G_{kj}F_{jl} & \cdots \\ \sum_i G_{li}F_{ik} & \sum_j G_{lj}F_{jl} & \cdots \\ \cdots & \cdots & \cdots \end{vmatrix} = \sum_{i,j,\cdots=1}^{3n-6} \begin{vmatrix} G_{ki} & G_{kj} & \cdots \\ G_{li} & G_{lj} & \cdots \\ \cdots & \cdots & \cdots \end{vmatrix} F_{ki}F_{lj}\cdots,$$

since $F_{ki}=F_{ik}$. This sum is over all values of $i, j, \cdots$, not just s values. However, if $i=j$, the determinant vanishes. Consequently the sum

$$\sum_{i,j,\cdots=1}^{3n-6} \text{ can be written as } \sum_{i<j<\cdots} \sum_P,$$

where P is a permutation of $ij\cdots$, since this will yield all sets $ij\cdots$ except those for which two or more indices are equal. But the minor $|G|_s$, which occurs in the above expression, is unaffected by permutations of $i, j, \cdots$ except for alteration of its sign, since these permutations represent permutations of the columns of a determinant. Therefore $|G|_s$ can be brought out in front of Σ_P if $\pm$ is inserted in the sum, $+$ for even, $-$ for odd permutations. This gives

$$\sum_{i<j<\cdots} |G|_s \sum_P (\pm) P F_{ki}F_{lj}\cdots. \quad (9)$$

But

$$\sum_P (\pm) P F_{ki}F_{lj}\cdots$$

is just another way of writing the s-rowed determinant $|F|_s$, so that the completely expanded secular equation is

$$\sum_{s=0}^{3n-6}(-\lambda)^{3n-6-s} \sum_{k<l<\cdots} \sum_{i<j<\cdots} \times \begin{vmatrix} G_{ki} & G_{kj} & \cdots \\ G_{li} & G_{lj} & \cdots \\ \cdots & \cdots & \cdots \end{vmatrix} \begin{vmatrix} F_{ki} & F_{kj} & \cdots \\ F_{li} & F_{lj} & \cdots \\ \cdots & \cdots & \cdots \end{vmatrix}, \quad (10)$$

where the sum is over all different sets of s letters k, l, etc. with $k<l$, $l<m$ etc. and over all different sets of s letters $i<j<\cdots$, these to be chosen from the $3n-6$ possible values.

Consequently, the process for setting up the expanded form of the secular equation for a

---

[2] The rule for multiplying determinants is the same as that for matrices so that the property $\sum_{i=1}^{3n-6} G_{ki}(G^{-1})_{il}=\delta_{kl}$ is made use of here.

[3] This result may be seen if the secular equation

$$\begin{vmatrix} (GF)_{11}-\lambda & (GF)_{12} & \cdots \\ (GF)_{21} & (GF)_{22}-\lambda & \cdots \\ \cdots & \cdots & \cdots \end{vmatrix} = 0$$

is expanded into a sum of 2^{3n-6} determinants by using repeatedly the property that

$$\begin{vmatrix} (GF)_{11}-\lambda & (GF)_{12} & \cdots \\ (GF)_{21} & (GF)_{22}-\lambda & \cdots \\ \cdots & \cdots & \cdots \end{vmatrix} = \begin{vmatrix} (GF)_{11} & (GF)_{12} & \cdots \\ (GF)_{21} & (GF)_{22}-\lambda & \cdots \\ \cdots & \cdots & \cdots \end{vmatrix} + \begin{vmatrix} -\lambda & (GF)_{12} & \cdots \\ 0 & (GF)_{22}-\lambda & \cdots \\ \cdots & \cdots & \cdots \end{vmatrix}.$$

These determinants can then be separated into groups having different numbers of λ's, and each determinant written as the product of the λ's which occur in it (on the diagonal only) and the remaining minor of $|GF|$.

molecule is as follows: Calculate from geometry the elements of the rectangular matrix B of $R=Bx$. Multiply these elements together in the proper way to secure the elements of G. Then evaluate the determinants which occur in Eq. (10) to obtain the coefficients of the various products of force constants which make up the coefficients of the powers of λ. All these calculations are best carried out numerically, at least for large molecules.

A Further Reduction

It is possible to carry the analysis still further and to obtain a result which is useful in special situations. A minor $|G|_s$ can be reduced as follows

$$\begin{vmatrix} G_{ki} & G_{kj} & \cdots \\ G_{li} & G_{lj} & \cdots \\ \cdots & \cdots & \cdots \end{vmatrix} = \begin{vmatrix} \sum_t B_{kt}B_{it}\mu_t & \sum_{t'} B_{kt'}B_{jt'}\mu_{t'} & \cdots \\ \sum_t B_{lt}B_{it}\mu_t & \sum_{t'} B_{lt'}B_{jt'}\mu_{t'} & \cdots \\ \cdots & \cdots & \cdots \end{vmatrix} = \sum_{t,\,t',\,\cdots}^{3n} \mu_t\mu_{t'}\cdots \begin{vmatrix} B_{kt} & B_{kt'} & \cdots \\ B_{lt} & B_{lt'} & \cdots \\ \cdots & \cdots & \cdots \end{vmatrix} B_{it}B_{jt'}\cdots$$

$$= \sum_{t<t'<\cdots} \mu_t\mu_{t'}\cdots \begin{vmatrix} B_{kt} & B_{kt'} & \cdots \\ B_{lt} & B_{lt'} & \cdots \\ \cdots & \cdots & \cdots \end{vmatrix} \begin{vmatrix} B_{it} & B_{it'} & \cdots \\ B_{jt} & B_{jt'} & \cdots \\ \cdots & \cdots & \cdots \end{vmatrix}. \quad (11)$$

Here $\mu_t=1/m_t$. Consequently, the calculation of the elements of G and the subsequent computation of the various minors of G is replaced by the calculation and combination of minors of B. This is not ordinarily easier, however, because the number of minors needed becomes very large. However, this form has the advantage of showing at a glance which coefficients are zero.

A modification which is more generally useful is the following. Since the mass associated with each of the three Cartesian coordinates of an atom is the same[4] and since there may be several atoms of the same mass,[5] the μ_t's will not all be different. It is therefore convenient to separate the sum in Eq. (11) into sets of terms with different coefficients $\mu_t\mu_{t'}\cdots$

$$\therefore \quad |G|_s = \sum_{\alpha,\,\alpha',\,\cdots} \mu_\alpha\mu_{\alpha'}\cdots \begin{vmatrix} H_{ki}^{(\alpha)} & H_{kj}^{(\alpha')} & \cdots \\ H_{li}^{(\alpha)} & H_{lj}^{(\alpha')} & \cdots \\ \cdots & \cdots & \cdots \end{vmatrix}, \quad (12)$$

in which

$$H_{ki}^{(\alpha)} = \sum_{t(\alpha)} B_{kt}B_{it},$$

summed over all values of t for which $\mu_t=\mu_\alpha$; i.e., summed over values of t having the same mass. The sum over α, α', $\cdots$ should include all the different masses, and permutations of α, α', $\cdots$ should be included separately since they are in general different. This result enables one to obtain the expanded form of the secular equation with both the force constants and the masses in algebraic form.[6] Indeed it is only a matter of patience to obtain the minors of H algebraically also, so that it is possible to secure the complete equation in algebraic form. In practice, however, for equations higher than a quartic, the algebraic form of these minors is so complicated that it is seldom desirable to obtain them algebraically, unless several molecules of the same configuration but different dimensions are to be treated.

Likewise, it is simpler to calculate the minors $|G|_s$ numerically directly unless isotopic species are to be studied.

Evaluation of Determinants

The most laborious part of the calculation is the evaluation of $|G|$ and its minors. In the general case in which all the minors are required, it is perhaps best to calculate the two-rowed minors first, then use these to calculate the three-rowed minors, etc. However, in special cases where not all the minors are required it may be more rapid to calculate $|G|$ first by the method

[4] But note one of the approximation methods described later.

[5] See, however, the section on the isotope effect.

[6] It is in addition possible to set up general tables for the elements of H for an atom. Thus the diagonal element corresponding to stretching of a bond attached to the given atom is always unity, etc.

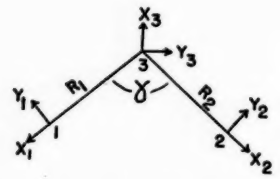

FIG. 1. The geometry and coordinates for the molecule ABC.

of reduction to triangular form.[7] The work sheet for this calculation will then contain much of the computation needed to calculate the various minors.

AN EXAMPLE

To illustrate the method a simple example will be worked out algebraically: the three-particle system with valence type force constants previously examined by Cross and Van Vleck and by Lechner.[8] The geometry and coordinates are shown in Fig. 1. By considering components one easily sees that

$$R_1=\Delta r_1=x_1+cx_3+sy_3,$$

$$R_2=\Delta r_2=x_2+cx_3-sy_3,$$

$$R_3=r_1r_2\Delta\gamma=r_2y_1+r_1y_2-sr_+x_3+cr_-y_3,$$

where $c=\cos\frac{1}{2}\gamma$, $s=\sin\frac{1}{2}\gamma$, r_i is the equilibrium length of bond $3\rightarrow i$, $r_+=r_2+r_1$, $r_-=r_2-r_1$. Consequently, the matrix B is

$$B=\begin{pmatrix}1 & 0 & 0 & c & s\\ 0 & 0 & 0 & c & -s\\ 0 & r_2 & r_1 & -sr_+ & cr_-\end{pmatrix},$$

where dotted lines are used to separate columns associated with different masses. Then

$$H^{(1)}=\begin{pmatrix}1&0&0\\0&0&0\\0&0&r_2^2\end{pmatrix};\quad H^{(2)}=\begin{pmatrix}0&0&0\\0&1&0\\0&0&r_1^2\end{pmatrix};$$

$$H^{(3)}=\begin{pmatrix}1 & c^2-s^2 & -2csr_1\\ c^2-s^2 & 1 & -2csr_2\\ -2csr_1 & -2csr_2 & s^2r_+^2+c^2r_-^2\end{pmatrix}.$$

[7] R. A. Frazer, W. J. Duncan, A. R. Collar, *Elementary Matrices* (Cambridge University Press, 1938), Chap. 4.

[8] P. C. Cross and J. H. Van Vleck, J. Chem. Phys. **1**, 350 (1933). F. Lechner, Sitzber. Akad. Wiss. Wien Math.-naturw. Klasse **141**, 291 (1932).

For simple valence forces the matrix for F may be written

$$F=\begin{pmatrix}f_{11}&0&0\\0&f_{22}&0\\0&0&f_{33}\end{pmatrix},$$

where the relation to the notation of Cross and Van Vleck is

$$f_{11}=k_1,\quad f_{22}=k_2,\quad f_{33}=[(r_1^{02}+r_2^{02})/r_1^{02}r_2^{02}]k_3.$$

The complete equation may now be written down almost by inspection and is

$$\begin{aligned}&\lambda^3-\lambda^2\{f_{11}(\mu_1+\mu_3)+f_{22}(\mu_2+\mu_3)\\&\quad+f_{33}[r_2^2\mu_1+r_1^2\mu_2+(s^2r_+^2+c^2r_-^2)\mu_3]\}\\&\quad+\lambda\{f_{11}f_{22}[\mu_1\mu_2+\mu_1\mu_3+\mu_2\mu_3+4c^2s^2\mu_3^2]\\&\quad+f_{11}f_{33}[r_2^2\mu_1^2+r_1^2\mu_1\mu_2+(s^2r_+^2+c^2r_-^2+r_2^2)\mu_1\mu_3\\&\quad+r_1^2\mu_2\mu_3+(s^2r_+^2+c^2r_-^2-4c^2s^2r_1^2)\mu_3^2]\\&\quad+f_{22}f_{33}[r_2^2\mu_1\mu_2+r_2^2\mu_1\mu_3+r_1^2\mu_2^2\\&\quad+(s^2r_+^2+c^2r_-^2+r_1^2)\mu_2\mu_3+(s^2r_+^2+c^2r_-^2\\&\quad-4c^2s^2r_2^2)\mu_3^2]\}-f_{11}f_{22}f_{33}[r_2^2\mu_1^2\mu_2+r_2^2\mu_1^2\mu_3\\&\quad+r_1^2\mu_1\mu_2^2+(s^2r_+^2+c^2r_-^2)\mu_1\mu_3^2+r_1^2\mu_2^2\mu_3\\&\quad+(s^2r_+^2+c^2r_-^2)\mu_2\mu_3^2\\&\qquad+(s^2r_+^2+c^2r_-^2+r_1^2+r_2^2)\mu_1\mu_2\mu_3]=0.\end{aligned}$$

The terms involving f_{12}, etc., the cross terms in the potential energy, could be introduced just as easily. For example the coefficient of λ will contain the term

$$(f_{12}f_{23}-f_{13}f_{22})[2csr_1\mu_2\mu_3+(4cs^3r_1-2csr_-)\mu_3^2].$$

There will be another term in $(f_{21}f_{32}-f_{31}f_{22})$ equal to this. When no cross terms are involved only diagonal minors are needed. It is evident from this example that it is necessary to be very systematic in order to be sure that all the necessary minors have been included.

UTILIZATION OF SYMMETRY

If the molecule possesses any symmetry whatever, the equation in λ can be factored into two or more factors of lower degree. The present method can be applied equally well to such cases.

It is only necessary to replace the coordinates x_i by the appropriate linear combinations of x's which form the basis of a completely reduced representation of the symmetry point group of the molecule, and likewise to replace the R's by the corresponding linear combinations[9] of R's. Coordinates of each different symmetry are treated completely separately and yield separate factors of the secular equation.

Isotope Effect

If the masses have been carried through the computation algebraically, the effect of introducing an isotopic atom can of course be computed exactly, provided that the substitution does not invalidate the symmetry coordinates, if any, used in calculating B. That is, if the problem has been factored by the use of symmetry and if the introduction of the isotopic atom lowers the symmetry, merely using the new mass in the old equations will not give an exact answer because the interaction between levels formerly of different but now of the same symmetry is thereby neglected. However, unless the pair of levels in question are close together, the loss of accuracy is usually small. Furthermore, if one isotopic atom is introduced in a molecule containing several atoms of that element, care must be used in making the original calculation to see that a separate H is used for the atom in question instead of one H for all the atoms of that element.

In large molecules where the completely numerical method has been used (i.e., calculation of G and its minors), the effect of a change in mass of one or more atoms may be obtained by using the second method (calculation of minors of B) for those terms which involve the altered atoms, and thus obtaining corrections to be added to the minors of G.

A Useful Method of Approximation

It has been found very convenient in treating normal vibrations by the standard methods to split off the high frequencies from the rest by an approximation technique.[10] This can be done even more easily with the expanded form of the secular equation. It is found in practice that each vibration frequency is determined chiefly by the values of a few force constants and much less affected by the others. This is particularly true if the frequencies are well separated from one another. Under these circumstances approximately correct results may often be obtained by setting the other force constants equal either to infinity or to zero or some to infinity and some to zero. If the equation is divided by the product of the force constants later put equal to infinity, it will be seen that the resulting equation will be of degree less than before by precisely the number of force constants put equal to infinity. This step enables the low frequencies to be more easily obtained, if they are not appreciably influenced by the high frequencies. To obtain the high frequencies, all the other force constants are put equal to zero, which again lowers the degree of the equation. In cases where experience has shown that it is unnecessary to go to a higher approximation—for example, in the splitting of the frequencies of hydrocarbons above 2800 cm^{-1}—much labor can be saved not only because of the reduction in the degree of the algebraic equation to be solved but because the coefficients which are eliminated in the approximation process do not need to be calculated.

It may even be possible in some cases to carry this process considerably further, at least for a preliminary set of results, and split the equation into one factor for each group of frequencies near to one another.

The general mechanical theorem[11] that the frequencies of a vibrating system can only increase when a constraint is added shows that when any force constant is put equal to infinity the resulting roots must be higher than the true ones. However, it is to be noted that care must be taken in correlating the new roots with the old ones. This theorem apparently does not apply, in general, to the case when force constants are put equal to zero and it is to be care-

[9] In other words "external symmetry coordinates" replace the x's and "internal symmetry coordinates" (or "geometrical symmetry coordinates") replace the R's. See E. B. Wilson, Jr., and B. L. Crawford, Jr., J. Chem. Phys. **6**, 223 (1938).

[10] B. L. Crawford, Jr., and J. T. Edsall, J. Chem. Phys. **7**, 223 (1939).

[11] E. T. Whittaker, *Analytical Dynamics* (Cambridge University Press, 1927), third edition, p. 191.

fully noted that these two approximations do not usually bracket the true roots.

Another approximation is obtained when one or more masses is put equal to infinity. Here again an upper limit to the true roots is obtained because making a mass infinite is equivalent to preventing the atom in question from moving. In some cases it is better to put the mass associated with only one of the three coordinates of an atom equal to infinity. This prevents motion in one direction but not in others.

Some Advantages and Limitations

The method described in this paper has the great advantage of giving an algebraic instead of a secular equation. Numerical methods of solution, such as Horner's method, are more highly developed for algebraic equations. In addition there is the advantage that as each root is found, the equation may be reduced to one of lower degree by dividing through by the root, so that the other roots become progressively easier to find.

Furthermore, the labor of setting up conservative coordinates in order to get a secular equation of degree $3n-6$ rather than $3n$ is avoided. Finally the algebraic form permits the use of the approximation technique in its most general and most convenient form.

The principal disadvantage of this method is the necessity of calculating a rather large number of determinants. This is a severe handicap when dealing with large factors and only experience will tell whether or not the older methods, especially as they have been modified recently, may not still be the most rapid for large molecules. For equations possibly up to the fifth or sixth degree and perhaps higher, however, this method should prove convenient.

I should like to thank Dr. B. L. Crawford, Jr. and Dr. Fred Stitt for reading and criticizing the manuscript of this paper.

Appendix

Define a new matrix D whose elements are $d_{ki}=B_{ki}(m_i)^{-\frac{1}{2}}$ and a new set of coordinates $q_i=(m_i)^{\frac{1}{2}}x_i$. Then $R=Dq$ and $2T=\dot{q}'\dot{q}$. The matrix D is rectangular but if the six conditions of zero linear and angular momentum are introduced as if they were extra coordinates r_k, later to be set equal to zero, then the matrix of the transformation is square and has an inverse. Call the augmented matrix $\mathfrak{D}$ and write it and its inverse in terms of submatrices:[12]

$$\mathfrak{D}=\begin{pmatrix} D \\ \cdots \\ D_0 \end{pmatrix}; \quad \mathfrak{D}^{-1}=(Q \vdots Q_0),$$

where D_0 is a $(6, 3n)$ matrix representing the momentum conditions. Q is $(3n, 3n-6)$, Q_0 is $(3n, 6)$ and both are to be determined. It is convenient to write also

$$\mathfrak{R}=\begin{pmatrix} R \\ \cdots \\ r \end{pmatrix}, \quad \text{so that} \quad q=\mathfrak{D}^{-1}\mathfrak{R},$$

where $r=D_0q$ $(=0)$ represents the 6 momentum conditions. Then the kinetic energy may be written as

$$2T=\dot{q}'\dot{q}=\dot{\mathfrak{R}}'\mathfrak{D}'^{-1}\mathfrak{D}^{-1}\dot{\mathfrak{R}}=\dot{R}'Q'Q\dot{R}+\dot{r}'Q_0'Q\dot{R}'$$
$$+\dot{R}'Q'Q_0\dot{r}+\dot{r}'Q_0'Q_0\dot{r}=\dot{R}'Q'Q\dot{R},$$

since $r=0$. But $\mathfrak{D}^{-1}\mathfrak{D}=E$ and $\mathfrak{D}\mathfrak{D}^{-1}=E$, whence

$$QD+Q_0D_0=E_{3n,\,3n} \quad \text{and} \quad DQ=E_{3n-6,\,3n-6}.$$

Therefore

$$D'Q'+D_0'Q_0'=E_{3n,\,3n}.$$

Multiplication by D and Q gives

$$DD'Q'Q+DD_0'Q_0'Q=DQ=E_{3n-6,\,3n-6}.$$

But the internal coordinates R are orthogonal to the translations and rotations r so that $DD_0'=0$ and therefore $DD_0'Q_0'Q=0$.

$$\therefore \quad Q'Q=(DD')^{-1}=G^{-1},$$

and $2T=\dot{R}'G^{-1}\dot{R}$, as previously stated.

[12] See reference 7, Chap. I.

Application of the Theory of Absolute Reaction Rates to Overvoltage

H. EYRING, S. GLASSTONE AND K. J. LAIDLER*
Frick Chemical Laboratory, Princeton University, Princeton, New Jersey

(Received August 3, 1939)

It is shown by means of the theory of absolute reaction rates that the current density I at an electrode is related to the overvoltage V by the expression $I=I_0e^{\alpha VF/RT}$ where I_0 is a constant for a given electrode, representing the current passing in each direction at the reversible potential, and α is the fraction of the added potential V operating between the initial and activated states. Since α is about 0.5 for many electrodes, it appears that the energy barriers at the electrode surface is a symmetrical one. The quantity I_0 is equal to $Be^{-\Delta H_1^{\ddagger}/RT}$, where $\Delta H_1^{\ddagger}$ is the heat of activation of the rate-determining process responsible for overvoltage, and B is $C_1(kT/h)F/N\cdot e^{\Delta S_1^{\ddagger}/R}$, where k, h, F, N and R are universal constants, T is the temperature, $\Delta S_1^{\ddagger}$ is the entropy of activation and C_1 is the concentration, per unit area, of the species involved in the slow process. Since $\Delta H_1^{\ddagger}$ and I_0 can be obtained from experimental data, it is possible to evaluate B, which is found to be independent of the nature of the cathode or the hydrogen ion concentration of the solution, and hence it appears that C_1 is almost constant for all electrodes in aqueous solutions. This suggests that the rate-determining step in the discharge of a hydrogen ion involves a water molecule, for only in this way could C_1 remain constant, and the slow process is believed to consist in the transfer of a proton from a molecule of water attached to the solution to another water molecule attached to the electrode surface. The suggested prototropic mechanism permits of an approximate estimate of $\Delta S_1^{\ddagger}$, and taking C_1 as 10^{15} molecules of water per sq. cm, the value of B calculated is in satisfactory agreement with experiment. The mechanism suggested immediately leads to the expectation of a symmetrical barrier at the electrode surface and so accounts for the value of 0.5 for α. The linear rate of attainment of overvoltage and the effect of changes in zeta-potential are readily explained, and it is shown that metals which form strong M−H bonds should have low overvoltages, as found in practice. The hydrogen-deuterium electrolytic separation factor is considered from the standpoint of the prototropic theory of overvoltage, and an explanation is proposed for the influence of the cathode material and of temperature. Oxygen overvoltage is attributed to a proton transfer in the opposite direction, i.e., from a water molecule on the electrode to one in a layer associated with the solvent, and so the striking similarities between cathodic and anodic phenomena can be readily understood. The high overvoltage accompanying the discharge of H_3O^+ and OH^- but not other ions is attributed to the fact that these ions are comfortably built into the structure of the solvent water.

INTRODUCTION

WHEN an electrode, immersed in a solution of its own ions (or of the ions of a gas with which it is saturated), is at its reversible potential the rate of deposition of ions on to the electrode is equal to the rate of re-ionization of the deposited substance: under these conditions there is no net flow of current and the resultant rate of deposition is zero. If material is to be deposited at an appreciable rate or, in other words, in order that an appreciable current may flow from electrode to solution, or vice versa, it is necessary to impose an additional electrical potential on the system; the magnitude of this excess potential determines the net rate of deposition, i.e., the current strength. The difference between the actual potential required to permit current to flow at a particular current density and the reversible value for the electrode in the given solution is called the "overvoltage" or "overpotential"[1] at that current density. In assessing the reversible potential it is the general practice to suppose that the substances deposited are in their standard states; a gas, e.g., hydrogen or oxygen, is supposed to be at 1 atmos. pressure if this is the external pressure at which electrolysis occurs. The overvoltage obtained in this manner is, of course, important from the practical point of view, but for theoretical treatment it is preferable to define the overvoltage as the potential in excess of the reversible potential of the electrode *under the experimental conditions*. In this way polarization phenomena resulting from changes in concentration of the electrolyte or from the fact that the solution may be supersaturated with gas, since this may be necessary

* Commonwealth Fund Fellow, 1938–40.

[1] For recent reviews, see S. Glasstone, *The Electrochemistry of Solutions* (Van Nostrand, Second edition, 1937), Chap. XVII; Ann. Reports Chem. Soc. **34**, 107 (1937); F. P. Bowden and J. N. Agar, *ibid.* **35**, 90 (1938); K. Wirtz, Zeits. f. Elektrochemie **44**, 303 (1938).

before bubbles can form, are excluded from the true overvoltage. As the latter is probably related to the energy of activation of the slowest stage involved in the process of deposition of material on the electrode, it may be called the "activation overvoltage."[2] The deposition of metals, except those of the iron group, generally requires only a small overvoltage, but appreciable values, rising sometimes to as much as one volt, accompany the liberation of hydrogen and oxygen.

The Rate-Determining Step

In the electrolysis of any aqueous solution the over-all reaction is the conversion of water into hydrogen and oxygen, and the various stages involved at the cathode are as follows: (1) the transport of H_3O^+ to the electrode layer; (2) the transfer of the ions, or possibly protons, to the electrode, and their discharge by electrons; (3) the combination of the hydrogen atoms on the electrode surface to form molecular hydrogen; and (4) the evolution of the hydrogen molecules in bubbles of gas. The slowest of these stages determines the overvoltage corresponding to a given current density. That stage (1) is not rate-determining is shown by the fact that the overvoltage depends on the nature of the metal used as cathode and is very small at an electrode of platinized platinum: further, the activation energy for the transport process is less than 3.5 kcal.,[3] which is much smaller than that usually associated with overvoltage (see Table I). Although (4) probably plays some part, it is apparently of relatively minor importance in determining overvoltage: the evolution of chlorine gas bubbles, as a result of the electrolysis of chloride solutions, for example, requires only a small overvoltage. The suggestion that stage (3) is the slow process was originally made by Tafel,[4] but this view leads to expectations in disagreement with the facts. If the electrode surface is sparsely covered with atomic hydrogen, the rate of the reaction $2H \rightarrow H_2$ is given by kn^2, where k is a constant and n is the number of atoms of adsorbed hydrogen per sq. cm of electrode surface. If the rate of the reverse process, that is the dissociation of hydrogen molecules into atoms, is negligible in comparison with that of the direct reaction, as it will be at appreciable current densities, the current flowing (I) is proportional to the rate of formation of molecular hydrogen: it is thus possible to write $I=kn^2$. The potential E of any atomic hydrogen electrode may be written in the form*

$$E=(RT/F)\ln n+\text{constant}, \qquad (1)$$

where the constant depends on the hydrogen ion concentration of the solution: the potential of the reversible electrode would then be

$$E_0=(RT/F)\ln n_0+\text{constant}, \qquad (2)$$

n_0 being the number of hydrogen atoms per sq. cm of surface at the reversible potential. The overvoltage V, equal to $E-E_0$, is then given by

$$V=(RT/F)\ln n/n_0. \qquad (3)$$

Combination of Eq. (3) with the result $I=kn^2$ then gives

$$I=kn_0^2e^{2VF/RT}$$

or, more generally,

$$I=I_0e^{2VF/RT}=I_0e^{\alpha VF/RT}, \qquad (4)$$

where I_0 is a constant, and α is equal to 2. According to Eq. (4) the plot of V against $\ln I$ should be a straight line of slope $RT/2F$, but it has been found experimentally for a number of metals that although the plot is linear, the slope is $2RT/F$, that is, α in Eq. (4) is 0.5 instead of 2. In order to account for this discrepancy Volmer and Erdey-Grúz,[5] Gurney,[6] and others[7] have suggested that part of stage (2), namely the neutralization of the hydrogen ion, is the slow process in the formation of gaseous hydrogen at an electrode, and hence is the fundamental cause of

[2] F. P. Bowden and J. N. Agar, reference 1, p. 91; Proc. Roy. Soc. **A169**, 206 (1938).

[3] A. E. Stearn and H. Eyring, J. Chem. Phys. **5**, 113 (1937).

[4] J. Tafel, Zeits. f. physik. Chemie **50**, 641 (1905).

* Strictly speaking the *activity*, and not the concentration of atomic hydrogen, should be used; under the conditions specified, however, i.e., a sparsely covered surface, n is probably a measure of the activity.

[5] T. Erdey-Grúz and M. Volmer, Zeits. f. physik. Chemie **150A**, 203 (1930).

[6] R. W. Gurney, Proc. Roy. Soc. **A134**, 137 (1931); see also R. H. Fowler, Trans. Faraday Soc. **28**, 368 (1932).

[7] See, A. Frumkin, Zeits. f. physik. Chemie **164A**, 121 (1933); J. A. V. Butler, Trans. Faraday Soc. **28**, 379 (1932); Proc. Roy. Soc. **A157**, 423 (1936); Zeits. f. Elektrochemie **44**, 55 (1938); J. A. V. Butler and G. Armstrong, Proc. Roy. Soc. **A137**, 604 (1932).

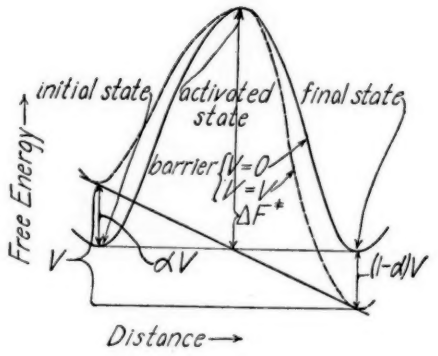

FIG. 1.

overvoltage: it has been shown, on the basis of these views, that α might reasonably have the value 0.5 as found experimentally.

ABSOLUTE REACTION RATE THEORY

Although it appears to be probable that a portion of stage (2) is the rate-determining step at most cathodes, some difficulty has been felt in accepting the suggestion that the addition of an electron to a hydrogen ion, or to a proton, requires an appreciable energy of activation. Since electrolysis may be considered as a rate process, the current strength being a measure of the velocity of reaction at a given overvoltage, it appeared possible that a further insight into the mechanism of electrode processes might be obtained by applying the theory of absolute reaction rates.[8] According to this theory[9] the specific rate k' of any reaction is given by the expression, assuming the transmission coefficient equal to unity,

$$k' = (kT/h)e^{-\Delta F^{\ddagger}/RT} \tag{5}$$

and for a *reversible* electrode the specific rate of the discharge process, i.e., of the direct reaction, may be written

$$k_1' = (kT/h)e^{-\Delta F_1^{\ddagger}/RT}, \tag{6}$$

while for the reverse reaction

$$k_2' = (kT/h)e^{-\Delta F_2^{\ddagger}/RT}, \tag{7}$$

where $\Delta F_1^{\ddagger}$, as usual, is the standard free energy required to form the activated state from the reactants, i.e., the free energy of activation for the direct reaction, whereas $\Delta F_2^{\ddagger}$ is the corresponding free energy of activation for the reverse process. These equations satisfy the thermodynamic requirement that k_1'/k_2' is equal to the equilibrium constant K of the process, since $\Delta F_1^{\ddagger} - \Delta F_2^{\ddagger}$ represents the standard free energy increase ΔF of the whole reaction, and K is $e^{-\Delta F/RT}$. At the reversible potential at which (6) and (7) hold good, no current passes, but if an overvoltage V is applied, the rate of the direct reaction exceeds that of the reverse process and current flows at a definite rate. Without making any assumptions as to the mechanism of the discharge process, it may be supposed that the effect of the excess potential is to diminish the free energy increase requisite for the formation of the activated state from reactants, thus assisting the direct process, whereas the reverse process is retarded.[10] If the additional potential V acts across the energy barrier between initial and final states, and α is the fraction of this electrical potential operative between the initial and activated states (Fig. 1), then the potential αV will facilitate the formation of the latter by decreasing the free energy by an amount αVF. At the same time the potential $(1-\alpha)V$ will oppose the reverse reaction, increasing the free energy required by $(1-\alpha)VF$. The specific reaction rates for direct and reverse reactions at the overvoltage V are then

$$k_1' = (kT/h)e^{-\Delta F_1^{\ddagger}/RT} \cdot e^{\alpha VF/RT}$$

and

$$k_2' = (kT/)he^{-\Delta F_2^{\ddagger}/RT} \cdot e^{-(1-\alpha)VF/RT}. \tag{8}$$

$$\therefore \quad k_1' = A_1 e^{\alpha VF/RT}, \quad k_2' = A_2 e^{-(1-\alpha)VF/RT}, \tag{9}$$

where A_1 and A_2 are constants. Since no assumption has been made concerning the nature of the reactants and resultants, their concentrations may be represented by C_1 and C_2 units, i.e., atoms, molecules or ions, per sq. cm, so that the direct and reverse reaction rates, in units per sq. cm, are

$$v_1 = A_1 C_1 e^{\alpha VF/RT} \text{ and } v_2 = A_2 C_2 e^{-(1-\alpha)VF/RT}. \tag{10}$$

[8] For reviews, see H. Eyring, Chem. Rev. **17**, 65 (1935); Trans. Faraday Soc. **34**, 41 (1938).

[9] A different application of the theory, based on an assumed mechanism, is given by G. Okamoto, J. Horiuti and K. Hirota, Sci. Papers Inst. Phys. Chem. Res. Tokyo **29**, 223 (1936).

[10] F. P. Bowden, Proc. Roy. Soc. **A126**, 107 (1929); T. Erdey-Grúz and M. Volmer, reference 5; R. W. Gurney, reference 6; J. Horiuti and M. Polanyi, Acta Physicochim. U. R. S. S. **2**, 505 (1935).

The current passing is determined by the difference between these rates, and if each reacting unit may be regarded as carrying the equivalent of a single charge, the current density I, in amp. per sq. cm, is given by

$$I=(v_1-v_2)F/N \tag{11}$$

$$=(C_1A_1e^{\alpha VF/RT}-C_2A_2e^{-(1-\alpha)VF/RT})F/N, \tag{12}$$

where F is the faraday, i.e., 96,500 coulombs, and N is the Avogadro number. If V is small, that is for very low overvoltages, the exponentials may be expanded and all terms other than the linear one neglected: thus

$$I=[C_1A_1(1+\alpha VF/RT) - C_2A_2\{1-(1-\alpha)VF/RT\}]F/N. \tag{13}$$

It will be seen from Eq. (10) that at the reversible potential, when V is zero, C_1A_1 is equal to C_2A_2, and if this equality may be assumed to hold also for small values of V,* then Eq. (13) becomes

$$I=(C_1A_1\cdot VF/RT)F/N. \tag{14}$$

At low overvoltages, therefore, there should be a linear relationship between current and overvoltage: this has been found for the evolution of hydrogen and the deposition of metals.[11] For higher values of V, the rate of the reverse reaction becomes negligibly small in comparison with that of the discharge process, so that it is possible to write

$$I=(C_1A_1e^{\alpha VF/RT})F/N=I_0e^{\alpha VF/RT}. \tag{15}$$

I_0, whose significance will be seen shortly, is equal to $C_1A_1\cdot F/N$. This is identical with Eq. (4), and, as already seen, it applies at many cathodes, α having the value of 0.5. Since α is the fraction of the overvoltage effective between initial and activated states of the discharge process, it follows (see Fig. 1) that the fall of potential between the initial and activated states must be, at least approximately, one-half that across the whole energy barrier;[12] in other words, the energy barrier at the electrode surface is almost symmetrical. This conclusion is of fundamental importance in deciding the nature of the essential electrode reaction.

Nature of Reacting Species

The next matter to consider is the species involved in the electrode process, and some information on this point may be obtained by calculating the value of C_1, the concentration of this substance. According to Eq. (12) the magnitude of the current passing in the forward direction, i.e., corresponding to the direct process, is

$$I(\text{forward})=(C_1A_1e^{\alpha VF/RT})F/N \tag{16}$$

and at the reversible potential, when $V=0$, this becomes

$$I_0=C_1A_1\cdot F/N \tag{17}$$

$$=C_1(kT/h)e^{-\Delta F_1^{\ddagger}/RT}\cdot F/N. \tag{18}$$

Since $\Delta F^{\ddagger}$ may be replaced by $\Delta H^{\ddagger}-T\Delta S^{\ddagger}$, it follows that

$$I_0=C_1(kT/h)F/N\cdot e^{\Delta S_1^{\ddagger}/R}e^{-\Delta H_1^{\ddagger}/RT} \tag{19}$$

$$=B\cdot e^{-\Delta H_1^{\ddagger}/RT}, \tag{20}$$

where B is equal to $C_1(kT/h)F/N\cdot e^{\Delta S_1^{\ddagger}/R}$: the quantities $\Delta S_1^{\ddagger}$ and $\Delta H_1^{\ddagger}$ are the entropy and heat of activation, respectively, of the direct electrode process. The value of I_0 may be determined by plotting ln I, or log I, against V, obtained experimentally for relatively high overvoltages and then extrapolating to $V=0$. The heat of activation $\Delta H_1^{\ddagger}$ can be derived from the temperature coefficient of overvoltage at constant current density, or from the temperature coefficient of current density at constant overvoltage, provided it is assumed that C_1 and $\Delta S_1^{\ddagger}$ are independent of temperature. From a knowledge of I_0 and $\Delta H_1^{\ddagger}$ it is possible to calculate B, by means of Eq. (20), and the results obtained from the available experimental data[13] are recorded in Table I. Except for the results with platinum in sodium hydroxide, which are

* According to the theory developed below C_1A_1 and C_2A_2 should be equal, irrespective of the magnitude of the overvoltage, for both hydrogen and oxygen evolution.

[11] J. A. V. Butler, Trans. Faraday Soc. **28**, 379 (1932); J. A. V. Butler and G. Armstrong, J. Chem. Soc. 743 (1934); M. Volmer and T. Erdey-Grúz, Zeits. f. physik. Chemie **159A**, 165 (1921); M. Volmer and H. Wick, *ibid.* **172A**, 429 (1935).

[12] T. Erdey-Grúz and H. Wick, Zeits. f. physik. Chemie **162A**, 53 (1932).

[13] F. P. Bowden and J. N. Agar, reference 1, p. 99.

TABLE I. *Hydrogen overvoltage at 25°.*

ELECTRODE	ELECTROLYTE	$12+\log I_0$	$\Delta H_1^\ddagger$ KCAL.	LOG B
Mercury	0.2N $-H_2SO_4$	0.8	18.0	2.0
Mercury	0.2N $-NaOH$	3.8	8.7	2.2
Gallium	0.2N $-H_2SO_4$	5.2	15.2	2.5 (87°C)
Wood's alloy	0.2N $-H_2SO_4$	4.0	16.4	2.0 (87°C)
Bright platinum	0.2N $-H_2SO_4$	6.2	11.5	2.6
Bright platinum	0.2N $-H_2SO_4$	6.8	9.5	1.7
Bright platinum	0.2N $-NaOH$	5.0	7.0	2.1
Bright platinum	0.2N $-NaOH$	6.3	6.0	2.7
Palladium	0.2N $-H_2SO_4$	7.3	9.0	1.9
Palladium	0.2N $-NaOH$	7.0	10.0	2.3

stated to be very dependent on the condition of the surface, and with mercury in the same electrolyte, where the low value of α, *viz.*, 0.24,[13] indicates the presence of complicating factors, e.g., the discharge of sodium ions to form a dilute amalgam, the figures in the last column are virtually constant, and B, which involves C_1 and $\Delta S_1^\ddagger$, is apparently independent of the nature of the electrode and electrolyte. This result suggests that the species whose concentration is represented by C_1 is *the same in all aqueous solutions and at all electrodes*, and the obvious conclusion to draw is that the substance is *water*. The provisional inference is, therefore, that the rate-determining step in the discharge of hydrogen ions involves a molecule of water. As a first approximation it may be assumed that a water molecule occupies 10^{-15} sq. cm: this is roughly the mean area of cross section of a single water molecule in pure water or of a metal atom of diameter 3A. The quantity C_1 would thus be about 10^{15} molecules per sq. cm, and since kT/h at 25° is about 6×10^{12}, F is 96,500 and N is 6×10^{23}, it follows that

$$B=9.6\times10^{8}\cdot e^{\Delta S_1^\ddagger/R}. \qquad (21)$$

MECHANISM OF CATHODE PROCESS

To determine whether the assumption that a molecule of water is involved in the rate-determining stage is in harmony with the experimental value of B it is necessary to assess $\Delta S_1^\ddagger$, at least roughly, and this can only be done if something is known of the nature of the initial and activated states. The next step, therefore, is to postulate a more detailed mechanism for the slow reaction at the cathode. It is suggested that in the absence of strongly adsorbed substances an electrode in aqueous solution becomes covered to a considerable extent by a unimolecular layer of water molecules, probably in the form of H and OH attached to atoms of the metal, which are at the same thermodynamic potential as and hence in equilibrium with the electrode itself. Adjacent to this layer there is another layer of water molecules attached to and at the same thermodynamic potential as the bulk of the electrolyte, and the excess potential V at the electrode may be regarded, as explained below, as operating entirely across these two layers of water molecules.* The slow stage in the discharge of a hydrogen ion is then believed to be the transfer of a proton from a molecule of water on the solution side to one attached to the electrode. The rate-determining step is thus a kind of prototropic change, and such processes are known to be associated with heats of activation of about 10 to 20 kcal.,[14] and hence are of the same order as those found for the cathodic liberation of hydrogen. Even when the proton has to move through a distance of the order of a molecular diameter, or less, as would be the case in the suggested cathode process, the heat of activation is of a similar magnitude: this is proved by the stability at ordinary temperatures of the keto- and enol-forms of tautomeric compounds such as acetoacetic ester. It will be noted that according to the above postulate the overvoltage acts across two layers of water molecules and since it is probable that the activated state lies midway between them, the requirement that half the excess potential V operates between the initial and activated states is satisfied.

The slow prototropic process, which is the essential cause of overvoltage, may then be represented as follows:

$$S\left\{\begin{matrix}H\\|\\O-H\end{matrix}\quad+\quad\begin{matrix}H\\|\\O-\\H-\end{matrix}\right\}^{\ominus}M\rightarrow S\left\{\begin{matrix}H\\|\\O\cdots H\cdots O-\\\ominus\quad\oplus\quad H-\end{matrix}\right\}^{\ominus}M\rightarrow S\left\{\begin{matrix}H\\|\\O\\\ominus\end{matrix}\quad+\quad\begin{matrix}H_2O-\\\\H-\end{matrix}\right\}M. \qquad (22)$$

Initial state — Activated state — Final state

* The layer attached to the solution may be somewhat diffuse, but for present purposes it can be regarded as being sharply defined without introducing any serious error.

[14] See, for example, G. F. Smith, J. Chem. Soc., 1744 (1934); 1824 (1936); 1413 (1937).

The symbol S refers to the solution and M to the electrode surface, the ⊖ sign on M being used to indicate an electron which is believed to be available at the cathode.[15] It is evident that the activated state consists virtually of H_3O^+ and OH^-, and so it appears that the entropy of activation $\Delta S_1^\ddagger$ will be very close to that accompanying the transfer of a proton from one water molecule to another, i.e., $H_2O+H_2O=H_3O^++OH^-$, which represents the ionization of water in any aqueous solution. Taking $a_{H_3O^+}\cdot a_{OH^-}$ as 10^{-14} at 25° and a_{H_2O} as 55 moles per liter, the equilibrium constant is found to be 3.3×10^{-18}: since ΔH for the ionization of water is 13.6 kcal., it follows that $e^{\Delta S/R}$ is 3.3×10^{-8}. According to the above arguments, therefore, $e^{\Delta S_1^\ddagger/R}$, required for the calculation of B by Eq. (21) should have the same value, and hence log B is approximately 1.5, in satisfactory agreement with that found from overvoltage measurements (Table I). The suggestion that the slow process at a cathode involves the transfer of a proton from one molecule of water to another is thus consistent with the experimental facts.

In the derivation of Eq. (21) it has been assumed that the concentration of water molecules is 10^{15} per sq. cm; strictly speaking this applies to the layer attached to the solution, but the concentration on the electrode surface will probably be much the same. In other words the electrode is supposed to be completely covered with water molecules. If strictly true this conclusion would be contrary to the observations made by various authors[16] on the quantity of electricity required to change a hydrogen electrode to an oxygen electrode, and vice versa: from these measurements it appears that the former is covered with a layer of hydrogen and the latter with a layer of oxygen atoms. It must be remembered that neither the calculations on which this conclusion is based nor those in the present paper are accurate within a factor of at least two and it is not impossible that the electrode surface is covered to the extent of one-half, or of that order, by water molecules and the remainder by hydrogen or oxygen atoms.

Rate of Attainment of Overvoltage

The increase of cathode potential, from the reversible to the overvoltage value, at a constant current is a linear function of the quantity of electricity passed:[17] this result implies that the attainment of overvoltage is equivalent to the charging of a condenser and is accompanied by the building up of an electrical double layer. The rate of the prototropic process at the cathode, which is $I_0e^{\alpha\pi F/RT}$, can only approach that required by the current strength when the potential π is close to the overvoltage value V for the given current: if the potential is below this point another process must be responsible for the removal of electrons brought up to the cathode. It is suggested, therefore, that while the overvoltage is building up the cathodic reaction is exclusively

$$\overset{\ominus}{M}\begin{cases}-H\\-OH\end{cases} \rightarrow M\begin{cases}-H\\-OH^{\ominus}\end{cases}. \qquad (23)$$

A water molecule exists on the surface as H and OH and the latter unites with an electron to form an OH^- ion on the electrode surface. Since (23) is the only cathodic process the number of these ions will be directly proportional to the quantity of electricity passed. If the OH^- ions in the electrode layer are balanced by an equal number of H_3O^+ ions in the solution layer, the double layer potential will increase with time in a linear manner, as found in practice. It is only when the potential approaches the overvoltage value that the velocity of process (22) becomes appreciable: the rate of growth of the potential due to (23) then falls off, and finally becomes zero at the steady overvoltage state when the prototropic process keeps pace with the current.*

[15] The so-called "electrochemical mechanism" described by J. Horiuti and G. Okamoto (Sci. Papers Inst. Phys. Chem. Res. Tokyo **28**, 231 (1936); K. Hirota and J. Horiuti, Bull. Chem. Soc. Japan **13**, 228 (1938) has some features in common with the above scheme: the theory which attributes overvoltage to the slow rate of neutralization of H_2^+ cannot, however, be regarded as satisfactory.

[16] F. P. Bowden, Proc. Roy. Soc. **A125**, 446 (1929); J. A. V. Butler and G. Armstrong, *ibid* **A137**, 604 (1932); G. Armstrong, F. R. Himsworth and J. A. V. Butler, *ibid* **A143**, 89 (1933); A. Frumkin and A. Šlygin, Acta Physicochim. U. R. S. S. **5**, 819 (1936); B. Ershler, *ibid.* **7**, 327 (1937).

[17] F. P. Bowden and E. K. Rideal, Proc. Roy. Soc. **A120**. 59 (1928); E. Baars, Sitzungsber. Ges. Beförd. Naturwiss, Marburg **63**, 213 (1928); T. Erdey-Grúz and M. Volmer, reference 5; A. Hickling, private communication.

* It should be emphasized that the scheme proposed for the establishment of the double layer potential measured as overvoltage does not involve any assumptions or implications as to the origin of the reversible electrode potential.

Influence of Electrolyte

Unless the electrolyte is more alkaline than *p*H 12, the cathodic overvoltage is independent of the hydrogen ion concentration:[18] this result is in agreement with the theory developed above. The number of water molecules per sq. cm of electrode surface will not differ appreciably in acid, neutral or alkaline media, and if $\Delta F_1^{\ddagger}$ for the activation process also remains unchanged, as is very probable, then it follows from Eq. (15) that the overvoltage, at constant current density, will not be dependent on the *p*H of the solution. This conclusion, however, may require some modification in certain circumstances, as will be seen below.

The effect of added electrolytes on overvoltage is not known with certainty, but it appears that when the zeta-potential at the interface between mercury and dilute sulfuric acid is made more positive, as a result of the adsorption of positive ions, the overvoltage is increased, whereas when the zeta-potential becomes more negative, that is when anions are taken up preferentially by the metal, the overvoltage is decreased.[19] These facts can be readily explained if the change in the zeta-potential resulting from the addition of a salt can be attributed to the preferential adsorption of one ion in the layer attached to the electrode and the other by the layer associated with the solution. For example, if the positive ions are in excess in the electrode layer, the zeta-potential will become more positive: the presence of these excess positive charges will tend to oppose the passage of protons over the energy barrier and hence the activation energy will be in excess of the normal value. If it is supposed that the fraction β of the increase $\Delta\zeta$ of the zeta-potential operates between the initial and activated states, then Eq. (15) becomes

$$I = I_0 e^{(\alpha V_1 - \beta\Delta\zeta)F/RT}, \qquad (24)$$

where V_1 is the new overvoltage. It follows, therefore, that for the same current density

$$V_1 = V + (\beta/\alpha)\Delta\zeta, \qquad (25)$$

where V is the overvoltage in the absence of the added salts. According to recent investigations[19] β/α is 0.5 to 0.7 for a mercury cathode, assuming $\Delta\zeta$ to be equal to the change in the potential at the mercury-solution interface at the electrocapillary maximum. If the ions causing the zeta-potential are adsorbed in the two water layers, as has been suggested, then this potential should operate over the same region as the overvoltage, and β/α should be unity. In view of the assumptions made in assessing $\Delta\zeta$, the agreement is as good as could be expected.

The lowering of overvoltage sometimes observed[20] when the *p*H of the electrolyte exceeds 12 is probably to be attributed to an effect similar to that just described. The adsorption of the negatively charged hydroxyl ions into the water layer near the electrode will facilitate the passage of protons over the energy barrier and so the overvoltage is diminished.[21] At a mercury cathode the overvoltage is apparently independent of the *p*H even in alkaline solutions:[22] if this is the case then it must be assumed that there is no preferential adsorption of hydroxyl ions on mercury.

If the electrolyte contains substances which are strongly adsorbed on the electrode surface, e.g., catalytic poisons, such as arsenic compounds, or long chain acids and alcohols, the area available for the adsorption of water molecules will be greatly decreased. The points available for the acceptance of protons is thus less than would be the case if the solution did not contain adsorbable compounds, and hence it is probable that a higher overvoltage would be required for the same apparent current density. Materials which are adsorbed to a small extent only, e.g., ethyl alcohol, acetone and acetic acid, sometimes lower overvoltage[23] because of other factors mentioned below.

---

[18] J. Tafel, reference (4); S. Glasstone, J. Chem. Soc. **125**, 2414, 2646 (1924); F. P. Bowden, Trans. Faraday Soc. **24**, 473 (1928); Proc. Roy. Soc. **A126**, 107 (1929); S. Lewina and V. Sarinsky, Acta Physicochim. U. R. S. S. **6**, 491 (1937); **7**, 485 (1937); C. Wagner and W. Traud, Zeits. f. Elektrochemie **44**, 391 (1938).

[19] S. Jofa *et al.* Acta Physicochim. U. R. S. S. **10**, 317 (1939).

[20] S. Glasstone, reference 16, p. 2414.

[21] The work of A. Frumkin *et al.*, Acta Physicochim. U. R. S. S. **3**, 791 (1935); **4**, 911 (1936) suggests that the adsorptive properties of a platinum electrode surface are different in acid and alkaline solutions.

[22] S. Glasstone, reference 16, p. 2646.

[23] S. Glasstone, Trans. Faraday Soc. **21**, 36 (1925).

Influence of Electrode Material

If the value of I_0 given by Eq. (19) is introduced into (15) it is seen that

$$I = C_1(kT/h)F/N \cdot e^{\Delta S_1^{\ddagger}/R} e^{-\Delta H_1^{\ddagger}/RT} e^{\alpha VF/RT}. \quad (26)$$

In the absence of strongly adsorbed substances, it appears that the different overvoltages of various metals must be attributed to differences in $\Delta H_1^{\ddagger}$, the heat of activation of the rate-determining process: the higher the value of $\Delta H_1^{\ddagger}$ the greater the overvoltage. If the metal is one that adsorbs hydrogen readily, that is it forms strong M—H bonds, then the oxygen atom of a water molecule held on such a surface will have increased affinity for the formation of a bond with hydrogen: the attachment of a proton to such an oxygen atom will, therefore, be facilitated and the heat of activation of the prototropic change responsible for overvoltage will be relatively low. This conclusion will be apparent from a consideration of the potential energy curves for the initial and final states of the rate-determining process (Fig. 2).[24] If the metal attracts the water molecule by forming strong M—H bonds, thus increasing the attraction of the proton, curve *A* will be less steep and $\Delta H_1^{\ddagger}$ will be diminished. Further, if the electrode material adsorbs atomic hydrogen readily, the position of curve *B* will be lowered, and this will also have the effect of decreasing $\Delta H_1^{\ddagger}$ and hence the overvoltage. Metals, such as platinum, palladium, copper, nickel, iron and silver, which adsorb hydrogen strongly should thus have low overvoltages, in agreement with experiment: these substances are as may be expected, good catalysts for the $2H \rightarrow H_2$ reaction,[25] but this is not to be taken as evidence for the view that atomic hydrogen is responsible for overvoltage, as was at one time suggested. The elements mercury, lead, zinc, tin and cadmium form only feeble M—H bonds, and hence these metals have high overvoltages. They should be poor catalysts for the recombination of atomic hydrogen and this has been verified for lead.[25]

[24] Cf. J. Horiuti and M. Polanyi, Acta Physicochim. U. R. S. S. **2**, 505 (1935); J. Horiuti and G. Okamoto, Sci. Papers Inst. Phys. Chem. Res. Tokyo, **28**, 231 (1936); J. A. V. Butler, Proc. Roy. Soc. **A157**, 423 (1936); Zeits. f. Elektrochemie **44**, 55 (1938).

[25] K. F. Bonhoeffer, Zeits. f. physik. Chemie **113**, 199 (1924).

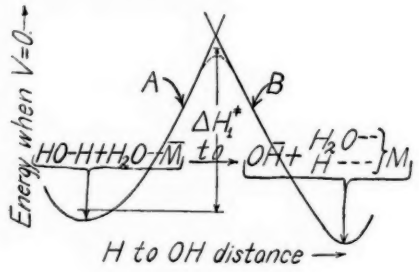

Fig. 2.

The constancy of the quantity *B* in Table I, and the prototropic theory of overvoltage, imply that the concentration of water molecules per *apparent* sq. cm of electrode surface is approximately constant: this can only be true if the surface is relatively smooth and the apparent and real areas are not very different. If the electrode surface is roughened, however, the quantity C_1 will be increased and as a consequence the overvoltage at an *apparent* constant current density will decrease. It is well known that roughening an electrode surface decreases the overvoltage, but it is possible that other factors besides mere increase of surface are responsible. The number of active adsorption centers probably increases more rapidly than does the actual surface area and, further, specially active centers may be developed: this is probably true for platinized platinum electrodes.

Alternative Electrode Processes

The model proposed here does not, of course, exclude the possibility that in certain circumstances other steps in the discharge process may become rate-determining: for example, on some electrodes the combination of atomic hydrogen to form molecules may be the slowest process. Since α is very close to 0.5 at electrodes of mercury, gallium, silver, nickel, etc., it is unlikely that the recombination reaction is the cause of overvoltage in these cases, but when α is large, for example at platinum, copper and palladium,[26] under certain conditions, where values of 0.8 and more have been observed, it is possible that this process is of importance in determining the

[26] C. A. Knorr and E. Schwartz, Zeits. f. Elektrochemie **40**, 38 (1934); Zeits. f. physik. Chemie **176A**, 161 (1936); M. Volmer and H. Wick, *ibid.* **172A**, 429 (1935); K. Wirtz, *ibid.* **36B**, 435 (1937).

current strength at a given overvoltage. When the electrode forms very strong M−H bonds the heat of activation of the prototropic process may become so low that the reaction $2H \rightarrow H_2$ becomes the rate-determining step. According to Tafel's calculations (p. 1054) α should then become equal to 2, and values of α between 2 and 0.5 are presumably due to the fact that the combination of atoms and the prototropic change have velocities of the same order, and hence both are effective in determining the rate of discharge of hydrogen ions. As the overvoltage is raised the rate of atom combination increases as the exponential of twice the overvoltage, and that of the prototropic reaction as the exponential of half the overvoltage; the former process will thus become very rapid as compared with the latter. It is evident, therefore, that the combination of atomic hydrogen can only be rate-determining, and hence the ultimate cause of overvoltage, when the latter is small.[27]

In the derivation of Eq. (4), with $\alpha=2$, it was assumed that the electrode surface was sparsely covered with atomic hydrogen so that the combination process is kinetically of the second order; if the surface becomes completely covered the reaction should become of zero order, and α should, apparently, decrease from 2 to 0.[28] This would only be true, however, if the concentration of atomic hydrogen was always a measure of its activity (see note, p. 1054), but this is certainly not the case. It is probable that as the surface becomes more fully covered and the apparent order of the combination of atomic hydrogen decreases, the activity coefficient increases, with the result that α would not diminish to zero. There is in fact reason for believing that α could not fall below 2 if the process $2H \rightarrow H_2$ were wholly responsible for overvoltage: from the viewpoint of energy barriers, the factor $e^{2VF/RT}$ in Eq. (4) arises because each of the two hydrogen atoms acquires additional energy $e^{VF/RT}$ when the ion becomes discharged by passing over the barrier across which the overvoltage V operates. If this is the case it is evident that provided H_2 molecules are formed, α should be 2, and it should not fall below this value unless some reaction other than $2H \rightarrow H_2$ is responsible for the overvoltage.

It may be remarked that according to the prototropic mechanism of overvoltage α is only 0.5 if the energy barrier is approximately symmetrical and the potential fall is uniform.[12] If for any reason there is distortion, then α may fall to zero if the activated state is pushed out towards the solution, or increase to unity if it approaches the electrode more closely.

Minimum Overvoltage, Surface Tension Effects, etc.

Various workers have found a connection between overvoltage and bubble formation: MacInnes and Adler,[29] for example, showed that the potential at a platinized platinum cathode fluctuated during the formation and liberation of a bubble of gas. These phenomena, as the aforementioned authors suggested, are undoubtedly due to supersaturation effects, and probably do not represent true, i.e., activation, overvoltage changes because the reversible potential of the hydrogen alters in a corresponding manner. Such changes of the reversible electrode potential are readily understandable but are outside the scope of the treatment by the theory of absolute reaction rates and are excluded from the present discussion by the definition of overvoltage given on p. 1053. It may be observed that the so-called "minimum overvoltage," which is the difference between the reversible potential for gas at 1 atmos. pressure and the measured cathode potential when hydrogen bubbles commence to be evolved, may not be a true overvoltage, since the concentration of gas in the vicinity of the cathode under these conditions probably exceeds the normal saturation value. Nevertheless, provided the surface forces at the electrode are not changed appreciably the extent of supersaturation requisite for steady bubble formation represents a fairly definite condition, irrespective of external influences, and so the measured minimum overvoltage is a constant for a given electrode under a variety of conditions.[30] Alterations in the electrode or electrolyte which influence the degree of

[27] L. P. Hammett, Trans. Faraday Soc. **29**, 770 (1933).
[28] Cf. G. Okamoto, J. Horiuti and K. Hirota, Sci. Papers Inst. Phys. Chem. Res. Tokyo **29**, 223 (1936); see also F. P. Bowden and J. N. Agar, reference 1, p. 104.
[29] D. A. MacInnes and L. Adler, J. Am. Chem. Soc. **41**, 194 (1919).
[30] See S. Glasstone and G. D. Reynolds, Trans. Faraday Soc. **28**, 582 (1932).

supersaturation, e.g., the presence of substances which influence interfacial tensions, will alter the observed "minimum overvoltage" to some extent, but the true overvoltage may remain unchanged unless, as is not improbable, there are corresponding appreciable changes in the quantities C_1, $\Delta H_1^\ddagger$ or ζ. There does not appear to be any means, however, of distinguishing between true and apparent overvoltage changes under these conditions.

Separation of Hydrogen and Deuterium

The electrolytic separation of hydrogen and deuterium is attributed to the difference in overvoltage for the deposition of the two isotopic forms, and the expected larger value for deuterium has been confirmed experimentally. It is necessary to demonstrate, therefore, that the higher overvoltage for deuterium is consistent with the theory developed above. The free energy of ionization of deuterium oxide, i.e., $D_2O+D_2O=D_3O^+ + OD^-$, calculated from the known ionic product, is about 1000 cal. greater than for ordinary water, and hence it may be supposed that the free activation energies for the transfer of a deuteron and a proton at a cathode differ by a similar amount. Utilizing the method described on p. 1058, and making the same assumptions it is found that $\Delta S_1^\ddagger$ is almost identical for proton and deuteron transfer, and hence it follows that the heat of activation for the deuterotropic change must be approximately 1000 cal. greater than for the cathodic prototropic change. Assuming the difference to be actually 1200 cal., it can be readily calculated that the specific rate of the discharge process involving hydrogen is 7.4 times as great as that for deuterium: this is of the correct order to account for the observed separation coefficients. From the limited data available it appears that $\Delta H_1^\ddagger$ for hydrogen evolution from 0.2 *N*-sulfuric acid at a mercury cathode is 18.0 kcal., whereas for deuterium discharge it is 20.9 kcal.[13] If $\Delta S_1^\ddagger$ for the cathodic process is the same for the transfer of a proton and a deuteron, as the approximate calculations suggest, then the difference is larger than expected. From the value of $\Delta H_1^\ddagger$ for deuterium $\log B$ is found to be 3.24, which is higher than those in Table I: if the heat of activation for deuterium evolution is assumed to be 19.2 kcal., however, i.e., 1200 cal. larger than for hydrogen, $\log B$ is calculated as almost exactly 2.0. A difference of 1200 cal., rather than 2900 cal., in the heats of activation would thus be consistent with the mechanism of hydrogen discharge proposed in this paper and the subject merits further experimental investigation. If the zero-point energies of the activated states do not differ greatly, the difference in the heats of activation for deuterotropic and prototropic reactions should be equal to the difference in the zero-point energies of the D−O and H−O bonds, i.e., about 1400 cal.: This is also in harmony with the arguments given above.

It is of interest that the hydrogen-deuterium separation factors obtained with different metals fall roughly into the same two groups as do overvoltages themselves: at low overvoltage metals, e.g., platinum, nickel and silver, the separation coefficient is about 6, whereas at high overvoltage electrodes, e.g., lead (in acid solution), mercury and tin, the value is in the vicinity of 3.[31] The latter figure is very close to that expected if the equilibrium

$$HD+H_2O \rightleftharpoons H_2+HDO \qquad (27)$$

were established at the cathode,[32] and this is presumably what happens on high overvoltage metals. It has been seen that elements of this type form only weak M−H bonds, so that the hydrogen and deuterium atoms on the surface, liberated by electrolysis, have a high energy content and hence are reactive.* It is probable, therefore, that the surface reaction

$$D+H_2O=HDO+H \qquad (28)$$

requiring a heat of activation of about 12 kcal.,[33] which will lead to the establishment of equilibrium conditions, takes place rapidly on a high overvoltage electrode. In order that complete equilibrium may be established it is necessary that the HDO molecule, which is presumably

[31] B. Topley and H. Eyring, J. Chem. Phys. **2**, 217 (1934); J. Horiuti and G. Okamoto, reference 24; H. F. Walton and J. H. Wolfenden, Trans. Faraday Soc. **34**, 436 (1938).

[32] See A. Farkas and L. Farkas, J. Chem. Phys. **2**, 468 (1934); Proc. Roy. Soc. **A146**, 623 (1934).

* The marked reduction efficiencies, e.g., of organic compounds, observed at high overvoltage cathodes can be accounted for in this manner.

[33] See K. H. Geib, Zeits. f. Elektrochemie **44**, 83 (1938) for summary of data.

attached to the electrode as OH and D (or OD and H), should be able to leave the surface readily and exchange with H_2O molecules: this will occur if the bonds holding the OH (or OD) and D (or H) to the surface are weak in comparison with the O−D (or O−H) bond. It is just at high overvoltage electrodes, where the strength of the M−H bond is small, that this condition is satisfied. At low overvoltage cathodes the activity of the hydrogen will be small and there will be little tendency for the equilibrium (27) to be attained.

Increase of temperature will not only increase the specific rate of reaction (28) but it will also speed up the recombination of hydrogen atoms on the surface and hence decrease their concentration. If the heats of activation of the two processes are such that the first reaction is favored more than the second when the temperature is raised, then there will be a closer approach to equilibrium and the separation factor will decrease: this is the case at platinum, nickel and silver cathodes. On the other hand, if increase of temperature favors the atom recombination process, so that there is a marked decrease in the concentration of atomic deuterium on the surface, the equilibrium state will be less readily attained and the separation factor may rise: a result of this type has been observed with a tin cathode.[34]

At a platinized platinum cathode the separation factor is about 3, in spite of the low overvoltage: at this electrode, however, departure from equilibrium can never be very appreciable, for on a platinized surface water reacts relatively rapidly even with molecular deuterium, or HD,[35] and so the separation factor is never likely to differ to any great extent from the theoretical value.

Although the hydrogen-deuterium separation coefficient is generally independent of the hydrogen ion concentration of the electrolyte, at a lead electrode it is as high as 6 in an alkaline solution as compared with 3 in acid solution: it may be significant that the overvoltage of lead is definitely less in media of high pH than in acid solution,[19] and cathodic reduction is generally more efficient in an acid electrolyte. The presence of excess of hydroxyl ions, however, also produces other changes in the conditions at an electrode surface.[36]

Oxygen Overvoltage

Interaction between the evolved oxygen and the electrode material leads to complications in the study of anodic phenomena, but in spite of the difficulties it has become evident that there is a fundamental similarity between the processes occurring at anode and cathode. The kinetics of the deposition of oxygen bears a marked resemblance to that for hydrogen evolution,[37] and both in acid and dilute alkaline solutions the variation of oxygen overvoltage with current density at a platinum anode is given by Eq. (15), with α having a value of approximately 0.5, as for hydrogen ion discharge.[37, 38] These results are in agreement with the suggestion that the rate-determining process for oxygen evolution is a prototropic change, similar to that postulated for hydrogen evolution but in the opposite direction. A proton from a water molecule attached to the surface is transferred to one in the layer associated with the electrolyte: thus

$$S\left\{\begin{matrix} H & HO- \\ | & + \\ H-O & H- \end{matrix}\right\}\overset{\oplus}{M}\rightarrow S\left\{\begin{matrix} H & & HO- \\ | & & \\ H-O\cdots H\cdots & \ominus & \end{matrix}\right\}\overset{\oplus}{M}\rightarrow S\left\{H_3O^{\oplus}+\begin{matrix} & HO- \\ & \end{matrix}\right\}M, \qquad (29)$$

the sign $\oplus$ on M representing the deficit of an electron. The hydroxyl radicals formed on the surface react in pairs with the ultimate formation of molecular oxygen, the intermediate stage, or stages, being relatively rapid. The connection between oxygen and hydrogen overvoltage is at once evident, and the fact that α in Eq. (15) is

[34] H. F. Walton and J. H. Wolfenden, reference 31.

[35] J. Horiuti and M. Polanyi, Nature **132**, 819 (1933); **133**, 142 (1934); K. F. Bonhoeffer and K. W. Rummel, Naturwiss. **22**, 45 (1934); A. Farkas and L. Farkas, Trans. Faraday Soc. **33**, 678 (1937).

[36] Cf. A. Šlygin and A. Frumkin, Acta Physicochim. U. R. S. S. **3**, 791 (1935); A. Šlygin, A. Frumkin and W. Medwedowsky, *ibid.* **4**, 911 (1936).

[37] F. P. Bowden, Proc. Roy. Soc. **A126**, 107 (1929).

[38] F. P. Bowden and H. W. Keenan, see F. P. Bowden and J. N. Agar, reference 1, p. 102.

about 0.5 in both cases is readily understood. If this mechanism for the slow process in oxygen evolution is correct, the value of log B should not be of a very different order from those in Table I. The only experimental data which permit the calculation to be made are those for a platinum anode in dilute sulfuric acid solution;[37] $12+\log I_0$ is 1.57, and $\Delta H_1^{\ddagger}$ is 18.7 kcal. at 14°C, and so log B is 3.83. This value is somewhat larger than for hydrogen evolution, but in view of the uncertainties associated with the nature of the anode, the agreement is reasonably good.

If there were no formation of surface oxides it would be expected that metals forming strong M−H bonds should have high overvoltages, since the attraction would tend to hinder the removal of a proton from the surface. It is true that smooth platinum, palladium and gold, which have the lowest hydrogen overvoltages, have the highest overvoltages for oxygen evolution,[39] but the parallelism does not always hold. Nickel and cobalt, for example, have low overvoltages both at the anode and the cathode: the oxidation of the surface is undoubtedly a complicating factor.

General Remarks.—Influence of Medium

One of the difficulties of the older theories of overvoltage is that they fail to explain why appreciable overvoltages are only observed when hydrogen and oxygen are evolved in electrolysis, whereas very little overvoltage accompanies the evolution of chlorine gas.[40] It appears, therefore, that a chlorine ion requires only a small heat of activation in order to pass through the two layers of water molecules at the surface of the anode. The question arises, at this point, why the discharge of hydrogen and hydroxyl ions requires a high energy of activation whereas that for chlorine, or other halogen or metal, ion discharge is small. The answer suggested is that as a consequence of the continuous interchange of protons in aqueous solution the hydrogen and hydroxyl ions are not individual entities which remain unchanged once they are formed by the addition of acid or alkali to the water. Interchanges of the type

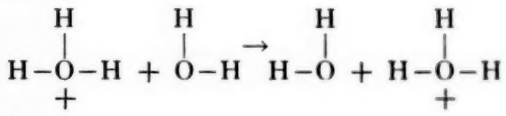

and

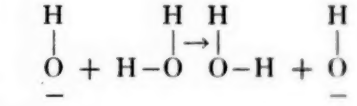

are taking place continuously in all directions, with the result that the H_3O^+ and OH^- ions must be regarded as part of the structure of the solvent water. Since the ions are so comfortably built into the structure of the bulk of the solution, it is evident that the direct passage of either an H_3O^+ or OH^- ion through the terminal layer of water molecules is likely to require a considerable rise in free energy, i.e., a higher free energy of activation is necessary. The transfer of a proton from one water molecule to another, as described in this paper, presumably requires a smaller heat of activation and so provides an alternative mechanism for bringing hydrogen or hydroxyl ions to the appropriate electrode for discharge.

The discharge of hydrogen ions in a non-aqueous solution will presumably depend on a prototropic change analogous to that suggested for aqueous solutions, but there are many factors which make it difficult to predict the relative overvoltages in different media. In alcoholic solutions both the molecule R·OH and the ion $R\cdot OH_2^+$ are less firmly bound to the bulk of solvent than are H_2O and H_3O^+, respectively, in water, because the replacement of H by R serves partially to break up the continuous structure. It is to be expected, therefore, that the transfer of a proton from a molecule of alcohol on the layer attached to the solvent to one on the electrode will require a smaller energy of activation than the corresponding process involving water molecules: further, there is a possibility, which apparently does not arise in aqueous solution, that a proton may be transferred from a $R\cdot OH_2^+$ ion on the solution side to an alcohol molecule on the cathode. In any case it would appear that the activation energy, and hence presumably the overvoltage, may be expected to be lower in alcoholic media than in

[39] A. Coehn and Y. Osaka, Zeits. f. anorg. Chemie **34**, 86 (1903).

[40] F. Chang and H. Wick, Zeits. f. physik. Chemie **A172**, 448 (1935).

aqueous electrolytes: this is so at various cathodes in methyl and ethyl alcohols.[41] It would appear, at first sight, that overvoltage should be low when acetic acid is the solvent, for the ion $CH_3 \cdot COOH_2^+$ would not be part of the structure of the medium: The situation is here complicated by the fact that most of the acetic acid exists in the associated form $(CH_3 \cdot COOH)_2$, and if single molecules only can take part in the prototropic change, overvoltages will be high. The very limited data suggest that the values are higher in acetic acid than in water.[42]

The addition of moderate amounts of methyl or ethyl alcohols, acetic acid or acetone to an aqueous solution lowers the overvoltage:[23] These substances have a depolymerizing effect on the solvent, tending to break up the continuous structure of the water,[43] and so the prototropic change at the boundary may well require a smaller energy of activation than in pure water. Small amounts of long chain alcohols and acids lower the overvoltage at a lead cathode, probably for the same reason, but larger amounts raise the value because of preferential adsorption on the surface.[23] It is probable that the addition of various organic compounds to an aqueous solution alters the zeta-potential: this, as already seen, might be expected to affect the overvoltage. Further, changes in the interfacial tensions may result in changes in the apparent overvoltage, as previously described.

The authors wish to express their thanks to Professor Hugh S. Taylor for helpful discussions.

[41] G. Carrara, Zeits. f. physik. Chemie **69**, 75 (1909); S. Lewina and M. Silberfarb, Acta Physicochim. U. R. S. S. **4**, 275 (1936).

[42] S. Swann and E. O. Edelmann, Trans. Electrochem. Soc. **58**, 179 (1930).

[43] See D. G. Beech and S. Glasstone, J. Chem. Soc. 67 (1938).

LETTERS TO THE EDITOR

This section will accept reports of new work, provided these are terse and contain few figures, and especially few halftone cuts. The Editorial Board will not hold itself responsible for opinions expressed by the correspondents. Contributions to this section should not exceed 600 words in length and must reach the office of the Managing Editor not later than the 15th of the month preceding that of the issue in which the letter is to appear. No proof will be sent to the authors. The usual publication charge ($3.00 per page) will not be made and no reprints will be furnished free.

The Spectroscopic Determination of the Carbon-Chlorine Distance in Methyl Chloride

About a year ago the writer pointed out[1] that there appeared to be a discrepancy between the values obtained for the C−Cl distance in methyl chloride by diffraction (1.77±0.02A) and by spectroscopic methods (1.66±0.05A). The latter value was based largely on an estimate for the larger moment of inertia of the molecule of 55.3×10^{-40} g cm². A paper by Nielsen and Nielsen[2] has recently appeared in which the rotational structure of a methyl chloride band is better resolved than in any previous work on the spectrum of this molecule. The value which these authors deduce for the moment of inertia is 48.0×10^{-40} g cm². If this were correct, it would mean an even more serious disagreement with the diffraction result as it would imply a C−Cl distance of about 1.55A. A careful examination of this recent work reveals, however, that the numbering of the lines is suspect for two reasons. On the low frequency side of the band, some of the weaker lines have been associated with the CH_3Cl^{35} isotopic form instead of the CH_3Cl^{37} to which they must clearly belong. This means that the numbering is out by at least one unit at that point. Again on the high frequency side the spacing between successive lines is frequently very much higher than the mean value accepted for the band as a whole *viz.* 1.15 cm^{-1} whereas exactly the opposite should be the case. The writer has found it possible to renumber the lines in such a way as to avoid the above difficulties and the mean spacing then comes out to be between 0.95 cm^{-1} and 1.0 cm^{-1} corresponding to a value for the moment of inertia of between 59×10^{-40} g cm and 56×10^{-40} g cm. This leads in turn to limiting values for the C−Cl distance of 1.71 and 1.66A. In other words the new work would appear to lessen, rather than to increase, the discrepancy between the spectroscopic and diffraction values. It should be emphasized, however, that more work must still be done, preferably on CH_3Cl^{35} or CH_3Cl^{37}, before an unequivocal numbering can be made.

G. B. B. M. SUTHERLAND*

Pembroke College,
Cambridge, England,
September 19, 1939.

* Leverhulme Research Fellow.

[1] G. B. B. M. Sutherland, Trans. Faraday Soc. **34**, 325 (1938).
[2] A. H. Nielsen and H. H. Nielsen, Phys. Rev. **56**, 274 (1939).

The Heat of Combustion of Isopropanol

The existing data on the heats of combustion of the first ten normal aliphatic alcohols have recently been reviewed and correlated by Rossini.[1] They may now be considered as quite satisfactory. On the other hand, the available data for the corresponding secondary and tertiary alcohols are old and relatively unreliable. In the present communication we shall present a modern combustion result which we have just obtained for liquid isopropyl alcohol.

Our measurements of the heat of combustion were made by burning samples of the liquid alcohol at 30 atmos. oxygen pressure and about 25°C in the precision bomb-calorimeter of Richardson and Parks.[2] The alcohol studied was a highly purified material—$d_4^{25°}$, 0.78134. According to standards previously used[3] in this laboratory, this density corresponds to 99.83 percent isopropanol and 0.17 percent water. The results for the four combustions which we have made are given in Table I in terms of the

TABLE I. *Experimental combustion data for isopropanol sample.*

EXPERIMENT	HEAT OF COMBUSTION (CAL./G)	PERCENT DEVIATION FROM THE MEAN
1	7944.3	+0.019
2	7947.8	+0.063
3	7937.7	−0.064
4	7941.6	−0.015
Mean	7942.8	±0.040

"defined" calorie (=4.1833 international joules). Column 2 contains the experimental heats of combustion per gram *in vacuum* for the bomb process at 25.0°C and column 3 the percentage deviations from our mean value. To convert this mean value to the ideal combustion process at 1 atmos. for pure isopropanol we have made changes of −0.03 percent for the Washburn correction[4] and +0.17 percent for the water content of our material. Using this corrected result ($-\Delta U_R/m=7953.9$ cal.) for the standard state combustion at constant volume and a molecular weight value[5] of 60.095, we next obtain $\Delta H_{298.16}=-478{,}880$ cal. per mole for the combustion process at 25° and 1 atmos. constant pressure. This result is 0.84 percent higher than the value of Zubow, as revised by Swietoslawski.[6] By the methods of Rossini[7] we estimate the uncertainty or

"accuracy error" in our final result to be ±300 cal. per mole.

Using Rossini's "best value" for *n*-propanol[1] and this new result for isopropanol, we now find for the isomerization reaction

$$n\text{-}C_3H_7OH(\text{liq.}) \rightarrow iso\text{-}C_3H_7OH(\text{liq.});$$
$$\Delta H_{298.16} = -3350(\pm 380) \text{ cal.}$$

By the third law of thermodynamics, $\Delta S_{298.16} = -3.1(\pm 0.5)$ e.u.[8] for this reaction; and hence

$$\Delta F^\circ_{298.16} = -3350 + (298.16)(3.1) = -2430(\pm 420) \text{ cal.}$$

GEORGE S. PARKS
GEORGE E. MOORE

Department of Chemistry,
Stanford University, California,
September 22, 1939.

[1] Rossini, Nat. Bur. Stand. J. Research **13**, 189 (1934).
[2] Richardson and Parks, J. Am. Chem. Soc. in a forthcoming issue.
[3] Parks and Kelley, J. Am. Chem. Soc. **47**, 2089 (1925).
[4] Washburn, Nat. Bur. Stand. J. Research **10**, 525 (1933).
[5] Baxter, Guichard, Hönigschmid and Whytlaw-Gray, J. Am. Chem. Soc. **61**, 223 (1939).
[6] Swietoslawski, J. Am. Chem. Soc. **42**, 1092 (1920).
[7] Rossini, Chem. Rev. **18**, 233 (1936).
[8] Parks and Huffman, *The Free Energies of Some Organic Compounds* (The Chemical Catalogue Co., New York, 1932), p. 109.

The Polymorphism of Cu_2S, and the Relations Between the Solid Phases in the System Cu_2S-CuS

The literature relating to the polymorphism of chalcocite and to the more general relations between the solid phases in the system Cu_2S-CuS contains numerous diverse conclusions. Because the solid phases in the system Cu_2S-CuS are of importance to mineralogists, a systematic x-ray study of them was undertaken. A special camera was designed to make x-ray photographs of powder-samples at high temperatures. This camera allows the specimen to remain heated continuously, and the heat treatment can be controlled as in a furnace. Samples were made up of annealed mechanical mixtures of the two end-members. The Cu_2S end-member came entirely from a single, homogeneous, pure orthorhombic crystal from Bristol, Connecticut. The CuS was chemically pure synthetic material which gave the covellite powder pattern.

The phase diagram for the system Cu_2S-CuS is shown in Fig. 1. This contains three compounds and six phases. The compounds are:

Chalcocite, ideally Cu_2S
Digenite, ideally $4Cu_2S \cdot CuS = Cu_9S_5$
Covellite, CuS

Several authorities have inferred that, on heating, chalcocite inverts from an orthorhombic to a cubic modification at about 91°C. In the present investigation it was found chalcocite undergoes three transformations, and none of the high temperature phases is cubic up to at least 250°C. The revised inversion scheme is:

above	105°C, nonisometric completely disordered basic structure
78°C to	105°C, nonisometric partially disordered basic structure
52°C to	78°C, nonisometric ordered basic structure
below	52°C, orthorhombic superstructure.

These temperatures are probably accurate to ±4°C. The 52° inversion is easily detectable by x-ray diffraction records, and makes itself known by the disappearance of superstructure lines on the powder photograph. The other inversions take place without obvious changes in the powder pattern except for certain intensity changes. The temperatures of these inversion points were determined by accurate thermal measurements. The superstructure phase is capable of dissolving up to 8 atomic percent CuS, while the ordered basic structure can dissolve only 2 atomic percent CuS. The solution of CuS by Cu_2S crystals almost certainly takes place by omission of Cu atoms from the Cu_2S structures.

The experimental evidence indicates a hitherto unrecognized compound, Cu_9S_5, whose powder pattern is

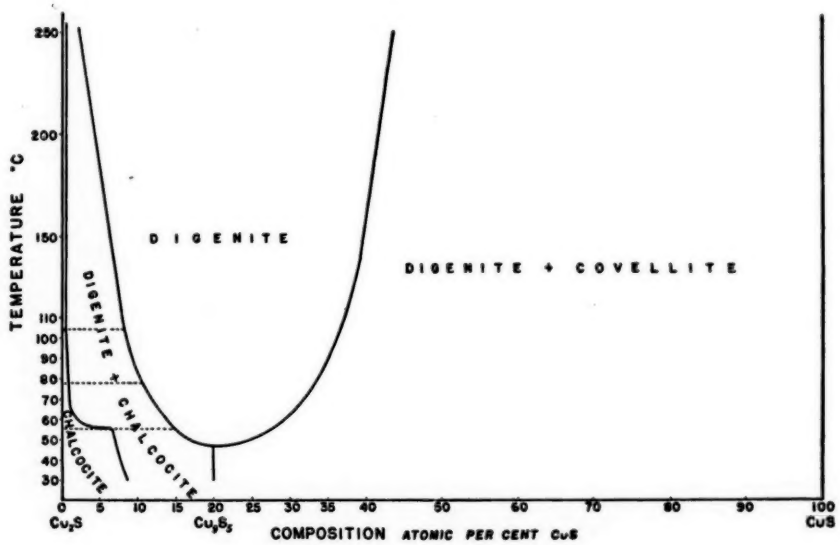

FIG. 1.

essentially identical with that of the discredited mineral digenite, to which the formula $2Cu_2S \cdot CuS = Cu_9S_5$ had been assigned. Below approximately 47°C digenite has the ideal composition Cu_9S_5 but above this temperature it takes increasing amounts of either Cu_2S or CuS into its composition. The mechanism of this solution is undoubtedly a variation in the number of copper atoms in the crystal structure. At 170°C, it is known that the copper atoms of this compound are in disorder. It is likely that at a temperature of 47°C or lower, the copper atoms in digenite become ordered and give rise to another modification.

Evidently digenite has been regarded as the phase of chalcocite stable above 91°C. Actually, the heat effect in this region is due to the transformation of ordered high chalcocite into the disordered high chalcocite, which is not isometric. The vanishing of this heat effect in preparations containing 8 percent and more by weight of CuS is evidently due to the fact that a heating run passes out of the chalcocite-digenite two-phase region and entirely into the digenite field before the chalcocite transformation is reached.

A full discussion of this investigation will appear elsewhere.

NEWTON W. BUERGER

Department of Mineralogy,
Queen's University,
Kingston, Ontario, Canada,
October 9, 1939.

Dipole Variation of Ether

Recently Byers[1] showed that the Cellosolves, whose structural formula resemble both ethers and alcohols, behave very similarly to the alcohols in respect to variation of dipole moment and not like the symmetrical ethers. The author stated that he was unable to find values for the electric moments of unsymmetrical ethers but predicted that these would vary in the manner of the Cellosolves and alcohols.

Reference to the values given in Table I shows that

TABLE I.

Mixed Ethyl Ethers Compound	Moment $\times 10^{18}$	Mixed Phenol Ethers Compound	Moment $\times 10^{18}$
Ethyl alcohol	1.70	Phenol	1.70
Diethyl ether	1.14	Anisole	1.20
Ethyl butyl ether	1.2	Phenetole	1.0
Ethyl isoamyl ether	1.2	Diphenyl ether	1.05
Ethyl phenol ether	1.0		

Byers' prediction, with respect to unsymmetrical ethers is true. There is an initial decrease in moment from ethyl alcohol to ethyl ether and from phenol to anisole, the decrease being due to the increased repulsion over the repulsion between an ethyl or phenyl group and hydrogen. Further lengthening of the chain does not alter its bulk in the neighborhood of the oxygen atom and therefore the moments remain sensibly the same. Essentially the same reasoning was applied by Smythe to account for the constant moment of the alcohols and by Byers for that of Cellosolves. The values given in the table are taken from Smythe.[2] The only exception is that of ethyl butyl ether which is taken from unpublished measurements from this laboratory. This unsymmetrical ether was prepared from interaction between butyl bromide and sodium ethylate. The product is purified by refluxing with sodium and repeated fractional distillation. The physical constants agree very well with those reported by Norris and Rigby.[3]

Meyer and Büchner[4] redetermined the moment of propyl ether and found it to be 1.16 ± 0.06. This value agrees with the electric moment of diethyl ether and together with the value of 1.0 for the moment of di-isoamylether,[2] indicates that even the symmetrical ethers shows similar dipole variation as that of unsymmetrical ethers.

NORMAN C. C. LI

Department of Chemistry,
Yenching University,
Peiping, China,
August 10, 1939.

[1] W. H. Byers, J. Chem. Phys. **7**, 175 (1939).
[2] Smythe, *Dielectric Constant and Molecular Structure* (Chemical Catalogue Co., New York, 1931).
[3] Norris and Rigby, J. Am. Chem. Soc. **54**, 2097 (1932).
[4] Meyer and Büchner, Physik. Zeits. **33**, 390 (1932).

Erratum: The Vapor Pressures of Ortho- and Parahydrogen and Ortho- and Paradeuterium

KARL COHEN AND H. C. UREY,
(J. Chem. Phys. **7**, 157 (1939))

During a conversation with Professor E. Teller on our paper on the vapor pressures of *o*- and *p*-H_2 and *o*- and *p*-D_2[1] he was kind enough to point out an error in the calculation of the centrifugal stretch of the rotating molecules. The stretch should be expressed as $\delta_c/c = 8B_o^2/\omega_o^2$, and not $4B_o^2/\omega_o^2$ as we had calculated. Since, in our view, the difference in heats of sublimation of 0°K caused by van der Waals attraction, ΔE_A, is proportional to this stretch, the calculated differences become doubled. Thus

$$\text{for } H_2 \quad \Delta E_A \text{ (calc.)} = -3.36 \text{ cal./mole},$$
$$\text{for } D_2 \quad \Delta E_A \text{ (calc.)} = -2.32 \text{ cal./mole},$$

while

$$\text{for } H_2 \quad \Delta E \text{ (exp.)} = -1.78 \text{ cal./mole} = E_{o\text{-}H_2} - E_{p\text{-}H_2},$$
$$\text{for } D_2 \quad \Delta E \text{ (exp.)} = -1.78 \text{ cal./mole} = E_{p\text{-}D_2} - E_{o\text{-}D_2},$$

where ΔE is the difference in sublimation heats computed from vapor pressure data, and naturally includes contributions from repulsive forces.

The corrected result is more satisfactory than the previously reported one. If, on the one hand, the stretch of rotating molecules increases their mutual attraction, on the other hand, the resultant increased penetration of the electron shells will also increase the repulsive forces. Thus a part of the increased binding energy caused by the increased van der Waals attraction will be canceled by the increased repulsion, and one must have $|\Delta E_A| > |\Delta E|$ if our explanation is to hold good.

If we calculate the required values of E_R to give agreement with experiment, namely $\Delta E_R = \Delta E - \Delta E_A$, we find

$$\text{for } H_2: \quad \Delta E_R = 1.58 \text{ cal./mole},$$
$$\text{for } D_2: \quad \Delta E_R = 0.54 \text{ cal./mole};$$

this agrees with the idea that ΔE_R will be larger for hydrogen because of the twice larger stretch.

[1] K. Cohen and H. C. Urey, J. Chem. Phys. **7**, 157 (1939); **7**, 438 (1939).